UNIVERSITY OF HAWAII
LIBRARY
JAN 9 '52

The
PHILOSOPHICAL MAGAZINE

FIRST PUBLISHED IN 1798

VOL. 42 SEVENTH SERIES No. 335 December, 1951

A Journal of Theoretical Experimental and Applied Physics

EDITOR
PROFESSOR N. F. MOTT, M.A., D.Sc., F.R.S.
EDITORIAL BOARD
SIR LAWRENCE BRAGG, O.B.E., M.C., M.A., D.Sc., F.R.S.
ALLAN FERGUSON, M.A., D.Sc.
SIR GEORGE THOMSON, M.A., D.Sc., F.R.S.
PROFESSOR A. M. TYNDALL, C.B.E., D.Sc., F.R.S.

PRICE 12s. 0d.
Annual Subscription £6 0s. 0d. payable in advance

TED AND PUBLISHED BY TAYLOR & FRANCIS LTD., RED LION COURT, FLEET ST., LONDON, E.C.4

ADVANCES IN PHYSICS

A QUARTERLY SUPPLEMENT OF THE PHILOSOPHICAL MAGAZINE

On 1st Jan., 1952, the Philosophical Magazine will publish the first number of a new quarterly supplement. The aim of this supplement will be to give those interested in physics comprehensive and authoritative accounts of recent important developments. It is felt by the Editor that in view of the rapid advances in many branches of physics, scientists will welcome a journal devoted to articles of this type.

VOLUME 1 JANUARY 1952 NUMBER 1

The Mean Free Path of Electrons in Metals.
By Dr. E. H. Sondheimer (Cambridge).
On the Generation of Vacancies by Moving Dislocations.
By Professor F. Seitz (University of Illinois, U.S.A.).
Crystal Growth and Dislocations. By Dr. F. C. Frank (Bristol University).

PRICE *per part* 15/- *plus postage* **PRICE** *per annum* £2 15s. 0d. *post free*

Editor: PROFESSOR N. F. MOTT, M.A., D.Sc., F.R.S.
Editorial Board: SIR GEORGE THOMSON, M.A., D.Sc., F.R.S.
PROFESSOR A. M. TYNDALL, C.B.E., D.Sc., F.R.S.
SIR LAWRENCE BRAGG, O.B.E., M.C., M.A., D.Sc., F.R.S.

Printed and Published by
TAYLOR & FRANCIS, LTD., RED LION COURT, FLEET ST., LONDON, E.C.4

CXXXIII. *Microscopic Studies on Beryl Crystals.*—II. *Dislocations and the Growth of* $\{10\bar{1}0\}$ *Prism Faces.*

By L. J. Griffin,
H. H. Wills Physical Laboratory, Bristol*.

[Received July 20, 1951.]

[Plates XLV.–LII.]

Summary.

It is shown that the type of growth predicted by the dislocation theory of growth takes place on $\{10\bar{1}0\}$ faces of beryl. The growth layers, in general, produce a complex topography. The behaviour of layers at surface obstacles is discussed. Examples are given of the propagation of a dominant layer group past lines of dislocations, and inactive dislocation groups, and the mode of propagation by cross-linking is discussed. Typical examples of lineage boundaries and limited slip zones are shown; these features are observed as lines of dislocations. The dependence of growth rate of the layers on crystallographic orientation is considered. The types of layer structure observed on natural and synthetic crystals are compared. It is shown that the dislocation theory of growth can be applied to give such information as the supersaturation and temperature at which growth took place.

---

§1. General.

The areas between the uni-molecular steps observed on prism faces of beryl (Griffin 1950, 1951) are in general plane. In some cases, however, the uni-molecular steps stop abruptly, and it is possible to describe a path from the low to the high side of a step without at any point crossing a discontinuity in height. The point of termination of the step must therefore mark a point of singularity of the surface corresponding to the point of emergence on the face of a dislocation with a screw component normal to the face. Any dislocation of this kind must necessarily mark one end of a step, which can only run off to the edge of the face or end at another screw dislocation.

§2. Spirals and Loops.

A case is shown in fig. 1 (Pl. XLV.) of a step, attached to a single dislocation, which takes a spiral form. Such behaviour has been predicted on purely theoretical grounds for the case of the advance of a layer attached to a single dislocation when the rate of advance of the layer is dependent on the crystallographic orientation (Burton, Cabrera and

---

* Communicated by the Author.

Frank 1951). The agreement between theoretical prediction and observation is so close that there can be no doubt but that the layer in fig. 1 (Pl. XLV.) has been winding itself up during growth.

The case of an edge joining two dislocations of opposite hand is shown in fig. 2 (Pl. XLVI.), this edge lying in the centre of the figure. The behaviour predicted by Frank was that the inner unclosed loop would expand during growth so as to generate successive closed loops, typified by the outer loop of fig. 2 (Pl. XLVI.). (The triangular area cutting into the closed loop of fig. 2 (Pl. XLVI.), probably consists of an overgrowth of foreign crystalline material.)

The dependence of growth rate upon crystallographic orientation of a layer can be represented by means of a two-dimensional polar diagram (Frank 1950). A close packed direction (Burton and Cabrera 1949) corresponds to a minimum growth rate and will manifest itself as an almost straight edge. The dislocation pair in fig. 2 (Pl. XLVI.) has been operating unhampered by the presence of other dislocations so that this case is almost ideal for consideration of growth rates. In this case the longitudinal edges must correspond to a close-packed direction. (These almost straight longitudinal edges are parallel to the *c*-axis and are most useful in defining the orientation of any area.)

Fig. 3.

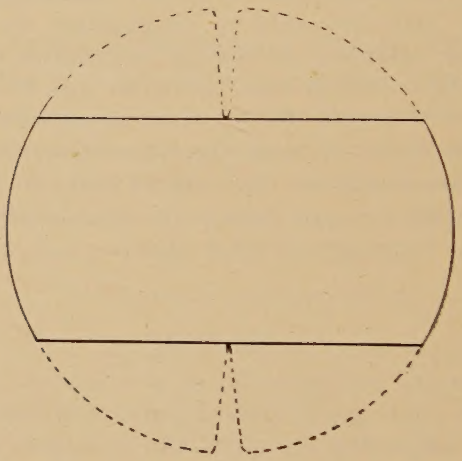

The two transverse edges of the outer closed loop are very nearly arcs of the same circle, so that the rate of growth must be independent of orientation for the range covered by these edges (±30°). It is therefore possible to construct a polar diagram as shown in fig. 3. This diagram coincides with the "razor-blade" outline over the circular arcs at the ends and at the mid points of the longitudinal edges. The dotted sections of the diagram are uncertain, and it is only possible to say, from the present information, that the polar diagram must lie outside these sections.

When two dislocations of the same hand are closer together than a certain distance (equal to 4π times the size of the critical nucleus) the theory predicts that the dislocations will work together cooperatively and produce steps which form two arms of a spiral. Examples of this behaviour have also been observed.

The examples so far quoted are the ideally simple cases and are comparatively seldom observed. More usually a complex layer system is seen on any area of a face, and we shall now consider some characteristic examples.

§3. BEHAVIOUR AT OBSTACLES.

A typical example of the behaviour of a layer system at a surface obstacle is shown in fig. 4 (Pl. XLV.). This layer system is of considerable extent and a small part of it has met with an obstacle to its steady growth, this obstacle being probably a crystal inclusion. The layers are forced to divide into two parts by the obstacle and as they advance towards the right of the figure the obstacle decreases in extent. It is therefore necessary for the layers to " fill in " by inward growth of the straight edges. Due to the fact that growth is more rapid parallel to the c-axis than perpendicular to it, the two sections of the system only unite at some distance beyond the obstacle. The points to be noted are :—

(*a*) The rapid elimination of the re-entrant angle at the junction of the two sections. As the re-entrant is parallel to the direction of rapid growth this would be expected on almost any theory of growth.

(*b*) The relative rate of growth parallel and perpendicular to the c-axis. The ratios of these rates are dependent upon the local conditions, being 1·7 and 2·1 for the two parts of this system, and in other similar cases 2·9 and 2·76, 2·36 and 2·37, 2·1 and 1·9.

(*c*) Each edge is a contour, with a vertical interval of 7·9 Å. The obstacle thus results in a triangular V-shaped valley with a maximum depth of 38 molecules (300 Å).

An obstacle of this kind appears to result in an increased curvature of the edges close to it, but as the effect on the two sections of the system is asymmetrical it is difficult to determine whether the effect is regular.

This difficulty can be overcome in the case of fig. 5 (Pl. XLVI.) in which the layers advancing from the right are split into three sections by a succession of crystal inclusions, which again act as obstacles. The central system formed in this way is affected equally on both sides and it can be immediately seen that it behaves as if a " virtual source " was present.

The approximate position of the virtual source can be found by producing back lines drawn through the points of junction of the curved and straight edges ; it lies on the upper edge of the narrow neck between the two obstacles. The ratio of the radius of curvature of the transverse edges of this small system to their distance from this " source " is constant and equal to unity. Moreover, this relation is still maintained, after junction with the lower section, for those parts of the first four layers of the joint system which originated from the central section. The system expanding from the "virtual source" thus behaves in precisely the same way as the closed loop in fig. 2 (Pl. XLVI.).

The behaviour of layer systems at obstacles provides valuable confirmatory evidence that the observed steps are normally uni-molecular. Thus in fig. 5 (Pl. XLVI.) the central and lower sections first combine again to form a single system. Counting from the last edge before division commences on the right, there are 37 edges in both the lower and central sections before a junction takes place. Similarly, considering the junction beyond the third obstacle there are 57 edges in both the upper and lower sections between the first division of the edge and the first joint edge. Similarly in fig. 4 (Pl. XLV.) in both the upper and lower systems there are 70 edges between the first division of the incident layer and the first joint layer. Such behaviour would be very difficult to comprehend for steps of more than one molecule high, for one would expect the steps in such circumstances either to split into smaller units or to combine to form multiple steps.

Fig. 6.

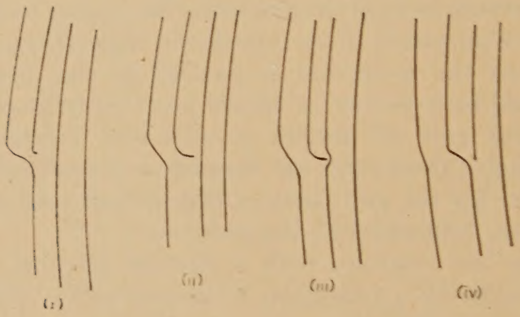

§4. PROPAGATION PAST INACTIVE DISLOCATIONS.

The theory predicted that certain dislocations and dislocation groups on a face could be more active than others, resulting in those active dislocations "dominating" less active dislocations (*i. e.* the layers emanating from active dislocations propagate past "dominated" groups or single dislocations with only a slight delay and a slight change in outline). The mode of propagation in such cases and the type of cross-linking which occurs is shown in fig. 6. The layers are advancing from right to left and in (i) one layer has just passed the dislocation. In (ii) the layer originating from the inactive dislocation has grown in the normal way, while the layer advancing from the right is quite close to it. The kink in the layer on the left is being eliminated as the layer extends. In (iii) the incident layer is being held up at the dislocation, as this layer is now close to the region of deformed lattice around the dislocation, and an effective small repulsion exists between the dislocation and the incident layer. By stage (iv) sufficient molecules have built on to the requisite section of the incident layer, probably because of a statistical fluctuation, to enable the layer to link across with the layer running from the dislocation. The dislocation is consequently attached to the shorter edge, which originally formed part of the incident layer. Meanwhile the kink in the left-hand layer has been almost eliminated. This type of behaviour can be repeated indefinitely.

Fig. 7 (Pl. XLVII.) and fig. 8 (Pl. XLVII.) show two examples of this kind of behaviour from the large number observed. In fig. 7 (Pl. XLVII.) a dominant layer system is advancing from the left and meets with a line of dislocations which are all of the same hand and all the stages of cross linking drawn in fig. 6 can be seen.

Fig. 8 (Pl. XLVII.) illustrates more clearly the kinking of the layers after the dislocations have been left behind, the dominant layer system moving from right to left in this case. In both figures it can be seen that the layers pass on with only very slightly modified outline, and, that some five layers after the dislocations are encountered, the layer outlines show no trace of the action of the dislocation groups.

Fig. 8 (Pl. XLVII.) is also of interest because of the evidence it provides of varying activities of layer systems, a subject which will be dealt with fully in a later paper. On the left of this figure there is a sudden considerable increase in layer spacing. Now layer spacing can most simply be equated against supersaturation, but in a case like this it is not likely that the supersaturation varied over this area. It would rather appear that the widely spaced layers on the left were produced by a dislocation group of low activity, this low degree of activity being due to a low supersaturation or other causes. At a later date in the history of the growth of this face another system has become active (possibly because of an increase in supersaturation, or the creation of new dislocations), producing more closely spaced layers which have gradually obliterated the old layer system, *i. e.* the new system has become the dominant one in this area. Thus the area in fig. 8 (Pl. XLVII.) shows the farthest point of advance of the new system before growth ceased.

§5. LINEAGE STRUCTURES.

It is generally accepted that most crystals consist of a lineage structure, *i. e.* of crystals blocks, sometimes macroscopic, which are slightly disoriented with respect to one another. The atomic structure of the boundaries between such blocks can be explained most satisfactorily in terms of dislocation systems lying in the boundaries, for dislocations necessarily produce a rotation of the lattice at distances far from the dislocation. Such a picture has proved valuable in investigations on grain boundaries in metals, but the evidence in favour of the presence of dislocations which results from such work, is necessarily indirect. On faces of beryl crystals, however, the structure of such boundaries can be observed directly. An example of a well marked lineage boundary is shown in fig. 9 (Pl. XLVIII.). There are some 85 dislocations in the boundary, the left-hand part of which is partially obscured by foreign material, all the dislocations being of the same hand. The distance between dislocations, measured in atomic spacings, is equal to the angle of rotation between the two crystal blocks. In this case the angle of rotation across the boundary is approximately 2·8 minutes of arc.

It is certain that these features consist of a line of dislocations. The layers would not curve round in this way if this feature was merely a surface step, for a considerable body of evidence shows that in all such cases the layer configuration would be quite different. For example, the behaviour at obstacles shown in fig. 4 (Pl. XLV.) and fig. 5 (Pl. XLVI.) can be contrasted with fig. 9 (Pl. XLVI.). Moreover, the layers running from lineage boundaries often terminate on neighbouring dislocations.

The step marking this boundary is very obvious under narrow pencil illumination and this is understandable for, because of the dislocation structure, the higher end of the boundary must project 670 Å. above the central region of fig. 9 (Pl. XLVIII.).

There are many tilt boundaries which are much smaller than the above example. One such case is shown in fig. 10 (Pl. XLV.). From each dislocation of the lower line a spiral edge starts, the straight sections being so closely packed that they are barely resolved. An edge also starts from each dislocation of the upper line, which again is marked as a series of dots, the two systems combining to form a large spiral. (The area blocking out part of the spiral is probably composed of foreign material.) The second, lower, set of straight edges forming the spiral is not parallel to the original set, a very unusual feature. These edges end in an irregular boundary which has been formed by the main growth region. From the position and behaviour of the series of edges above the dislocation system it appears probable that these may originally have formed part of the spiral. The angle of rotation at the two parallel boundaries is approximately 8 seconds of arc in each case.

A very heavily lineaged area is shown in fig. 11 (Pl. XLVIII.). Almost every layer in this figure runs from a lineage boundary, these boundaries lying close together in the lower part of the figure. (The obvious black feature which runs diagonally across the figure is a crack.) The layers are so closely spaced that the longitudinal edges are not resolved. On one side of this lineaged area there are some 140 dislocations of one hand, with some 180 dislocations of opposite hand on the other side. The result of these two groups being almost equal is that the difference in orientation of the lattice on either side of the area will be small, and will in fact amount only to approximately 20 seconds of arc. The actual difference in orientation produced by either group is much greater, being about 2·4 minutes of arc.

The position and nature of these lineages make it possible that they originated in the form of limited slip-zones, a type of feature discussed immediately below. The constituent halves of these zones would grow apart if the dislocation lines were set at a slight angle to each other, so that each half of a zone could eventually act independently as a lineage boundary.

It will be noticed that the examples of lineage boundaries which have been shown are all parallel to the *c*-axis of the crystal. This appears to be true for the majority of such features which have been observed.

§6. LIMITED SLIP-ZONES.

Another type of dislocation distribution very often observed is that corresponding to a limited slip-zone. Such features will be composed of a line of dislocations which is divided about the centre into two equal groups of opposite hand, the line lying along the trace of the appropriate glide plane in the face. A feature of this kind which lies parallel to the *c*-axis is shown in fig. 12 (Pl. XLIX.). This is unusually large and consists of two groups of approximately 90 dislocations each. (Evidence supporting the interpretation of these features as limited slip-zones will be given in a later paper. We are only concerned here with these slip-zones as typical dislocation groups.)

An example of a limited slip-zone perpendicular to the *c*-axis is shown in fig. 13 (Pl. XLIX.). Isolated slip-zones of this orientation are much less common than cases parallel to the *c*-axis. However, a not uncommon feature consists of a number of contiguous small slip-zones which form a long, closely packed line of dislocations perpendicular to the *c*-axis. In fig. 13 (Pl. XLIX.) the dislocation group has been sufficiently active to cause a local variation in the shape of the dominant layer system which is advancing from the left.

§7. PROPAGATION OF LAYERS PAST A DISLOCATION GROUP.

The case of the propagation of layers past dominated dislocations of the same hand has already been discussed. The more general case consists of the propagation of a dominant layer system through an inactive group of dislocations, and there are some significant differences in behaviour in this case.

In fig. 14 (Pl. L.) the dominant system is advancing from the right and meets a group of dislocations which are only sufficiently active to cause local variations in the outline of the layers. Almost all the steps in the bottom part of this figure run between pairs of dislocations and several of the layers tend toward the characteristic razor-blade shape.

Several steps in this group have a reversed S-shape. Such behaviour is not contrary to the theory but, as we shall see, is merely due to the dominant characteristics of the incident system. For example, a very acute elbow runs from a single dislocation in the upper part of the figure. It is obvious that this edge, which originally curved downwards, must form a re-entrant of this type on junction with the incident layers. Moreover, this re-entrant cannot be rapidly eliminated as it lies in the direction corresponding to a minimum growth rate.

In order to illustrate some of the points which arise a part of the dislocation group is isolated and drawn in full line in fig. 15 (i). It is necessary to consider a limited area only in order to simplify the actual

Fig. 15 (i).

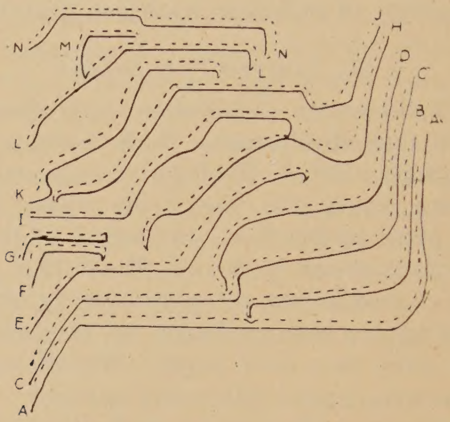

Fig. 15 (ii).

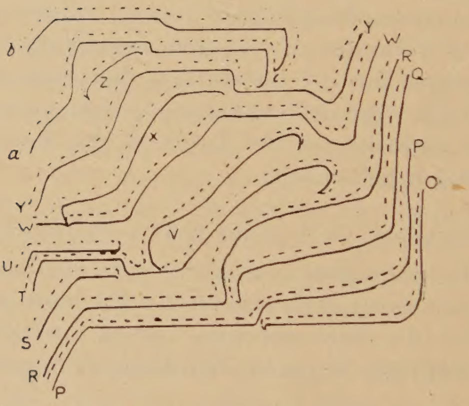

Fig. 15 (iii).

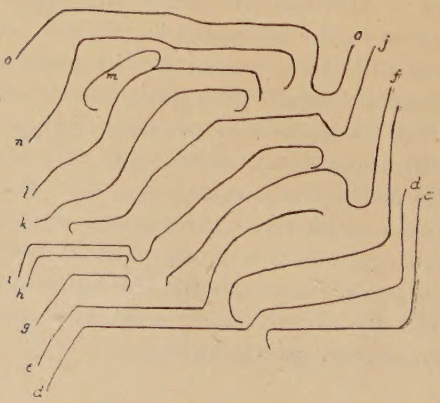

behaviour. Thus, the curved edges running down on the left of fig. 14 (Pl. L.) terminate at dislocations which are all of one hand. These terminations have not been shown in order to keep the diagrams down to a reasonable size, and also because only a simple type of cross linking takes place in this area. Hence, over the area shown in fig. 15, these curved edges can be considered to propagate regularly without any considerable deviation from the true conditions.

In these diagrams the propagation of the layers has not been drawn exactly to scale but only approximately so. This means that deviations from the order of events shown in these diagrams might have occurred had the crystal continued to grow, but the aim is to show the general way in which propagation by cross-linking takes place.

In (i), (ii) and (iii) five successive positions of the layers are shown. The advance of the layers from their original position in any of these diagrams is shown by a dotted line, and the position of layer I, for example, after an advance will be referred to as I′.

Let us consider the position of the layers in fig. 15 (i) after a slight advance has taken place. A′ is held up at the parent dislocation of B′, and cross-linking will soon take place. Similarly, C′ is now very close to the dislocation of D′. E′ and F′ show no important change (G′ is growing normally, but G was initially of an anomolous shape due to causes to be discussed in a later paper). The advance of H has caused cross-linking to take place with I, so that the joint layer I′H′ and a new double dislocation loop are formed. J′ and K′ show little change, but L and M have cross-linked to form the layer L′M′ and a double dislocation loop L′ has been formed. A further stage of advance of these layers is shown in full line in (ii). The lowest four layers have now cross-linked to give O and P and Q and R, R continuing with a considerable kink because of the cross-linking. E′ has cross-linked with F′ to give S and the layer T which is held up at the lower dislocation of the loop V. J′ has linked with K′ to form the double dislocation loop X, and cross-linking of this loop with W is imminent. No marked change has taken place in the other layers.

Another advance immediately causes T to cross-link with the double loop V, so that a dislocation is now attached to the right-hand section of T, and the layer T′U′ carries on with an obvious re-entrant. W and X have linked so that the two dislocations of the loop X now function separately. Y and *a* have linked so that the left-hand part of Y′ is attached to a dislocation. Meanwhile the joint layer *a*′Y′ almost immediately links with *b*′ so that *a*′ is again attached to a dislocation, while the joint layer *b*′Y′ passes on with a large re-entrant due to the rapid cross-linkings. The edge *b*′Y′ being nowhere attached to a dislocation (in this figure at least), is thus the first layer to pass through this group.

The position after a final advance is shown in fig. 15 (iii). O′, P′, Q′ have advanced undisturbed to the positions *c*, *d* and *e*. (In fact, of course, another layer would by now have advanced from below to cross-link with *c*.) R′ has linked with the double loop T′, leaving the two dislocations attached to the layers *e* and *f*. T′ has linked with U′ to give the layers L and *i*. Layer L is held up by one of the dislocations of the loop *m* and linking is about to take place. Otherwise there is no considerable change.

This group of dislocations which has been studied is both small and comparatively widely spaced. In the case of many of the larger closely packed groups it is obvious that the general outline of the layers will be complicated and varying very rapidly, so that any one layer in its passage through the group must very soon lose any semblance of composition from its original layer and will undergo a great many changes in outline.

It can be seen from fig. 15 (i) and (iii) that the original and final positions of the layers are similar. This would be more marked if the original position of the layers did not show certain slight anomalies explicable in terms other that growth. A certain periodicity is bound to occur if the conditions remain uniform, and if the incident edges advance in a regular way, a cycle of quite short period should result. Normally the conditions may fluctuate sufficiently to prevent the establishment of such a cycle, although a semi-periodic behaviour should result.

Fig. 15 shows that when dislocations, whatever their hand, are spaced with one or more layers between them, only a considerable kinking of the layer edges is likely to result. However, when successive layers run from dislocations of opposite hand, a succession of double-dislocation loops and single dislocation layers must be formed very rapidly. If a considerable number of such dislocations of opposite hand lie together, then a complicated pattern of looping and linking must ensue as any one layer progresses through the system.

§8. ADDITIONAL EVIDENCE OF THE DEPENDENCE OF GROWTH RATE ON ORIENTATION.

In fig. 16 (Pl. L.) a dominant system is advancing from the left when it meets a barrier formed by a closely spaced line of dislocations. The main system is forced to spread downwards from the upper limit of this barrier, until it meets the independent layer system running from the dislocations. At the junction between the two systems a slightly curving edge results which runs at a slight angle to the *c*-axis and continually encroaches on the curved edges of the upper system. This encroachment continues until the slightly curved edges spread across to make a junction with the straight longitudinal edges (see fig. 17 (Pl. LI.)) and so completely eliminate the curved edges. At this point the edges are slightly concave in curvature and make an angle of approximately 25° with the *c*-axis.

This junction continues for some 5 mms. along the face (*i. e.* some 1,000 layers) and the edges gradually become straighter and progressively less inclined to the *c*-axis. A locally dominant system then altered the conditions, and these edges were replaced by the normal type of curved edges. The general conclusion to be drawn from this behaviour appears to be that edges inclined at small angles to the *c*-axis can grow more rapidly than the normal curved edges. This conclusion is supported by observations of other similar events which gave a total range of inclinations of these rapidly growing edges of 4°–25°. It is therefore possible to make additions to the polar diagram shown in fig. 3 to produce the more complete diagram, fig. 18. The dotted lines still indicate the uncertain sections. It should be noted that these polar diagrams are only strictly applicable to other beryl crystals if they have grown in identical conditions. Considerable variations are observed in the proportions of these diagrams, but the shape is usually of the same kind. However, examples have been observed when even the shape is quite different.

Fig. 18.

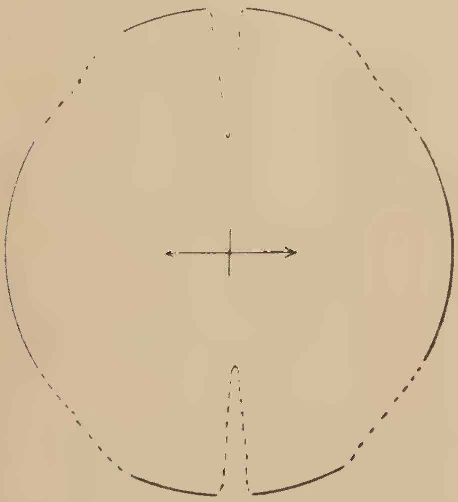

§9. SYNTHETIC EMERALD.

In addition to naturally occurring beryl crystals originating from various sources, two synthetic emeralds were examined. These crystals had been grown by Nacken by a hydrothermal process (Van Praagh 1948), the details of which have not been revealed. The faces of both crystals were very rough on a microscopic scale and a regular structure could only be detected on some of the faces. In all cases the surfaces were too irregular to allow very fine structure to be observed.

All the faces suitable for observation showed a number of very similar hills standing out above the surface. A typical feature of this kind as seen under oblique illumination is shown in fig. 19 (Pl. LI.). All the steps appear to be multi-molecular and the hill builds up to a definite point, the inference being that one central group of dislocations has been responsible for the growth of the hill.

This type of behaviour can be contrasted with the typical plateaus seen on natural crystals, as shown for example, in figs. 20 and 21 (Pl. LII.). These plateaus stand some wavelengths above the general surface level, but they still retain the typical shape characteristic of a simple unimolecular layer as shown in fig. 2 (Pl. XLVI.). The main plateaus of these figures are very flat, very few uni-molecular steps being visible. The single spiral shown in fig. 1 (Pl. XLV.) lies on the plateau of fig. 20 (Pl. L.) and its position can be identified by the gross black feature. This appeared to be one of the very few dislocations active on this plateau.

The two other main points of difference between the structures on natural and synthetic crystals are :—

(i.) The differing shapes of the layers. The longitudinal edges on the synthetic crystal have a considerable curvature; the significance of this point is discussed below.

Fig. 22.

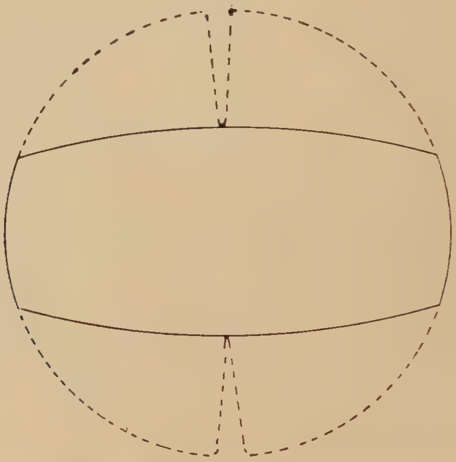

(ii.) The presence of a rough structure on the transverse gradients of the natural crystals. This rough structure actually consists of close-packed "rods"—features which will be fully discussed in a later paper. It need only be said that they invariably occur on steep gradients parallel to the c-axis on the natural crystals studied. No trace of such features was observed on the synthetic crystals.

It is possible to construct a polar diagram of growth rate for these synthetic crystals. The transverse edges are again almost arcs of the same circle, so that the growth rate must be independent of orientation over a range of $\pm 20°$. The polar diagram is shown in fig. 22 where the dotted lines again indicate uncertain areas.

§ 10. APPLICATION OF DISLOCATION THEORY OF GROWTH.

The theory predicts that for directions not far removed from a close-packed direction an edge will have a radius of curvature $(1+2\mathrm{B})$ times its distance from the point of origin, where $\mathrm{B}=\frac{1}{8}\exp(\phi/k\mathrm{T})$ and ϕ is a neighbour-neighbour interaction energy. The radius of curvature of the almost straight edges of the outer loop of fig. 2 (Pl. XLVI.) is some 120 times the distance from the centre. Therefore $\phi/k\mathrm{T}$ is about 6·2.

The average values of these constants for the two synthetic emeralds examined were :—

	B	$\phi/k\mathrm{T}$
Specimen 1	3·83	3·42
Specimen 2	3·71	3·39

These values are very similar and it appears probable that both specimens have grown in almost identical conditions. If one assumes that both the natural and synthetic crystals have grown from similar media then the differing values of $\phi/k\mathrm{T}$ can be ascribed to variations in T, and the natural crystal must have grown at an absolute temperature of a little more than half that of the synthetic crystals. The value of Nacken's operating temperature is not known, but it was probably close to the critical temperature of water. The natural crystal must therefore have grown at a temperature of approximately 80° C. This may appear surprisingly low, but it is of interest to note that the temperature of growth of a beryl crystal found in a pegmatite vein was 175° C., as determined by a liquid inclusion method (Ingersoll 1947). Moreover, the temperature of 80° C. can probably be taken as the lower limit, for the values of B were determined from measurements on multi-molecular steps, and such steps usually give results which are inaccurate unless one concludes that the values of B are greater than would hold for uni-molecular steps.

It is possible to estimate the size of the critical nucleus (ρ_c) by measurement of the distance between two dislocations of opposite hand which are linked by an edge which has been expanding outwards. The distance between the dislocations must be equal to, or greater than, $4\pi\rho_c$ where ρ_c is defined by $\rho_c = a\phi/k\mathrm{T}\sigma$, where a is the inter-atomic spacing and σ is the supersaturation. Knowing the value of $\phi/k\mathrm{T}$ we can deduce from fig. 2 (Pl. XLVI.) that the supersaturation in this area was about 0·5 per cent.

The accuracy with which the supersaturation in any area can be determined will always be dependent on the presence of two dislocations with a spacing of just $4\pi\rho_c$. This means that the closest spacing should be taken as giving the most accurate value, but it is sometimes difficult to be sure whether a given edge has been expanding. As an example there are tabulated a number of observations on another face of the crystal on which fig. 2 (Pl. XLVI.) was taken. In this case an asterisk denotes loops which may possibly not have been expanding.

From this table it would seem that the loops corresponding to values of 0·29 and 0·35 microns had not been expanding. Neglecting these two values and the rather high final value, the average value of ρ_c over this region of the face was probably quite close to 0·49 microns. Taking $\phi/k\mathrm{T}=6{\cdot}2$ this is equivalent to an average supersaturation of about 1 per cent.

Area	ρ_c (microns)
Active group	0·5 0·35*
Groups of fig. 13..................	0·46 0·41*
Centre of very large dominant group	0·55 0·29*
—	0·75

§11. CONCLUSIONS.

The observations show that the dislocation theory of growth is not only correct in principle, but also in detail. This is the more surprising when it is recalled that this theory was derived primarily for homopolar crystals, formed from spherical or cubic molecules, growing from the vapour phase. In this case beryl is an ionic crystal with complex molecules and growth has taken place from solution.

The dislocation theory of growth provides, for the first time, a quantitative account of crystal growth, and it is possible to learn a good deal about the conditions under which any crystal has grown from simple measusements on the faces. This theory also marks a considerable advance in the unification of growth phenomena and modern theories of the solid state, two fields which had previously been largely divorced.

Lineage and transition surfaces have been explained for some time in terms of dislocation theory as arrays and grids of dislocations. The observations provide direct visual evidence that this explanation is correct.

ACKNOWLEDGMENTS.

I am indebted to Dr. F. C. Frank for much valuable discussion; to the Mineralogy Department, British Museum, for the loan of specimens; to Dr. G. Van Praagh for the loan of synthetic beryl crystals; and to the Department of Scientific and Industrial Research for grants which have made this work possible.

REFERENCES.

BURTON, W. K., and CABRERA, N., 1949, Discussions, *Farad. Soc.*, **5**, 33.
BURTON, W. K., CABRERA, N., and FRANK, F. C., 1951, *Phil. Trans. Roy. Soc.*, **243**, 299.
FRANK, F. C., 1950, *Phil. Mag.*, **41**, 200.
GRIFFIN, L. J., 1950, *Phil. Mag.*, **41**, 196.
GRIFFIN, L. J., 1951, *Ibid.*, **42**, 775.
INGERSOLL, E., 1947, *Am. Min.*, **32**, 375.
VAN PRAAGH, G., 1948, Research, **1**, 458.

EXPLANATION OF THE PLATES.

Plate XLV.

Fig. 1.

The dislocation lies at the origin of the spiral. The kink in the right-hand edge of the spiral has possibly been caused by impurity obstructing steady growth.

Fig. 10.

The black area at the top is a hole in the crystal surface. The two boundaries lie a little down from this. This is a case where resolution has to be sacrificed to visibility.

Plate XLVI.

Fig. 2.

The inner step-line runs between two dislocations of opposite hand, the points of emergence of these dislocations being imaged as obvious black dots.

Plate XLVII.

Fig. 7.

The line of inactive dislocations lies close to the centre of the figure, and its presence is made noticeable by the kinking of the edges close to it. The dislocations are shown as black dots. In the top part of the figure the layer edges are running parallel to the *c*-axis, but are too closely spaced to be resolved.

Fig. 8.

The dark band at the bottom marks the edge of the face. The line of dislocations starts near the centre of the edge and from there runs upward and slightly to the right, almost to the top.

Plate XLVIII.

Fig. 9.

The lineage boundary runs from left to right just below the centre, its left-hand extremity being partially obscured. To the left of the mid-point of the boundary the step-lines become much more closely spaced and less clearly visible, while the corresponding longitudinal sections are too closely packed to be resolved.

Fig. 11.

The position of the different boundaries can be most easily found by following the downward path of the curved edges. There are at least six boundaries, all situated in the lower central part of this area.

Plate XLIX.

Fig. 12.

The slip-zone is the line running horizontally from which all the curved edges commence.

Fig. 13.

The dislocations are quite widely spaced along this slip-zone which runs vertically upwards to the left of centre. Most of the layers to the right of this line run between pairs of dislocations of opposite hand.

PLATE L.

Fig. 14.

The black band at the bottom marks the edge of the face. The inactive group lies centrally in the lower two-thirds of this area.

Fig. 16.

The closely spaced line of dislocations runs vertically upwards on the left of this area; individual dislocations cannot be distinguished at this magnification. The edges at an angle to the *c*-axis form at the junction of the two systems a little to the left and down from the centre of the figure.

PLATE LI.

Fig. 17.

The orientation is, as usual, given by straight edges which are barely resolved in the upper third of this area. The system which is being eliminated lies on the left and the rapidly growing layers are seen on the right.

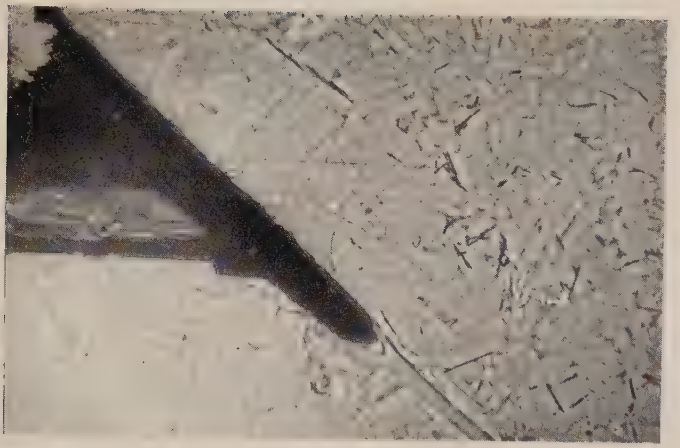

Fig. 1.

×280

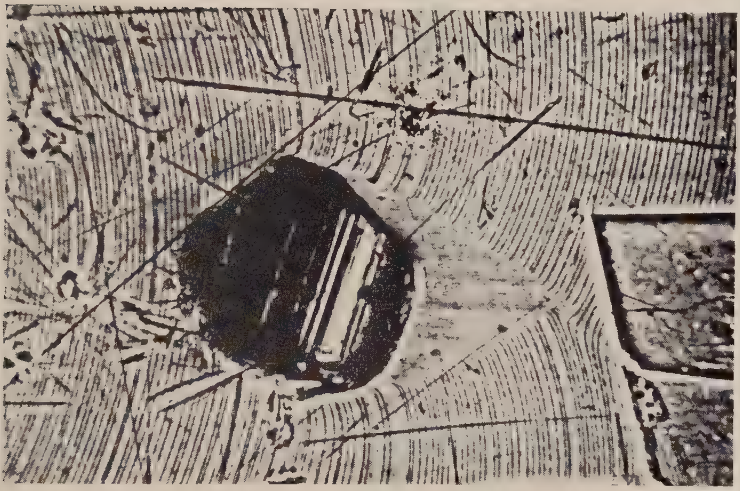

Fig. 4.

×400

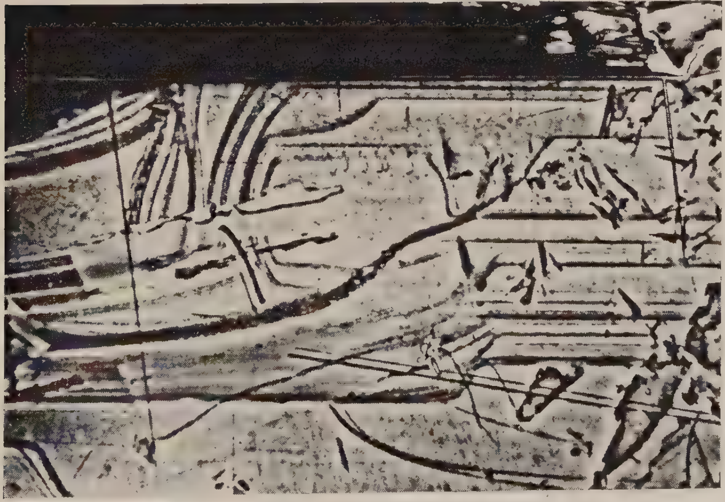

Fig. 10.

×400

To face page 1352

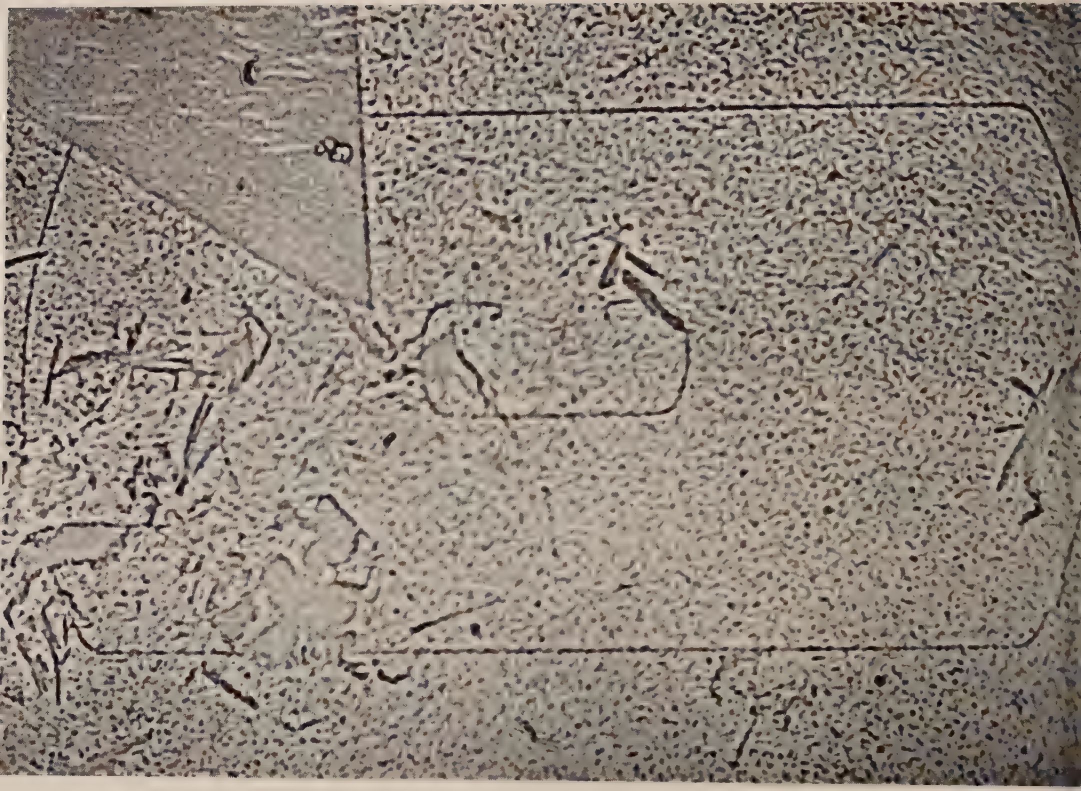

Fig. 2. ×1

Fig. 5. ×650

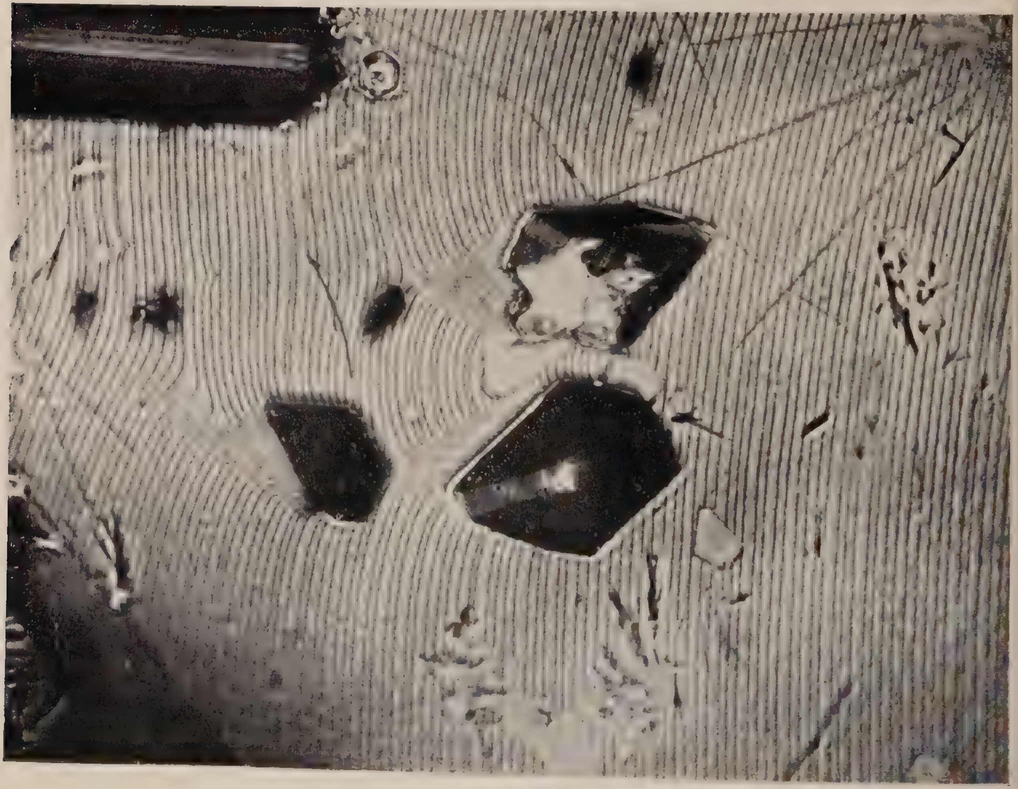

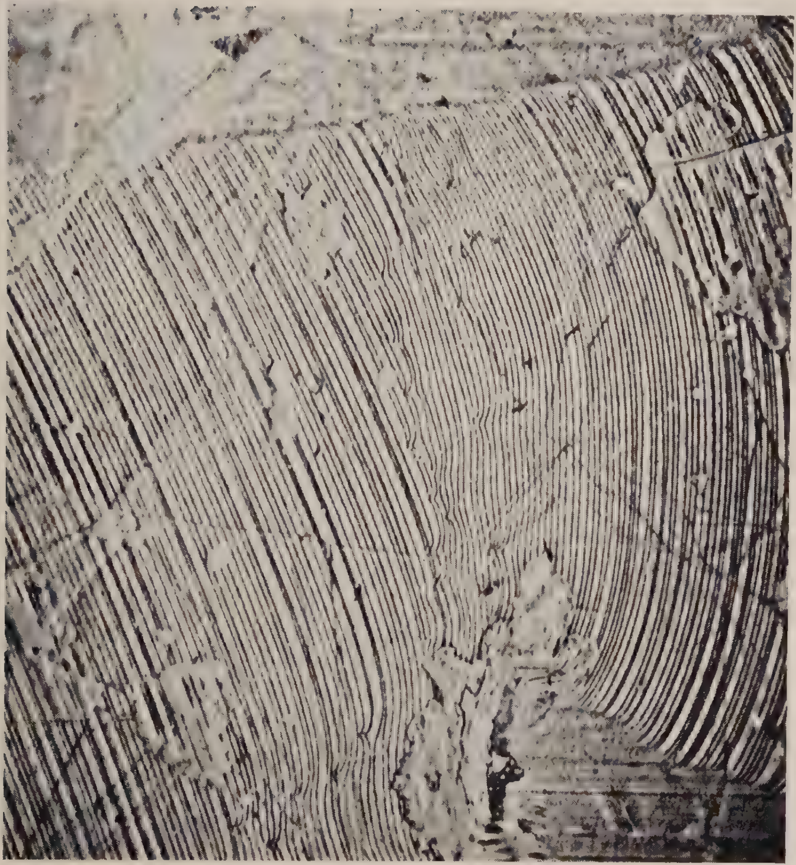

Fig. 7. ×650

×400

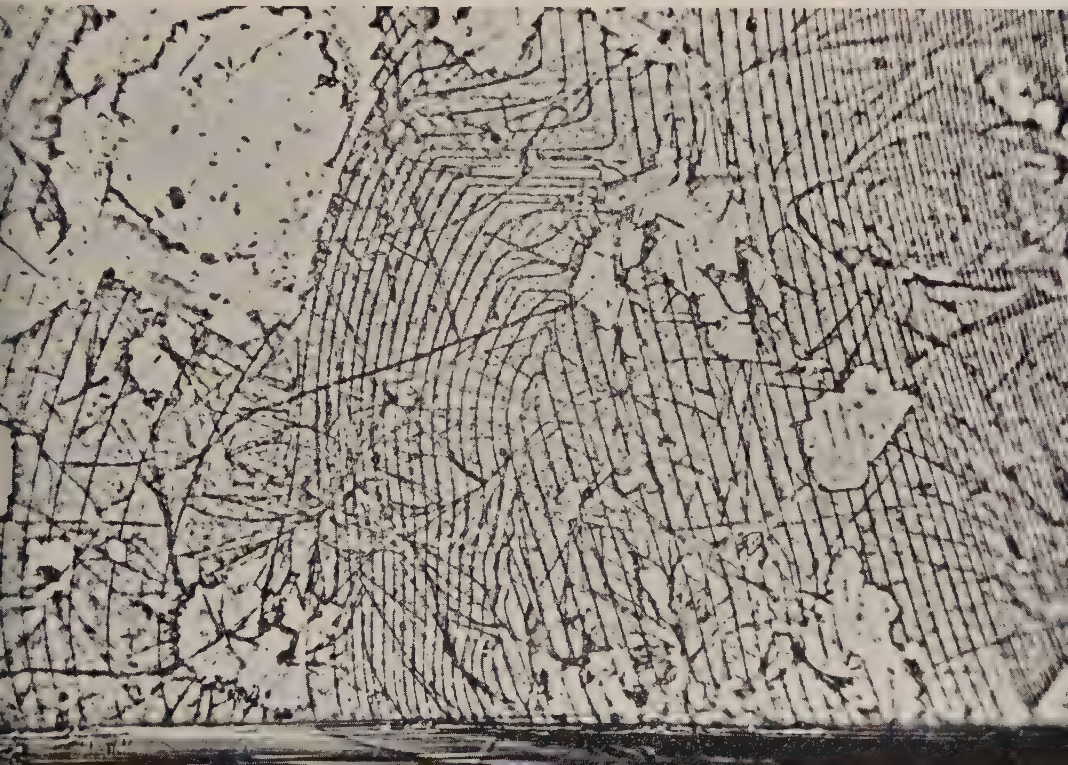

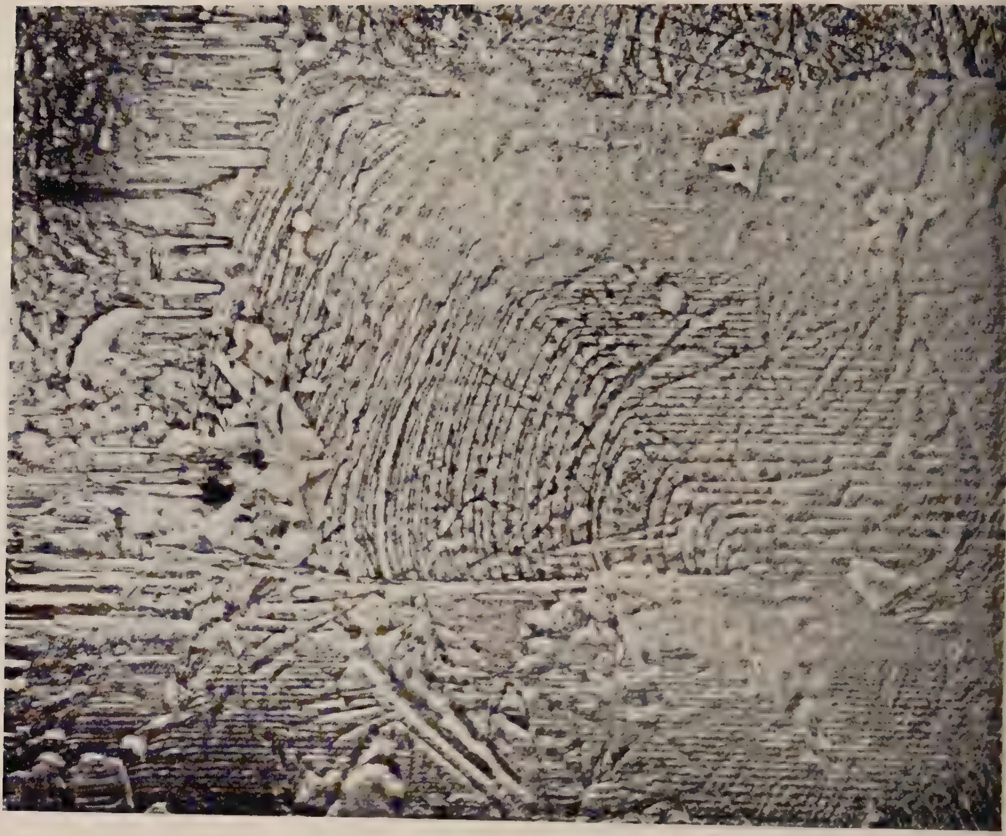

Fig. 9. ×650

Fig. 11. ×250

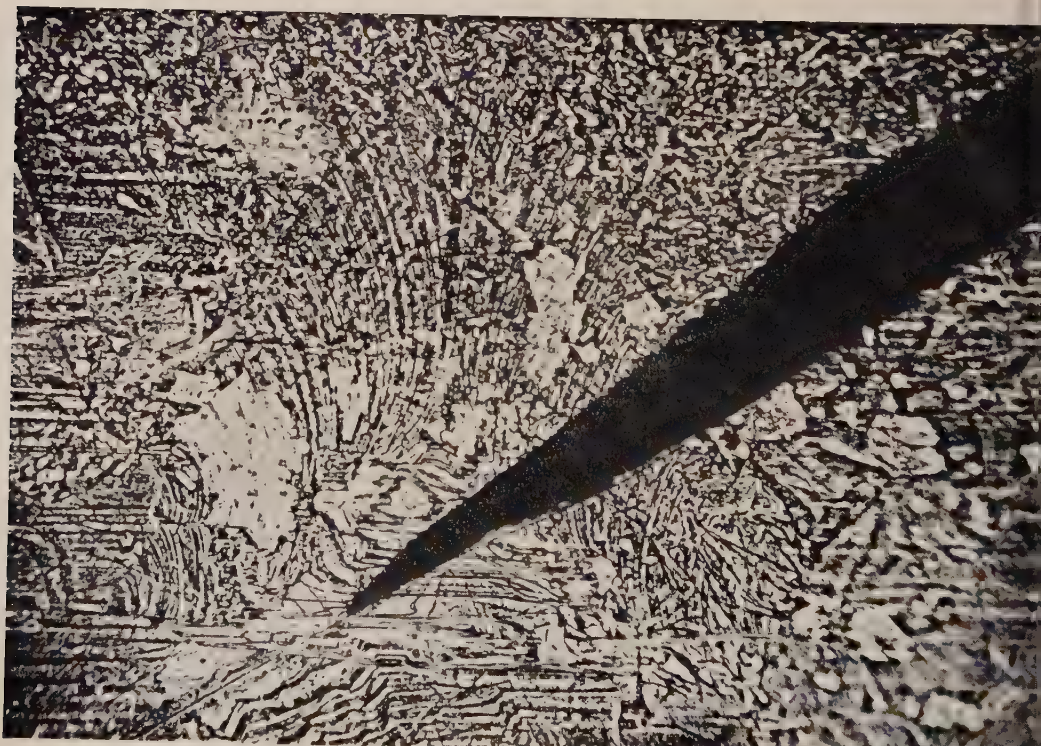

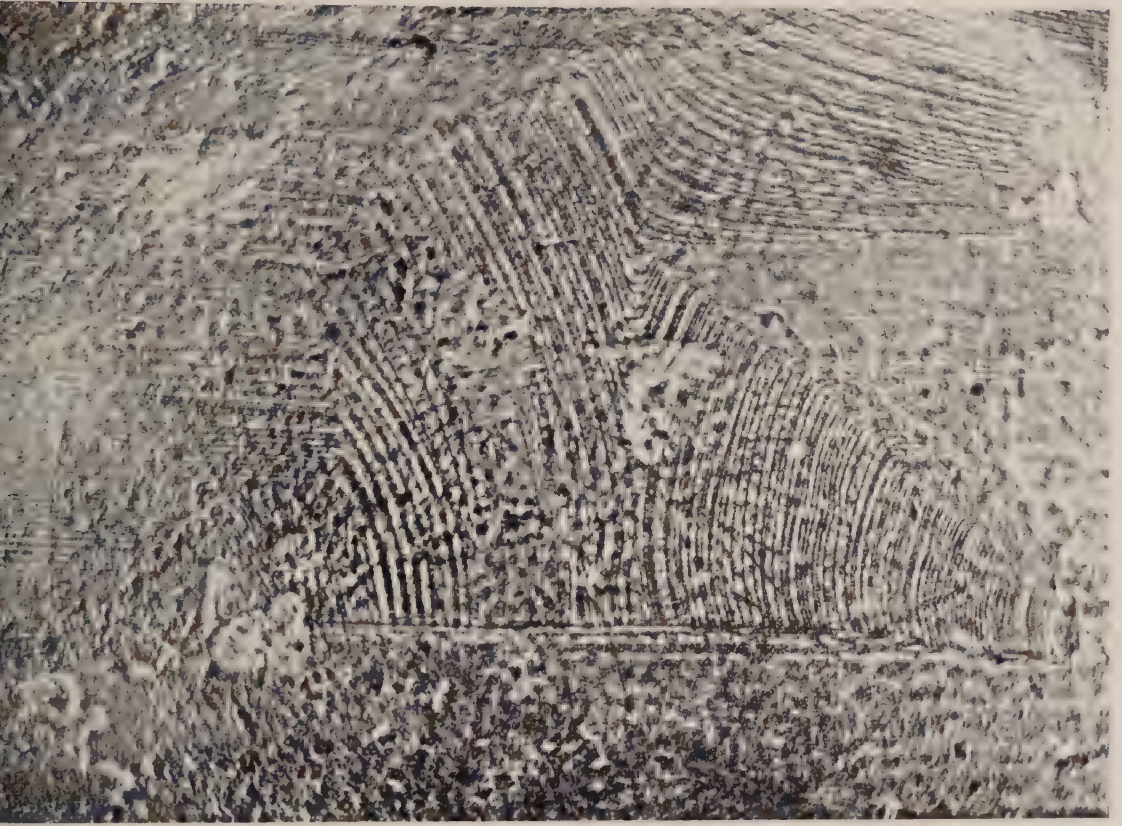

Fig. 12. ×650

Fig. 13. ×650

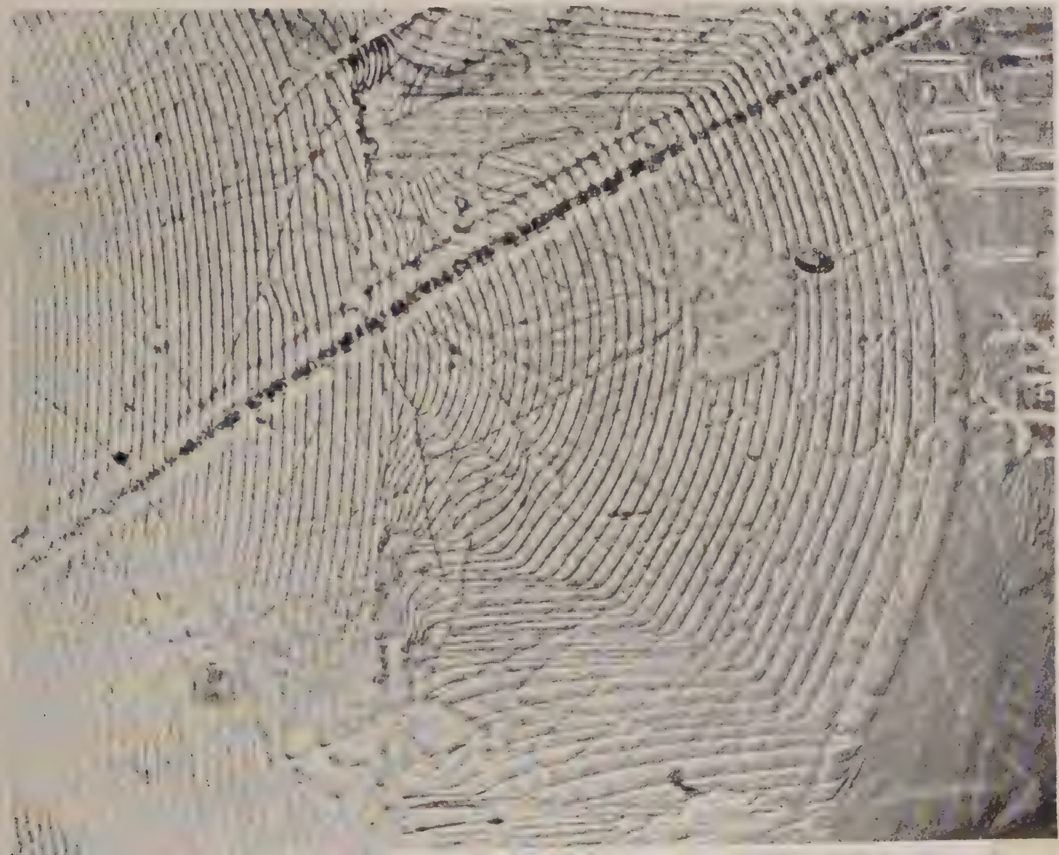

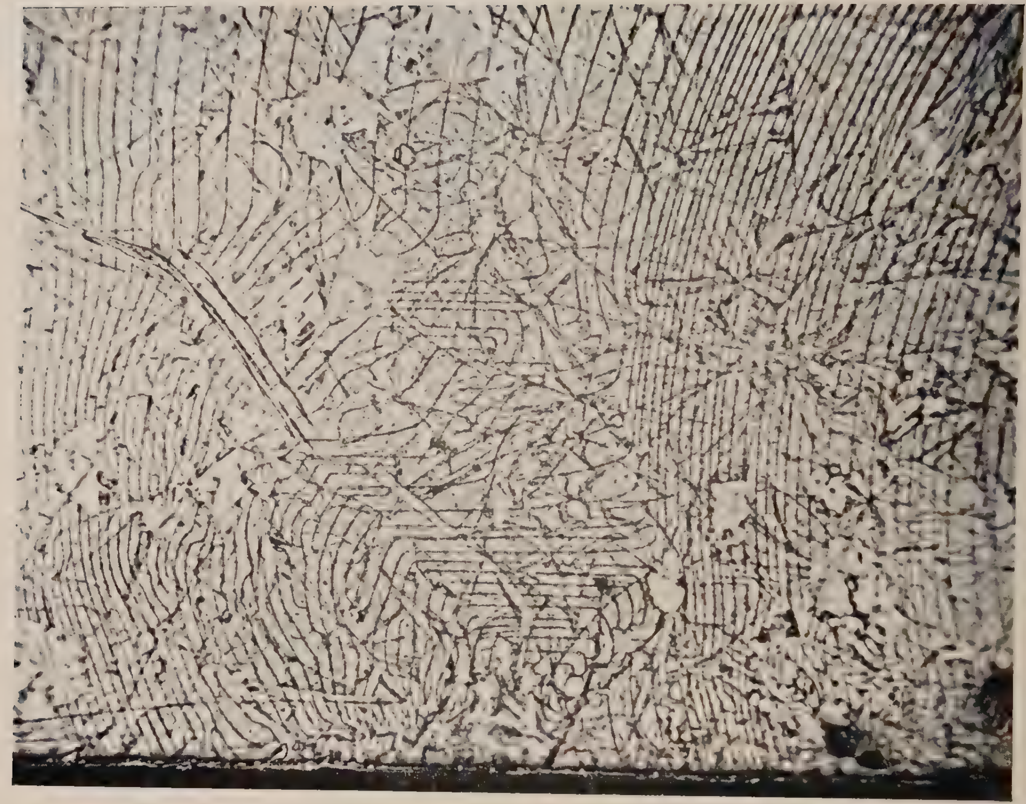

Fig. 14. ×312

Fig. 16. ×250

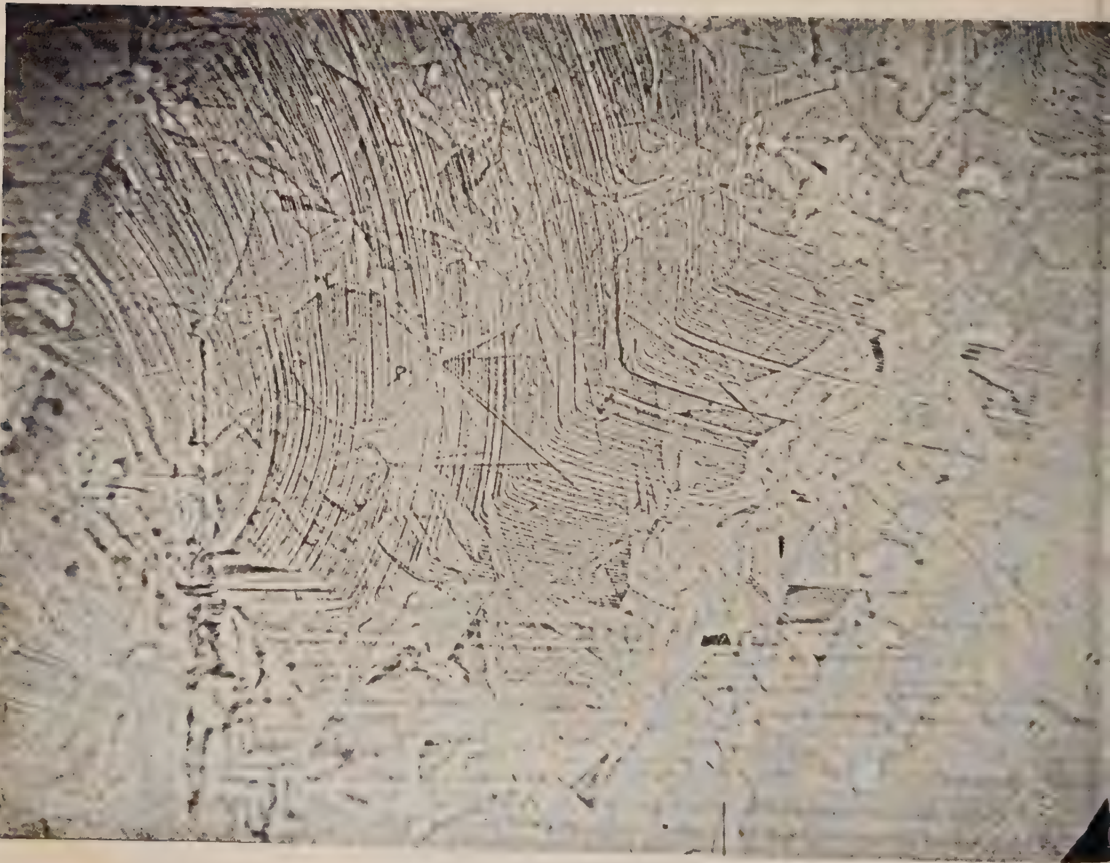

Fig. 17.

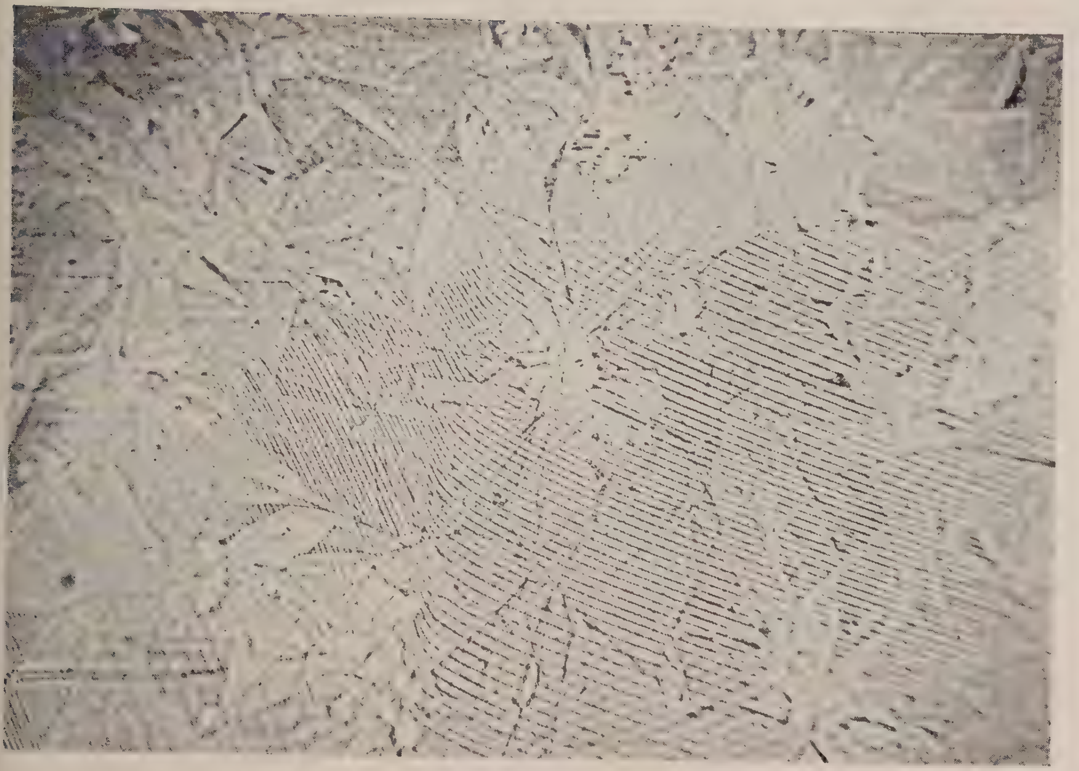

×250

Fig. 19.

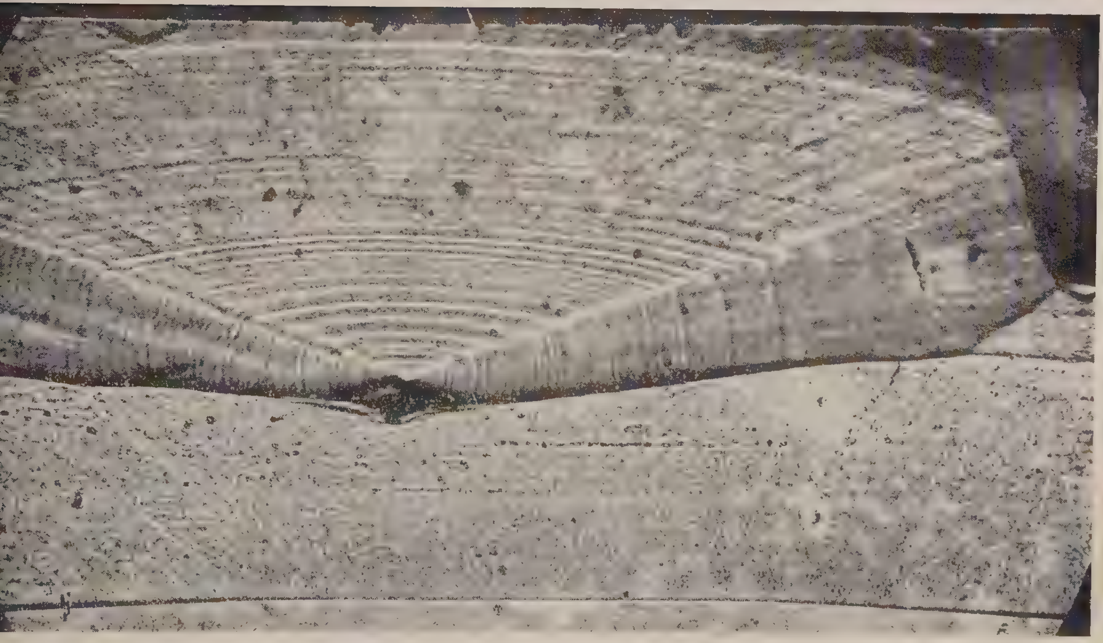

×120

Fig. 20.

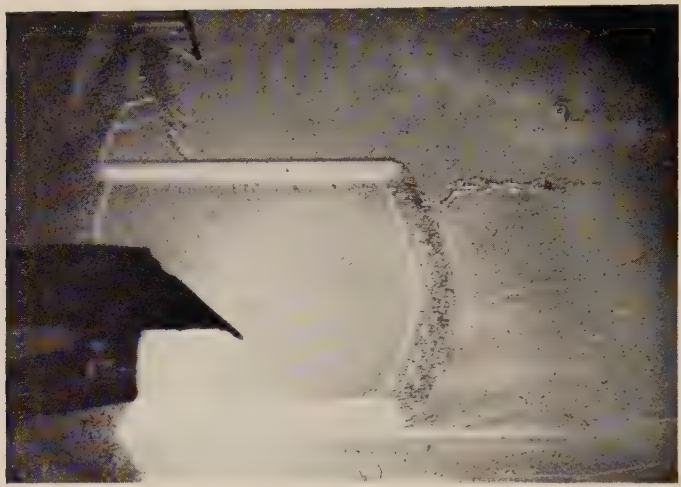

×44

Fig. 21.

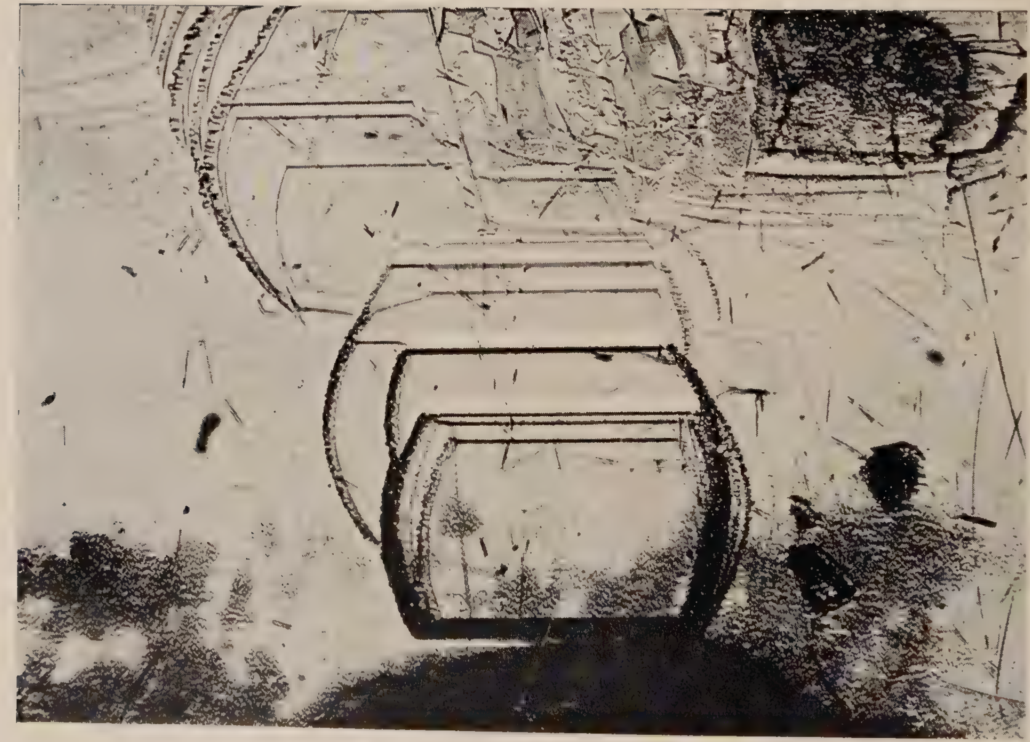

×36

CXXXIV. *The Photo-electric Disintegration of Three- and Four-Particle Nuclei.*

By J. C. Gunn and J. Irving,
Department of Natural Philosophy, University of Glasgow*.

[Received June 12, 1951.]

Abstract.

The two-particle and complete photo-electric disintegration cross-sections for three- and four-particle nuclei are calculated, using Gaussian and new exponential wave-functions. By suitable adjustment of a scale constant photo-disintegration, curves can be found with the maximum cross-section at any chosen energy above the threshold. For a given position of the maximum the Gaussian wave functions require a bigger nucleus than the exponential, and then give a larger maximum cross-section. The theoretical predictions are concerned with the small amount of experimental data available, mainly from the inverse processes of p-D and p-T capture. The exponential wave functions appear to fit more reasonably with this evidence.

§ 1. Introduction.

Since the detailed study of the deuteron and two-nucleon scattering data has not yet yielded a satisfactory nuclear interaction, it is of interest to investigate further nuclear problems involving more than two nucleons so that the adequacy or inadequacy of the proposed two-body interaction for such problems may be demonstrated. The n-D and p-D scattering problems have already been investigated by Buckingham, Burhop and Massey (1941, 1948) with various forms of the two-body interaction, using the resonating group structure method, first introduced by Wheeler. Comparison with experiment should then indicate the best form of the interaction. These authors also deduced the photo-electric disintegration cross-section of tritium into a neutron and deuteron. Their method, however, while neglecting the polarization of the deuteron, involves a great deal of computation. The object of the present investigation was to see how far an account could be given of the three- and four-body photo-disintegration problems with the use of simple analytical wave functions. Verde (1950) has treated the photo-disintegration of the three-particle system with Gaussian wave functions in an elementary manner. While the present work was in progress there has also appeared a discussion of the He^4 photo-disintegration, using Gaussian wave functions, by Flowers and Mandl (1951).

---

* Communicated by the Authors.

In this paper the photo-electric disintegration of both three- and four-particle systems is considered, attention being limited to electric dipole transitions. The treatment is crude in the sense that the final states of the systems are taken to be plane waves. Equally, for the initial tritium and helium nuclei, only the space symmetric part of the wave function is considered. The calculations, however, indicate the great sensitivity of the cross-sections to the value of the parameters occurring in the wave functions of the initial states. Cross-sections for inverse processes are calculated by the method of detailed balance.

Calculations were first carried out with Gaussian wave functions at about the same time as those of Verde. Since the Gaussian wave function has an incorrect asymptotic behaviour, it seemed worthwhile to investigate the effect of a wave function with a better behaviour in this respect. The wave functions worked out by Svartholm (1945), using the variation-iteration method, were found to be rather complicated to handle in photo-disintegration calculations, as also were wave functions of the form $\exp\{-\alpha(r_{12}+r_{13}+\ .\ .\ .)\}$ which have been used by a number of authors in binding energy calculations, for example, Fröhlich *et al.* (1947). The new wave functions, used by Irving (1951) for calculations of the binding energies of three- and four-particle systems, however, were found to lead to fairly simple analysis in the calculation of photo-electric disintegration cross-sections. Detailed calculations have been carried out for these wave functions and the results compared with those for Gaussian wave functions. The theoretical results are compared with the experimental data from p-D capture by Fowler *et al.* (1949) and p-T capture by Argo *et al.* (1950)*. If the parameters appearing in the wave functions are determined by variational calculations of the binding energies of three- and four-particle systems, very low values for the cross-sections are obtained. One reason for this is that the variational calculations of the binding energies with a central two-body interaction are incorrect and lead to values of the variation parameter which, in the case of the new wave functions, concentrate the nucleus too much. Calculations of the binding energies, when a mixture of central and tensor forces is used, indicate that more reasonable values of the variation parameters are then obtained.

It is to be hoped that when detailed experimental evidence of p-D and p-T capture cross-sections—or, alternatively, the inverse processes—is available, the theoretical formulae arising from the exponential wave functions may be found to give the correct variation of the cross-section with energy. In fact, if the parameter can then be chosen to give the correct magnitude for the cross-section, thus determining the " size " of the nucleus, the value obtained should agree with the value calculated by a variational method which takes into account non-central forces. A characteristic difference between the exponential and Gaussian wave functions may be mentioned here. This is that the exponential wave functions, for a given "size" of nucleus, lead to an earlier maximum cross-section, than the Gaussian. For a given position of the maximum above the threshold the magnitude of the cross-section is smaller with the exponential wave functions.

---

* Experiments with the Glasgow 30 MeV. Synchrotron have demonstrated the γ -p process with He^4, but are not yet complete (private communication from J. R. Atkinson). Preliminary measurements with the G.E.C. betatron (Gaertner and Yeater) on the same process indicate an integrated yield of 4×10^{-26} cm.^{2} MeV. with mean quantum energy about 27 MeV. We are very grateful to these authors for a report of their results.

§ 2. GENERAL FORMALISM.

As we intend to deal in this paper with the photo-disintegration of both three- and four-particle systems, it seems worthwhile first to summarize the general formalism applicable to the photo-disintegration of a system of A particles of equal mass. It is in the first place convenient to separate the motion of the mass-centre by the change to the coordinates

$$\mathbf{R}=\frac{1}{\mathrm{A}}\sum_{j=1}^{\mathrm{A}}\mathbf{r}_j\,, \qquad \ldots \ldots \ldots \qquad (1)$$

$$\mathbf{r}_{1j}=\mathbf{r}_j-\mathbf{r}_1, \quad j\neq 1$$

where $\mathbf{r}_j$ denotes the coordinates of the A particles. In the problem chiefly considered in this paper one of the particles only is ejected, say, particle 1 ; a suitable set of coordinates is then

$$\left.\begin{aligned}\boldsymbol{\rho}_1&=\mathbf{r}_1-\mathbf{R}'=-\frac{1}{(\mathrm{A}-1)}\sum_{2}^{\mathrm{A}}\mathbf{r}_{1j}\\ \mathbf{R}'&=\frac{1}{(\mathrm{A}-1)}\sum_{j=2}^{\mathrm{A}}\mathbf{r}_j=\mathbf{R}+\frac{1}{\mathrm{A}(\mathrm{A}-1)}\sum_{2}^{\mathrm{A}}\mathbf{r}_{1j}\\ \mathbf{r}_{2m}&=\mathbf{r}_{1m}-\mathbf{r}_{12}, \quad m=3,4\ldots\mathrm{A}.\end{aligned}\right\} \quad \ldots \quad (2)$$

It may easily be verified that the Jacobian of each of these transformations has unit modulus. The second set of coordinates corresponds physically with the mass-centre and relative coordinates of the residual nucleus of (A—1) nucleons, together with the coordinates relative to this mass-centre of the ejected nucleon.

The wave function of the initial motion may be taken in the form

$$\Psi_i=u_i(\mathbf{r}_{1j})\exp i(\mathbf{P}_0\,.\,\mathbf{R})$$

and similarly for the final state

$$\Psi_f=u_f(\mathbf{r}_{2m})\exp i(\mathbf{p}\,.\,\mathbf{r}_1+\mathbf{P}'\,.\,\mathbf{R}').$$

These wave functions will in general have to be given the right spin, isotopic spin and symmetry properties. It is most simple, however, to consider these for individual cases. We shall, in this investigation, limit consideration to electric dipole transitions for which the matrix element reduces to the form

$$\int u_f^*(\mathbf{r}_{2m})\exp\{-i(\mathbf{p}\,.\,\boldsymbol{\rho}_1)\}\left\{\sum_{i=1}^{\mathrm{A}}\tau_i(\mathbf{r}_i-\mathbf{R})\,.\,\mathbf{E}_0\right\}u_i(r_{1j})\,d\boldsymbol{\rho}_1\,d\mathbf{r}_{2m}.$$

Here τ_i is the usual isotopic variable, $\mathbf{E}_0$ represents the electric field vector at, say, the mass centre of the system, and the integral corresponding with overall momentum conservation has been removed. The probability per unit time of disintegration into a group of final states F by a quantum of energy k, with its polarization vector along the z-axis, is

$$w=4\pi^2ke^2\left|\int u_f^*(\mathbf{r}_{2m})\exp(-i\mathbf{p}\,.\,\boldsymbol{\rho}_1)\left\{\sum_{i=1}^{\mathrm{A}}\tau_i(\mathbf{r}_i-\mathbf{R})_z\right\}u_i(r_{1j})\,d\boldsymbol{\rho}_1\,d\mathbf{r}_{2m}\right|^2\rho(\mathrm{E_F}). \quad . \quad . \quad . \quad (3)$$

Here $\rho(\mathrm{E_F})$ is the density of the final states per unit energy interval, and the necessary averaging over the initial nucleon spin states, and sum over the final spin states must be carried out. Natural units $\hbar=c=1$ are employed.

§ 3. CHOICE OF WAVE FUNCTIONS.

For analytical simplicity Gaussian wave functions immediately suggest themselves. Their bad asymptotic behaviour, however, seems likely to lead to an underestimate of the photo-disintegration cross-sections. These, however, have been worked out using wave functions of the space symmetric form

$$\psi=\mathrm{N}^{\frac{1}{2}}\exp\Big(-\mu^2\sum_{i>j}r_{ij}^2\Big). \quad . \quad . \quad . \quad . \quad . \quad . \quad . \quad (4)$$

In order to obtain an improvement on the Gaussian wave functions it seemed desirable to find functions, which, whilst retaining reasonable analytical simplicity would have a more correct asymptotic behaviour. The wave functions developed by Svartholm were considered for this purpose, but in fact greater analytical simplicity is given by the general form

$$\psi=\mathrm{N}^{\frac{1}{2}}\exp\Big\{-\mu\Big(\sum_{i>j}r_{ij}^2\Big)^{\frac{1}{2}}\Big\}\Big/\Big(\sum_{i>j}r_{ij}^2\Big)^n. \quad . \quad . \quad . \quad . \quad . \quad (5)$$

An extensive series of variational calculations has been carried out for wave functions of this form, and has been separately described by one of us (Irving 1951).

With both types of wave function a choice has to be made of the appropriate value of μ for the deuteron, tritium and helium ground states, denoted subsequently by μ_D, μ_T and μ_α. This choice is discussed later when the photo-disintegration cross-sections are derived.

§ 4. PHOTO-DISINTEGRATION OF H^3 AND He^3 (TWO-PARTICLE).

For electric dipole transitions the probability per unit time of disintegration into a group of final states F is

$$w=4\pi^2ke^2\left|\Big(F\,\Big|\sum_{i=1}^{\mathrm{A}}\tau_i(\mathbf{r}_i-\mathbf{R})_z\Big|\,0\Big)\right|^2\rho_{\mathrm{E_F}}$$

where the initial quantum is regarded as polarized in the z-direction. The initial state O, say, for the tritium case, is the ${}^2S$ ground state of

H^3. The final state F contains one neutron moving as a plane wave with momentum $\mathbf{p}$, the resultant deuteron being in either the ${}^3(\sigma)_{\pm 1}$, or the ${}^3(\sigma)_0$ state. Carrying out the elementary spin summations leads to the result

$$w=\frac{2}{3}\pi^2 ke^2\left|\int u_f^* \rho_{1z} \exp\{-i(\mathbf{p}\cdot\boldsymbol{\rho}_1)\}\, u_i\, d\boldsymbol{\rho}_1\, d\mathbf{r}_{23}\right|^2 \rho(\mathrm{E_F}) \quad . \quad . \quad (6)$$

or, for the differential cross-section for the absorption of a quantum k with the neutron ejected into a solid angle $d\Omega$

$$d\sigma=\frac{e^2}{18\pi}\, kp\mathrm{M}\left|\int u_f^* \rho_{1z} \exp\{-i(\mathbf{p}\cdot\boldsymbol{\rho}_1)\}\, u_i\, d\boldsymbol{\rho}_1\, d\mathbf{r}_{23}\right|^2 d\Omega. \quad . \quad . \quad (7)$$

Here u_i, u_f are the initial tritium, and final deuteron wave functions expressed as functions of $\boldsymbol{\rho}_1$ and $\mathbf{r}_{23}$. For the case of He^3 the result is exactly similar except that allowance must be made for the Coulomb force between the outgoing proton and deuteron.

(a) *Photo-disintegration of Tritium.*

Using the Gaussian wave functions defined in equation (4) the differential cross-section for disintegration of H^3 with ejection of a neutron of momentum p is

$$d\sigma=\sqrt{\left(\frac{\pi}{6}\right)}\, e^2kp^3\mathrm{M}\cos^2\theta\,\frac{\mu_{\mathrm{D}}^3}{\mu_{\mathrm{T}}^4(3\mu_{\mathrm{T}}^2+2\mu_{\mathrm{D}}^2)^3}\exp\left(-\frac{\mathrm{ME}}{3\mu_{\mathrm{T}}^2}\right) d\Omega \quad . \quad (8)$$

where E is the kinetic energy available for the disintegration so that $p^2=\frac{4}{3}\mathrm{ME}$, with M the nucleon mass. The total cross-section σ is then given by

$$\sigma=\frac{16\sqrt{2}}{27}\pi^{3/2}e^2\,\frac{\mathrm{M}^{5/2}\mu_{\mathrm{D}}^3}{\mu_{\mathrm{T}}^4(3\mu_{\mathrm{T}}^2+2\mu_{\mathrm{D}}^2)^3}\,k\mathrm{E}^{3/2}\exp\left(-\frac{\mathrm{ME}}{3\mu_{\mathrm{T}}^2}\right). \quad . \quad . \quad (9)$$

Suitable values of μ_{T} are found from variational calculations with different Gaussian wells, $1/\mu_{\mathrm{T}}=4{\cdot}2\times10^{-13}$ cm. corresponding with the results of Margenau and Warren (1937), and $1/\mu_{\mathrm{T}}=3{\cdot}65\times10^{-13}$ cm. with the more recent force constants (Rosenfeld 1948)

$$1/\kappa=1{\cdot}9\times10^{-13}\ \text{cm.},\quad {}^3\mathrm{J}^{(0)}=43{\cdot}7\ \text{MeV.},\quad {}^1\mathrm{J}^{(0)}/{}^3\mathrm{J}^{(0)}=0{\cdot}62.$$

This second value gives a Coulomb energy of about 0·75 MeV. for He^3. The cross-section is plotted in fig. 1 (*a*) with those values of μ_{T}, and with $\mu_{\mathrm{D}}/\mu_{\mathrm{T}}=1{\cdot}12$.

The calculations were then repeated with the new form of wave functions. For simplicity in the evaluation of the integral (6) these were taken in the form

$$\psi_{\mathrm{T}}=\mathrm{A}\,\frac{\exp\{-\mu_r(r_{12}^2+r_{23}^2+r_{31}^2)^{\frac{1}{2}}\}}{(r_{12}^2+r_{23}^2+r_{31}^2)^{\frac{1}{2}}}=\frac{\mathrm{N}_{\mathrm{T}}^{\frac{1}{2}}\exp\{-\sqrt{2}\mu_{\mathrm{T}}(\rho^2+r^2)(\rho^2+r^2)^{\frac{1}{2}}\}}{(\rho^2+r^2)^{\frac{1}{2}}} \quad . \quad . \quad . \quad (10)$$

with

$$\left.\begin{aligned}\boldsymbol{\rho}&=\mathbf{r}_1-\tfrac{1}{2}(\mathbf{r}_2+\mathbf{r}_3)\\ \mathbf{r}&=\frac{\sqrt{3}}{2}(\mathbf{r}_3-\mathbf{r}_2).\end{aligned}\right\} \quad . \quad . \quad . \quad . \quad . \quad . \quad . \quad (11)$$

and

Figs. 1 (*a*) and 1 (*b*).

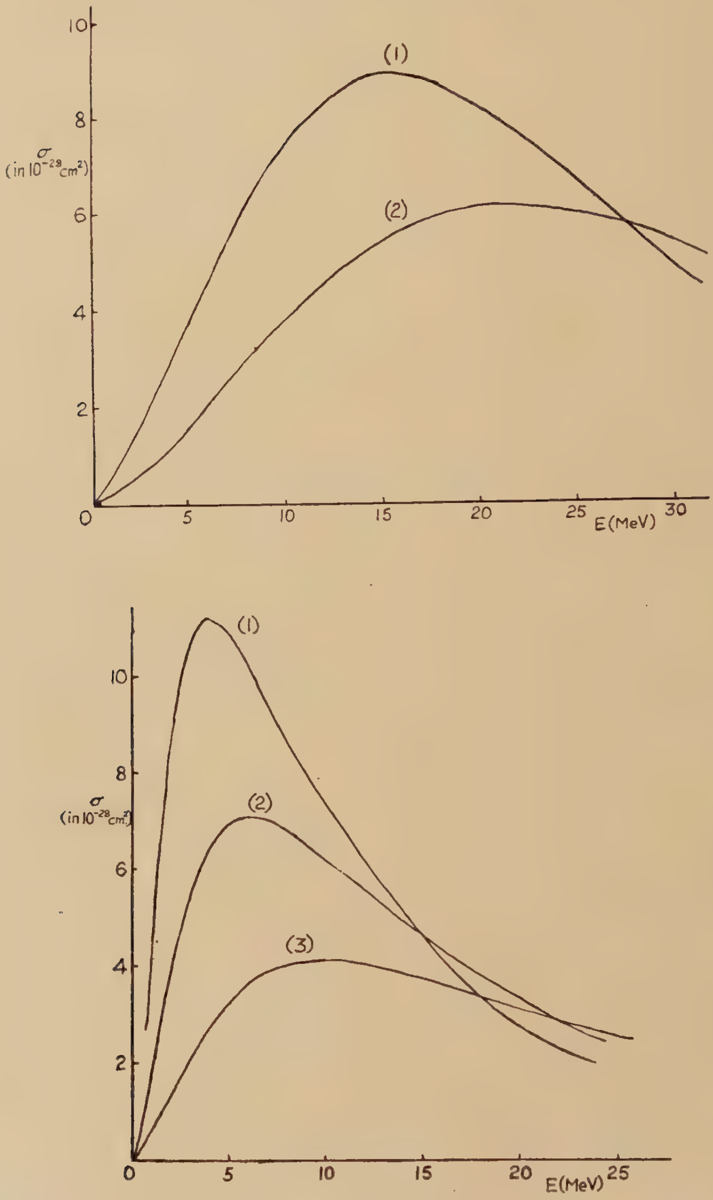

Cross-sections for two particle photo-disintegration of H^3

(*a*) for Gaussian wave functions with the values

(1) $1/\mu_T=4{\cdot}2\times10^{-13}$ cm., (2) $1/\mu_T=3{\cdot}65\times10^{-13}$ cm.

(*b*) for exponential wave functions with

(1) $1/\mu_T=3{\cdot}0\times10^{-13}$ cm., (2) $1/\mu_T=2{\cdot}5\times10^{-13}$ cm., (3) $1/\mu_T=2{\cdot}0\times10^{-13}$ cm.

The variational calculations of binding energy then show that $1/\mu_T = 2\cdot0\times10^{-13}$ cm. is a suitable value of the parameter, corresponding to a binding energy of 7·1 MeV. for a standard Yukawa potential

$$1/\kappa = 1\cdot17\times10^{-13}\text{ cm.},\quad {}^3J^{(0)} = 67\cdot3\text{ MeV.},\quad q = 0\cdot69 \quad . \quad . \quad (12)$$

(*cf.* Irving (1951)). If, rather than using the best variational value, μ_T is chosen to fit the Coulomb energy of He^3, then $1/\mu_T = 2\cdot5\times10^{-13}$ cm., corresponding with a Coulomb energy of 0·8 MeV. (binding energy of $H^3 = 6\cdot3$ MeV.) is suggested. In the curves of fig. 1*b* the rather extreme case of $1/\mu_T = 3\cdot0\times10^{-13}$ cm. is also shown. The binding energy with the potential (12) is then 5 MeV.

For the deuteron we take

$$\psi_D = N_D\sqrt{3}e^{-\gamma r}/(2r), \quad . \quad . \quad . \quad . \quad . \quad . \quad . \quad . \quad (13)$$

with r as defined in (11) and γ determined by the deuteron binding energy W_D, $\gamma = 2(MW_D/3)^{\frac{1}{2}}$. The integrals involved are long but quite elementary and lead to the result for the total cross-section

$$\sigma = 2^5e^2\frac{kE^{3/2}}{W_D^{5/2}}\frac{\mu_T^4}{M^3W_D^3}\{f(\lambda)\}^2 \quad . \quad . \quad . \quad . \quad . \quad . \quad (14)$$

with $$f(\lambda) = \frac{7\lambda-2}{\lambda^2(\lambda-1)^2} - \frac{15}{(\lambda-1)^3} + \frac{15}{(\lambda-1)^{7/2}}\cos^{-1}\left(\frac{1}{\sqrt{\lambda}}\right),$$

and $\lambda = (p^2 + 2\mu_T^2)/\gamma^2$. This cross-section is shown plotted as a function of photon energy in fig. 1*b*.

(b) *Photo-disintegration of* He^3.

In this case allowance must be made for the Coulomb interaction between the outgoing proton and deuteron; otherwise the general formulae are as for H^3. In view of the approximate nature of the calculation, it is felt that this allowance can be adequately made by multiplying the H^3 form of cross-section by a barrier penetration factor (Bethe 1937), at the same time taking note the of different binding energy of He^3 (7·74 MeV.), which brings the threshold to $k = 5\cdot5$ MeV. Detailed curves are not drawn for this case but the *p*-wave barrier penetration factors for a few energies are shown in Table I.

TABLE I.

E (MeV.)	0·5	1·0	1·5	2·0	2·5
exp $(-P_n)$ ($R = 4\cdot0\times10^{-13}$ cm.)	0·02	0·11	0·27	0·49	0·81
exp $(-P_n)$ ($R = 5\cdot0\times10^{-13}$ cm.)	0·05	0·25	0·64	1·0	—

E = energy in mass centre system.
R = barrier range.

Reviewing the results, we have found for the two-particle disintegrations it must be admitted that neither the results for the Gaussian nor for the exponential wave functions can be very accurate. Considering for the moment, for comparison, the case of photo-disintegration of the deuteron, it is known that a fairly good result can be obtained with the use of an asymptotic form for the initial wave functions and plane waves for the final neutron and proton. This possibility arises from the fact that the neutron and proton forming a deuteron exist for the greater part of the time outside the range of the nuclear forces. For the three- and four-particle nuclei this effect becomes successively weaker, and the central portion of the dipole matrix element integral becomes more important. Allowance for distortion of the outgoing waves is difficult to make, but it will probably tend in the direction of increasing the cross-sections at low energies and bringing the maxima nearer to low energies. In favour of the exponential wave functions it can at least be stated that they have a fairly correct asymptotic form, and should give the general shape of the cross-section better than the Gaussian form. (It may be recalled that even for the case of photo-disintegration of the deuteron Gaussian wave functions give a rather poor result.)

Unfortunately, only very little experimental information is available with which to compare the theoretical predictions. It is limited to the p-D capture cross-section reported by Fowler *et al.* (1949). These measurements indicate an approximate cross-section

$$\sigma_c = 0{\cdot}74\mathrm{E}_p^{0{\cdot}72} \times 10^{-29}\ \mathrm{cm.}^2 \quad . \quad . \quad . \quad . \quad . \quad . \quad . \quad (15)$$

for the $\mathrm{H}^2(p\,,\gamma)\,\mathrm{He}^3$ capture process in the region 0·5—1·5 MeV. The capture cross-section for this process is given in terms of the corresponding inverse photo-disintegration by

$$\sigma_c(\mathrm{E}_p) = (k^2/2\mathrm{ME})\sigma_d(k). \quad . \quad . \quad . \quad . \quad . \quad . \quad . \quad (16)$$

Here E_p is the proton bombarding energy in the laboratory system (deuteron stationary), and related to the earlier E (energy in the mass centre system) by $\mathrm{E}_p = \frac{3}{2}\mathrm{E}$. The corresponding quantum energy k is given by $k = \mathrm{E} + \mathrm{B}$, where in this case B=5·5 MeV. From (16) the theoretical capture cross-sections may be derived using the earlier (9) and (14). For the present we merely note that for small energies $\sigma_c \propto \mathrm{E}_p^{\frac{1}{2}}$. It has, thus, neglecting Coulomb barrier effects, a very swift rise above threshold, for any type of wave function or choice of parameters. The difference between different theoretical models is only observable when measurements beyond the initial rise are available. This is by no means true in the present case. Indeed, the experimental results given in (15) apply only up to $\mathrm{E}_p = 1{\cdot}5$ MeV., when the Coulomb barrier effects are still appreciable, and can easily be fitted, at least in shape, with either type of wave function using the barrier penetration factors of Table I. The most significant use to make of (15) seems to be to derive the magnitude of the corresponding photo-disintegration cross-section. We find that this should have the value 4×10^{-28} cm.^{2}, for E=1 MeV. The corresponding cross-section without barrier should be at least 16×10^{-28} cm.^{2} This should be approximately equal to the cross-section for the $H^3(\gamma, n)H^2$ process at 1 MeV. above the threshold. Comparison with figs. 1 (*a*) and (*b*) shows that none of the theoretical cross-sections has such a rapid rise above the threshold. Even the exponential wave functions with $1/\mu_T=3{\cdot}0\times10^{-13}$ cm. gives only a cross-section of 5×10^{-28} cm.^{2} In this energy range the distortion of the outgoing wave may be important and give rise to the discrepancy noted.

§ 5. PHOTO-DISINTEGRATION OF H^3 AND He^3 (THREE-PARTICLE).

As most of the binding energy of H^3 or He^3 is lost when the disintegrations $H^3\rightarrow n+D$, $He^3\rightarrow p+D$ are carried out, we might expect, in view of the greater phase space available, that, except just near the threshold, the three-particle disintegrations, of which $H^3\rightarrow n+n+p$ is typical, should predominate. Calculations along the lines of the preceding ones confirm this belief. They have been carried out both for the Gaussian and for the new exponential form of wave functions, once more using the approximation of plane waves for the outgoing particles. With the same notation as previously the two cross-sections are

Gaussian

$$\sigma=\frac{\pi^2ke^2}{3^7\mu_T^{10}}M^4E^3\exp\left(-\frac{ME}{3\mu_T^2}\right). \qquad (17)$$

Exponential

$$\sigma=\frac{150\pi^2e^2}{M^2}\left(\frac{\mu_T}{M}\right)^4\frac{kE^3M^3}{\left(E+\frac{3\mu_T^2}{2M}\right)}. \qquad (18)$$

For the Gaussian wave functions the maximum cross-section comes approximately when

$$E=500\text{ MeV.}\Big/\left\{\frac{1}{\mu_T}\text{ in }10^{-13}\text{ cm.}\right\}^2$$

and the magnitude of the cross-section varies approximately as $1/\mu_T^2$. In Table II. these maximum cross-sections are shown for various values of $1/\mu_T$, for the disintegration of H^3.

TABLE II.

Maximum cross-sections for $H^3\rightarrow n+n+p$ (Gaussian wave functions).

$1/\mu_T$ (units 10^{-13} cm.)	3·65	4·2	5·48
E_{max} (MeV.)	35	28·4	17
σ_{max} (units 10^{-27} cm.^{2})	2·2	2·9	4·8

For the exponential type wave functions rather similar values of cross-sections are obtained; for reasonable values of $1/\mu_T$, however, the maxima of the cross-sections again occur at lower energies. The maximum cross-section is approximately proportional to $1/\mu_T^2$, and the corresponding energy to μ_T^2. In fig. 2 the results are shown with $1/\mu_T=2{\cdot}5\times10^{-13}$ cm. It will be noted how these values dwarf the two-particle disintegration cross-sections of § 4, except at the threshold where only the two-particle process is possible. This will add to the already considerable experimental difficulties in the way of observation of the $He^3(\gamma, p)H^2$, $H^3(\gamma, n)H^2$ processes.

We have earlier noted the dangers in the use of the Born approximation, *i. e.* plane waves in the final state, in excitation problems of this sort. The method is to some extent consistent in that, for the initial state also, wave functions are used which have only asymptotic validity.

Fig. 2.

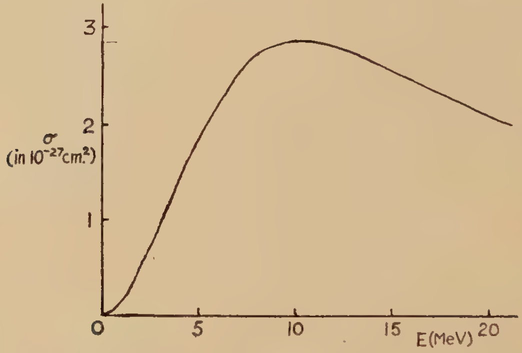

Three particle photo-disintegration cross-section of H^3, for exponential wave function, $1/\mu_T=2{\cdot}5\times10^{-13}$ cm.

§ 6. TWO-PARTICLE PHOTO-DISINTEGRATION OF α-PARTICLE.

Here we consider only the transition $He^4(\gamma, p)\,H^3$, neglecting at first the Coulomb interaction between the outgoing proton and triton. This is, in any case, negligible for quanta above about 22 MeV. From the general formulae given in § 2 we have

$$w=\pi^2ke^2\left|\int u_f^*\rho_{12}\exp\left(-i\mathbf{p}\cdot\boldsymbol{\rho}_1\right)u_i\,d\boldsymbol{\rho}_1\,d\mathbf{r}_{23}\,d\mathbf{r}_{24}\right|^2\rho_{EF}. \quad . \quad . \quad (19)$$

The initial state is the ${}^1S$ ground state of He^4, and the final state F contains one proton moving as a plane wave with momentum $\mathbf{p}$, the resultant triton being in a ${}^2S$ state.

Introducing the coordinates

$$\left.\begin{aligned}\mathbf{u}&=-\mathbf{r}_1+\tfrac{1}{3}(\mathbf{r}_2+\mathbf{r}_3+\mathbf{r}_4)\\ \mathbf{v}&=\tfrac{1}{2}(\mathbf{r}_3+\mathbf{r}_4)-\tfrac{1}{3}(\mathbf{r}_2+\mathbf{r}_3+\mathbf{r}_4)\\ \mathbf{w}&=\mathbf{r}_3-\mathbf{r}_4\end{aligned}\right\} . \quad . \quad . \quad . \quad (20)$$

we have

$$\left.\begin{aligned}\tfrac{1}{2}\sum_{i,j=1}^{4}\mathbf{r}_{ij}^{2}&=3u^{2}+24v^{2}+2w^{2}\\ \tfrac{1}{2}\sum_{i,j=1}^{3}\mathbf{r}_{ij}^{2}&=\tfrac{3}{4}(24v^{2}+2w^{2}).\end{aligned}\right\} \quad . \quad . \quad . \quad . \quad . \quad (21)$$

Gaussian wave functions : The calculations are elementary leading to

$$\sigma=3\times 4^{4}\pi^{3/2}e^{2}\mathrm{M}^{5/2}\frac{\mu_{\mathrm{T}}^{6}}{\mu_{\alpha}(3\mu_{\mathrm{T}}^{2}+4\mu_{\alpha}^{2})^{6}}k\mathrm{E}^{3/2}\exp\left\{-\frac{\mathrm{ME}}{4\mu_{\alpha}^{2}}\right\} \quad . \quad . \quad . \quad (22)$$

The parameters μ_α and μ_T may be determined by variational calculations of the binding energies of the α-particle and triton, assuming, for example, a Gaussian well. The nuclear parameters

$$1/\kappa=1{\cdot}9\times 10^{-13}\ \text{cm.},\quad {}^{3}\mathrm{J}^{(0)}=43{\cdot}7\ \text{MeV.},\quad q=0{\cdot}62$$

then give $1/\mu_\mathrm{T}\simeq 1/\mu_\alpha=3{\cdot}65\times 10^{-13}$ cm. yielding binding energies of approximately 4 MeV. and 23 MeV. for the triton and α-particle respectively. The Coulomb energy of He^3 is then approximately 0·75 MeV. The nuclear parameters $1/\kappa=2{\cdot}25\times 10^{-13}$ cm., ${}^3\mathrm{J}^{(0)}=35{\cdot}6$ MeV., $q=0{\cdot}6$ determined by Margenau and Warren (1937) to fit the triton binding and deuteron data give slightly too small a value for the α-particle binding energy. For this case $1/\mu_\alpha\simeq 1/\mu_\mathrm{T}=4{\cdot}2\times 10^{-13}$ cm. In fig. 3 (*a*) σ is graphed against E for $1/\mu_\alpha=1/\mu_\mathrm{T}$, several values of the parameters being taken to show the dependence on them. $1/\mu_\alpha=1/\mu_\mathrm{T}=5{\cdot}25\times 10^{-13}$ cm. has already been considered by Flowers and Mandl (1951).

The calculations were repeated with exponential wave functions of the form

$$\begin{aligned}\psi_\alpha&=\mathrm{N}_\alpha^{1/2}\exp\{-\mu_\alpha(\sum_{i>j}r_{ij}^2)^{\frac{1}{2}}\}/\{\sum_{i>j}r_{ij}^2\}^{\frac{1}{2}}\\ &=\frac{\mathrm{N}_\alpha^{1/2}\exp\{-\mu_\alpha(3u^2+24v^2+2w^2)^{\frac{1}{2}}\}}{(3u^2+24v^2+2w^2)^{\frac{1}{2}}} \quad . \quad . \quad . \quad . \quad . \quad . \quad (23)\end{aligned}$$

and

$$\begin{aligned}\psi_\mathrm{T}&=\mathrm{N}_\mathrm{T}^{1/2}\exp\{-\mu_\mathrm{T}(r_{12}^2+r_{23}^2+r_{31}^2)^{\frac{1}{2}}\}/(r_{12}^2+r_{23}^2+r_{31}^2)^{\frac{1}{2}}\\ &=\frac{\mathrm{N}_\mathrm{T}^{1/2}\exp\{-\frac{1}{2}\sqrt{3}\mu_\mathrm{T}(24v^2+2w^2)^{\frac{1}{2}}\}}{\{\frac{1}{2}\sqrt{3}(24v^2+2w^2)^{\frac{1}{2}}\}} \quad . \quad . \quad . \quad . \quad . \quad . \quad . \quad (24)\end{aligned}$$

The cross-section is then given by

$$\sigma=\frac{7\times 4^{11}\pi}{3^{9}\sqrt{2}}e^{2}\mathrm{M}^{5/2}\frac{\mu_\alpha^{7}}{\mu_\mathrm{T}^{14}}k\mathrm{E}^{3/2}z^{20}\{f(z)\}^{2} \quad . \quad . \quad . \quad . \quad . \quad . \quad (25)$$

where $$f(z)=\Big[(735+3465z^2)/8+21/(1+z^2)+2/(1+z^2)^2 \\ -\frac{3\cot^{-1}z}{8z}(1155z^4+630z^2+35)\Big]$$

and $$\frac{1}{z^2}=\frac{2\mathrm{ME}}{3\mu_\mathrm{T}^2}+\frac{4\mu_\alpha^2}{3\mu_\mathrm{T}^2}-1.$$

The graph of σ against E is shown in fig. 3 (*b*) for different values of the parameters. $1/\mu_T = 2{\cdot}5 \times 10^{-13}$ cm. gives the correct Coulomb energy of He^3. $1/\mu_\alpha = 1{\cdot}7 \times 10^{-13}$ cm. gives a binding energy of 28 MeV. for He^4; $1/\mu_\alpha = 2{\cdot}0 \times 10^{-13}$ cm. a binding energy of 20·5 MeV.; $1/\mu_\alpha = 2{\cdot}5 \times 10^{-13}$ cm., a binding energy of 12·5 MeV. The rapid rise of the cross-section is evident. The exponential wave functions give earlier maxima than the Gaussian, the values of the parameters being smaller as well; that is, a more concentrated nucleus is found for cross-sections of comparable magnitude.

Fig. 3 (*a*).

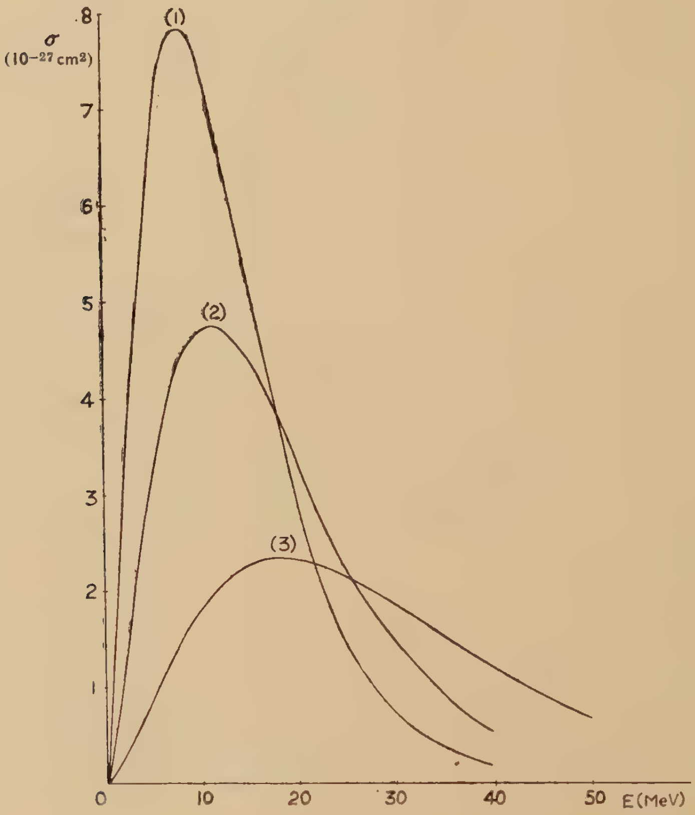

Cross-sections for two particle photo-disintegration of He^4
(*a*) Gaussian wave functions with $1/\mu_\alpha = 1/\mu_T$ having values (1) $6{\cdot}10 \times 10^{-13}$ cm., (2) $5{\cdot}25 \times 10^{-13}$ cm., (3) $4{\cdot}20 \times 10^{-13}$ cm.

The cross-section for the inverse capture process can again be calculated by the method of detailed balance yielding

$$\sigma_c(E_p) = (k^2/3ME)\sigma_d(k). \quad . \quad . \quad . \quad . \quad . \quad . \quad (26)$$

Here, as previously, E_p denotes the proton bombarding energy in the laboratory system, $E(=\frac{3}{4}E_p)$ is the corresponding energy in the centre of mass system, and $\sigma_d(k)$ denotes the photo-disintegration cross-section for quantum energy k. To illustrate the general form of the theoretical capture curves, the capture cross-section is given in fig. 4 for the exponential form of wave function with $1/\mu_T=1/\mu_\alpha=2{\cdot}5\times10^{-13}$ cm., and for the Gaussian form of wave function with $1/\mu_T=1/\mu_\chi=6{\cdot}10\times10^{-13}$ cm.

Fig. 3 (*b*).

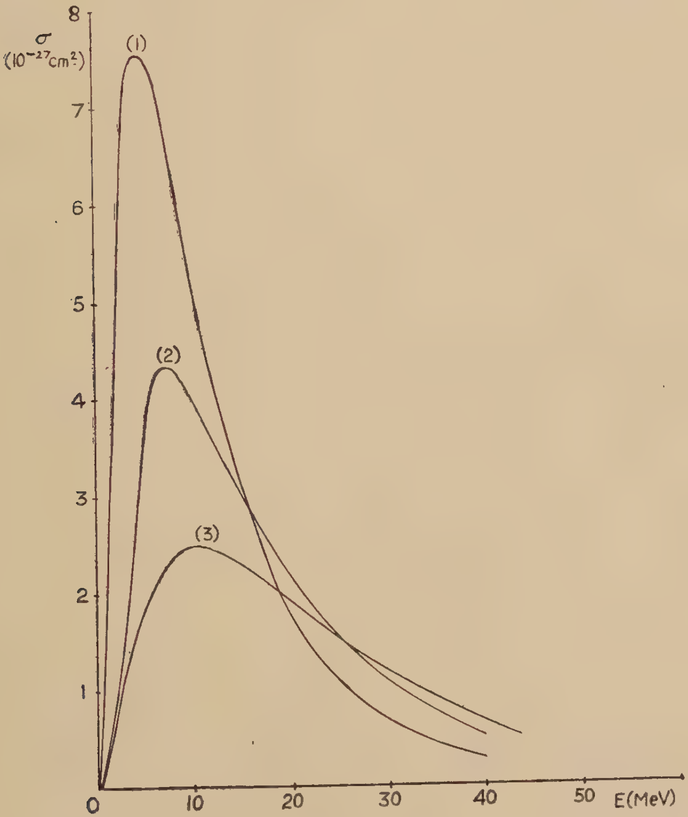

Cross-sections for two particle photo-disintegration of He^4

(*b*) Exponential wave functions with (1) $1/\mu_\alpha=1/\mu_T=2{\cdot}5\times10^{-13}$ cm., (2) $1/\mu_\alpha=2{\cdot}0\times10^{-13}$ cm., $1/\mu_T=2{\cdot}5\times10^{-13}$ cm., (3) $1/\mu_\alpha=1{\cdot}7\times10^{-13}$ cm., $1/\mu_T=2{\cdot}5\times10^{-13}$ cm.

The experimental evidence available relates mainly to the capture process, coming from the measurements of Argo *et al.* (1950). Experiment has only been carried out up to a bombarding energy $E_p=2{\cdot}6$ MeV., which is just approaching the top of the barrier for *p*-wave protons. It is clear that the shape of the experimental curve can, as noted by Flowers and Mandl (1951), be explained by a combination of the initial shape without barrier $\sigma_c \propto E_p^{\frac{1}{2}}$, and suitable barrier penetration factors, more particularly in view of the rather arbitrary calculations involved in the latter. Once again, however, the magnitude of the capture cross-section is interesting. This is quoted as approximately 10^{-27} cm.^{2} at $E_p = 2{\cdot}6$ MeV. The corresponding photo-disintegration cross-section is about 10^{-26} cm.^{2} at $k=2$ MeV. None of the theoretical curves predicts so sharp a rise in the cross-section above the threshold, though once again the exponential wave functions give a better agreement. If the experimental evidence regarding the photo-disintegration process mentioned in a footnote in § 1 is confirmed, then support is provided for a cross-section approximately of the form given by the exponential wave functions with $1/\mu_T = 1/\mu_\alpha = 2{\cdot}5 \times 10^{-13}$ cm. These measurements give an integrated yield of 4×10^{-26} cm.^{2} MeV. for the cross-section, with about 40 per cent of the events below $k=24$ MeV., which could not be reconciled with any of the curves based on Gaussian wave functions.

Fig. 4.

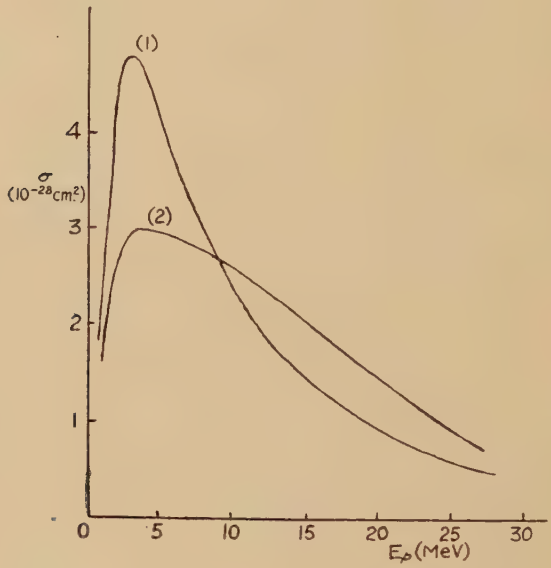

Cross-section for proton capture by tritium, neglecting Coulomb barrier (1) with exponential wave function, $1/\mu_T = 1/\mu_\alpha = 2{\cdot}5 \times 10^{-13}$ cm., (2) with Gaussian wave function, $1/\mu_T = 1/\mu_\alpha = 6{\cdot}10 \times 10^{-13}$ cm.

In conclusion then it appears that a reasonably good fit to the photo-disintegration and inverse processes for the three- and four-particle nuclei may be hoped for with the exponential wave functions. They are at least superior to the Gaussian functions in predicting the early rise of the cross-sections above the threshold. There is at present, however, too much uncertainty regarding the choice to be made of the parameters, μ_T and μ_χ. The binding energy calculations with central forces (Irving 1951) are certainly inadequate for this purpose, but the hope is that their extension to include non-central forces may yield a consistent picture. We should then, in the exponential wave functions, have an analytical model of reasonable simplicity for three- and four-particle nuclei, with the possibility of extension to other light nuclei.

Complete disintegration of He^4.

Using the same approximations as in the case of the three-particle system, the cross-section for the process

$$\mathrm{He}^4+\gamma\rightarrow n+n+p+p$$

is easily calculated.

For the Gaussian wave functions, we have

$$\sigma=\frac{1}{945}\frac{\pi^{3/2}}{4^4}e^2\frac{\mathrm{M}^{11/2}}{\mu_\alpha^{13}}k\mathrm{E}^{9/2}\exp\left\{-\frac{\mathrm{ME}}{4\mu_\alpha^2}\right\}. \quad . \quad . \quad . \quad . \qquad (27)$$

The values of $\sigma_{\max}$ for several values of the parameter are then as follows :

$1/\mu_\alpha$ (10^{-13} cm.)	E (MeV.)	$\sigma_{\max}$ (10^{-27} cm.^{2})
3·6	66·4	3·04
4·2	48·0	4·58
5·25	30·0	8·66
6·1	22·0	13·7

For the exponential wave function,

$$\sigma=\frac{2^{21}\sqrt{2\pi}}{45}e^2\frac{1}{\mathrm{M}^{9/2}}\frac{\mu_\alpha^7 k\mathrm{E}^{9/2}}{(\mathrm{E}+2\mu_\alpha^2/\mathrm{M})^{10}} \quad . \quad . \quad . \quad . \quad . \qquad (28)$$

yielding the following results for $\sigma_{\max}$:

$1/\mu_\alpha$ (10^{-13} cm.)	E (MeV.)	$\sigma_{\max}$ (10^{-27} cm.^{2})
1·7	28·7	3·7
2·0	20·0	6·2
2·5	12·2	12·8

The maxima for the exponential wave function again occur at much lower energies than those for the Gaussian wave function. It would be interesting if experimental information could be obtained on this point.

ACKNOWLEDGMENT.

One of us (J. I.) wishes to thank the Nuffield Foundation for the award of a Fellowship, during the tenure of which this work was carried out.

REFERENCES.

ARGO, A. V., GITTINGS, H. T., HEMMENDINGER, A., JARVIS, G. A., and TASCHEK, R. F., 1950, *Phys. Rev.*, **78,** 691.

BETHE, H. A., 1937, *Rev. Mod. Phys.*, **9,** 177.

BUCKINGHAM, R. A., and MASSEY, H. S. W., 1941, *Proc. Roy. Soc.* A, **179,** 123.

BURHOP, E., and MASSEY, H. S. W., 1948, *Proc. Roy. Soc.* A, **192,** 156.

FLOWERS, B. H., and MANDL, 1951, *Proc. Roy. Soc.* A, **206,** 131.

FOWLER, W. A., LAURITSEN, C. C., and TOLLESTRUP, A. V., 1949, *Phys. Rev.*, **76,** 1767.

FRÖHLICH, H., HUANG, K., and SNEDDON, I. N., 1947, *Proc. Roy. Soc.* A, **191,** 61.

IRVING, J., 1951, *Phil. Mag.*, **42,** 338.

MARGENAU, H., and WARREN, D., 1937, *Phys. Rev.*, **52,** 790.

ROSENFELD, L., 1948, *Nuclear Forces* (Amsterdam : North Holland Publishing Co.), p. 131.

SVARTHOLM, N., 1945, *The binding energies of the lightest atomic nuclei*, Thesis, Lund.

VERDE, M., 1950, *Helv. Phys. Acta*, **23,** 453.

CXXXV. *The Recrystallization Texture of Drawn Aluminium Wire.*

By J. Sawkill and N. Thorley,
Physics Department, King's College, Newcastle-upon-Tyne*.

[Received June 26, 1951. Revised August 9, 1951.]

[Plate LIII.]

Abstract.

The recrystallization texture of high purity (99·995 per cent) cold drawn aluminium wire has been found to be double, viz., [322], [100]. The [100] component is relatively weak. The scatter in the major [322] component increases, and the amount of the [100] component decreases, the higher the temperature of anneal.

Recently it has been suggested (Hibbard 1950) that the double [111], [100] deformation texture of drawn face-centred cubic metal wires previously described (*e. g.* Schmid and Wassermann 1927) is actually an intermediate texture which changes to a single [111] texture with sufficient deformation. The [111] texture has been predicted on theoretical grounds (Hibbard and Yen 1948, Calnan and Clews 1950). Observations Hibbard made on drawn wires of six metals showed that for a large deformation (98 per cent reduction in diameter) all the wires had essentially a single [111] texture. In the case of aluminium, however, there was a minor [100] component, which Hibbard ascribed to room temperature recrystallization. His reasons for this were that aluminium of the purity used (99·994 per cent) has been known to recrystallize at room temperature; that the [100] component on the X-ray photograph was characteristic of diffraction from large recrystallized strain-free grains (*i. e.* " spotty " rather than diffuse); that the [100] component increased in intensity with increasing deformation above 90 per cent; and that the deformation texture of less pure drawn aluminium wire has been reported previously as single [111].

It is interesting to observe that v. Göler and Sachs (1927) working with less pure aluminium (99·93 per cent) did find evidence of a [100] recrystallization texture. The wire they used had been reduced in diameter by 80·6 per cent and the deformation texture was [111] with a trace of [100]. An annealing temperature of at least 200° C. was required before recrystallization was evident as faint spots on the Debye–Scherrer rings of the X-ray photographs. After complete recrystallization, requiring temperatures of at least 375° C., the [111] deformation texture was observed to be preserved and an appreciable amount of [100] texture was also present.

---

* Communicated by the Authors.

Recent experiments in this department have also shown the existence of a minor [100] component in the recrystallization texture of high purity aluminium wire. The actual texture is double, viz., [322], [100]. The majority of grains have the [322] texture, the minor [100] component being relatively weak.

The aluminium, kindly supplied by the British Aluminium Co. Ltd., was of 99·995 per cent purity and had received a 95·2 per cent reduction in diameter. Plate LIII. (*a*) is a flat film X-ray photograph showing the deformation texture, taken with partially filtered MoKα radiation with the beam perpendicular to the vertical wire axis. It shows the [111] texture on a background of complete rings from the randomly oriented grains. On the first ring there is a weak reflection at A (Plate LIII. (*a*)) which can be accounted for if a small percentage of the grains have the [100] direction along the wire axis. In this case a slight intensity maximum would be expected at B on the second ring, and this can be seen on the original negative. A weak [100] component then exists in addition to the strong [111] component and the small percentage of grains of random orientation. The reflections at A due to the [100] component are not spotty, *i. e.* not characteristic of large recrystallized strain-free grains. The wire was annealed at various temperatures and in all cases a new texture appeared. Plate LIII. (*b*) is a typical photograph. Here the wire had been annealed at 275° C. for two hours and a comparison with Plate LIII. (*a*) shows the change in texture. At regions A and B (Plate LIII. (*b*)) on the first and second rings respectively the fairly weak reflections are at the positions predicted by a [100] texture. For these reflections the maximum angular deviation of the [100] direction from the axis of the wire is about 5°. For the remainder of the reflections an analysis has shown that the texture can be accounted for almost exactly with the [322] direction along the wire axis. The randomly oriented grains disappear. Anneals were given from approximately 150° C. to 550° C. and this new texture was always found. It is due to primary recrystallization; subsequent grain growth did not affect the texture. The amount of the [100] component decreased, and the scatter in the [322] component increased, the higher the temperature of anneal. In Plate LIII. (*b*) the maximum angular deviation of the [322] direction from the axis of the wire is between 2° and 3°.

v. Göler and Sachs (1927) used aluminium of three different purities and found the minor [100] recrystallization component strongest for the purest metal.

Their results were as follows :—

(i.) a preservation of the [111] deformation texture and the appearance of a [100] component with recrystallization of 99·93 per cent aluminium (previously mentioned) ;

(ii.) a partial preservation of the [111] deformation texture and a suggestion of a [100] component with recrystallization of 99·0 per cent aluminium ; and

(iii.) a partial preservation of the [111] deformation texture with recrystallization below 500° C. but increasing randomness with recrystallization above this temperature and no [100] recrystallization component for 98·7 per cent aluminium.

Other observers (Schmid and Wassermann 1928) found no evidence of a [100] recrystallization component for 99·95 per cent aluminium.

Nevertheless, the results of v. Göler and Sachs suggest that the amount of the [100] recrystallization component depends on purity, and it may be significant that with the higher purity material in the present work temperatures lower than the 375° C. of v. Göler and Sachs produced this component. This seems to support Hibbard's suggestion that the room temperature [100] component in his aluminium wire is due to recrystallization. In the particular case observed here, however, the existence of the minor [100] recrystallization component does not definitely establish that the room temperature component is due to recrystallization. Two possibilities exist :—

(i.) that it is due to deformation only and that recrystallization preserves it ; and

(ii.) that it is already present due to recrystallization and higher temperature anneals merely retain it.

The fact that the room temperature [100] component here was not " spotty " and that temperatures of at least 150° C. were required before the X-ray rings did become " spotty " tends to discount (ii.) while some of Hibbard's previously mentioned observations would seem to discount the first possibility. It is evident that further investigations are necessary to determine the true origin of this room temperature [100] component in aluminium wires after large deformations.

The major [322] recrystallization component has not hitherto been reported. It may be characteristic of this wire only, as purity, prior deformation and mode of recrystallization are determining factors for the resulting texture. In many cases in face-centred cubic metals a certain relative orientation, corresponding to a rotation of 30° to 40° about the [111] axis, has been found between a highly oriented cold worked matrix and strain-free grains growing in this matrix (Beck and Hu 1949). The same relative orientation was found with coarsening or secondary recrystallization. The retention of the [111] drawing texture on annealing, previously observed, would be in keeping with this orientation relationship, but the production of the [322] texture on annealing from the [111] drawing texture, observed here, does not agree with this relationship.

With increasing purity of available metals it is more necessary than ever, when stating recrystallization textures, to quote the purity, temperature of anneal, mode of recrystallization and the magnitude of the previous deformation.

REFERENCES.

BECK, P. A., and HU, H., 1949, *Trans. Amer. Inst. Min. Met. Eng.*, **185,** 627.
CALNAN, E. A., and CLEWS, C. J. B., 1950, *Phil. Mag.*, **41,** 1085.
VON GÖLER, F., and SACHS, G., 1927, *Z. Metallkunde*, **19,** 90.
HIBBARD, W. R., 1950, *J. Inst. Metals, Lond.*, **77,** 581.
HIBBARD, W. R., and YEN, M.-K., 1948, *Trans. Amer. Inst. Min. Met. Eng.*, **175,** 126.
SCHMID, E., and WASSERMANN, G., 1927, *Z. Physik*, **42,** 779; 1928, *Z. Tech. Physik*, **9,** 106.

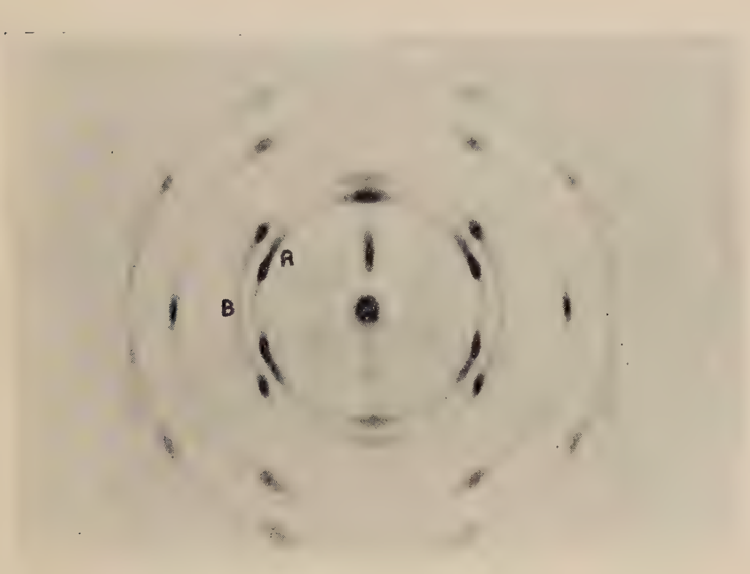

(*a*)

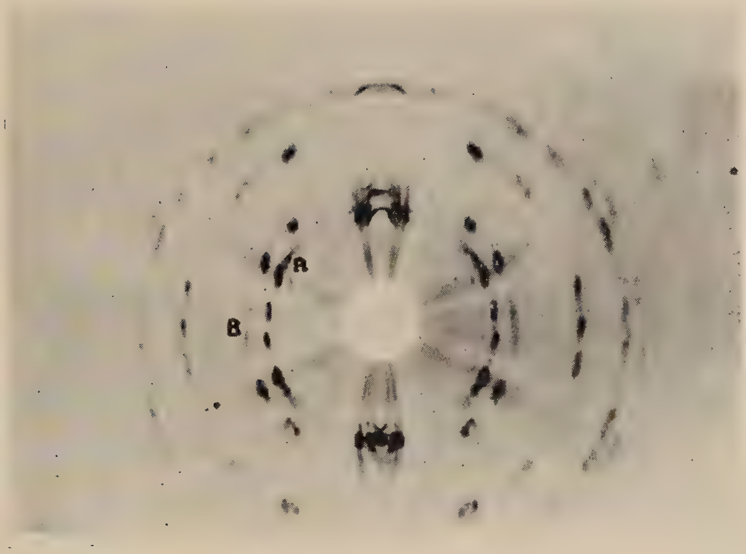

(*b*)

CXXXVI. *On the Quantum Mechanics of Helium II.*

By O. PENROSE,
Royal Society Mond Laboratory, Cambridge*.

[Received June 2, 1951 ; revised June 29, 1951.]

ABSTRACT.

The quantum mechanics of a system of identical interacting particles must lead to the classical hydrodynamic equations of motion at high temperatures, because of the correspondence principle. On the other hand, the behaviour of helium II shows that this is not always the case at low temperatures. In this paper it is shown that in certain cases the quantum description requires an extra parameter, which is the potential of a new velocity field superimposed on the classical motion. Expressed in semi-classical terms, the condition for the existence of this new parameter is that the probability, in the equilibrium state, of a particle having a very large de Broglie wavelength (that is, a negligible momentum) is finite. This condition is satisfied in one model of a superfluid system, a condensed Bose–Einstein gas, but not in a crystal. A tentative theoretical interpretation of two basic equations of the empirical two-fluid theory of helium II is given, in which this new parameter determines the velocity of the superfluid.

§ 1. INTRODUCTION.

BORN AND GREEN (1947, 1948) described a method of studying transport processes in a system of identical interacting particles obeying quantum mechanics by using the analogy with the corresponding classical system. Gurov (1948, 1950) carried out a similar calculation. In both cases the conclusion was that the equations of hydrodynamics and heat transfer were identical in form with the classical equations. These treatments assumed that the three quantities describing a " normal " state of the system (Born and Green 1947, Chapman and Cowling 1939) were the same as for a classical system : the density, velocity and temperature fields. In other words, if at one instant the system is in a state described by given fields of these three parameters, its state at a later time is sufficiently described by the new fields of the parameters resulting from the thermo-hydrodynamical equations of motion. From the correspondence principle it is clear that the three parameters of classical mechanics are sufficient in quantum mechanics at high temperatures, but, as we shall see, this is not always true at low temperatures.

---

* Communicated by the Author.

§ 2. PROPERTIES OF THE REDUCED DENSITY MATRICES.

Suppose the system consists of N identical particles of mass m interacting by central forces whose potential is U, and let the Schrödinger representative of the density matrix of the corresponding Gibbs ensemble (Dirac 1947) be

$$\mathrm{D}(\mathbf{q}_1, \ldots \mathbf{q}_N\, ;\, \mathbf{q}_1', \ldots \mathbf{q}_N'),$$

where $\mathbf{q}_1, \ldots \mathbf{q}_N$ are the position vectors of the N particles, and D is Hermitian. The reduced density matrices, which are also Hermitian, are defined by

$$\mathrm{R}_k(\mathbf{q}_1, \ldots \mathbf{q}_k\, ;\, \mathbf{q}_1', \ldots \mathbf{q}_k') = [\mathrm{N}\,!/(\mathrm{N}-k)\,!] \times \int \ldots \int \mathrm{D}(\mathbf{q}_1 \ldots \mathbf{q}_N\, ;\, \mathbf{q}_1' \ldots \mathbf{q}_k', \mathbf{q}_{k+1} \ldots \mathbf{q}_N)\, d\mathbf{q}_{k+1} \ldots d\mathbf{q}_N \,. \quad . \quad (1)$$

The equation of motion for D is

$$i\hbar\, \partial \mathrm{D}/\partial t = \mathrm{HD} - \mathrm{DH}, \quad . \quad . \quad . \quad . \quad . \quad . \quad . \quad . \quad (2)$$

where H is the Hamiltonian operator of the system. After setting $\mathbf{q}_2 = \mathbf{q}_2', \ldots \mathbf{q}_N = \mathbf{q}_N'$, this may be integrated over $\mathbf{q}_2, \ldots \mathbf{q}_N$, giving

$$i\hbar \partial \mathrm{R}_1(\mathbf{q}_1\, ;\, \mathbf{q}_1')/\partial t = -(\hbar^2/2m)(\nabla_1^2 - \nabla_1'^2)\mathrm{R}_1(\mathbf{q}_1\, ;\, \mathbf{q}_1') + \int [\mathrm{U}(\mathbf{q}_1 - \mathbf{q}_2) - \mathrm{U}(\mathbf{q}_1' - \mathbf{q}_2)]\mathrm{R}_2(\mathbf{q}_1, \mathbf{q}_2\, ;\, \mathbf{q}_1', \mathbf{q}_2)\, d\mathbf{q}_2, \quad . \quad . \quad . \quad (3)$$

where $\nabla_j = \partial/\partial \mathbf{q}_j$, etc.

By using Wigner's result (Wigner 1932, Moyal 1949) that a density matrix $\mathrm{R}_1(\mathbf{q}_1\, ;\, \mathbf{q}_1')$ corresponds to a classical probability density $\mathrm{F}(\mathbf{x}, \mathbf{p})$ for the position $\mathbf{x}$ and momentum $\mathbf{p}$ of one particle such that

$$\mathrm{R}_1(\mathbf{q}_1\, ;\, \mathbf{q}_1') \sim \int d\mathbf{p} \mathrm{F}(\tfrac{1}{2}[\mathbf{q}_1 + \mathbf{q}_1'], \mathbf{p}) \exp [i\mathbf{p} \cdot (\mathbf{q}_1 - \mathbf{q}_1')/\hbar], \quad . \quad . \quad (4)$$

combined with the classical result

$$\mathrm{F}(\mathbf{x}, \mathbf{p}) \propto \exp [-\mathbf{p}^2/2mk\mathrm{T}], \quad . \quad . \quad . \quad . \quad . \quad . \quad . \quad (5)$$

or alternatively by approximately solving the Bloch equation $\partial \mathrm{D}/\partial (k\mathrm{T})^{-1} = -\mathrm{HD}$ (Husimi 1940), we obtain a high temperature approximation

$$\mathrm{R}_1(\mathbf{q}_1\, ;\, \mathbf{q}_1') \propto \exp [-(\mathbf{q}_1 - \mathbf{q}_1')^2 mk\mathrm{T}/2\hbar^2], \quad . \quad . \quad . \quad . \quad (6)$$

for equilibrium at the temperature T. Therefore

$$\lim_{|\mathbf{q}_1 - \mathbf{q}_1'| \to \infty} \mathrm{R}_1(\mathbf{q}_1\, ;\, \mathbf{q}_1') = 0. \quad . \quad . \quad . \quad . \quad . \quad . \quad . \quad (7)$$

At low temperatures (7) may not be satisfied for every type of system. To see the physical significance of the failure of (7) let us assume for the moment that $\mathrm{R}_1(\mathbf{q}_1\, ;\, \mathbf{q}_1')$ depends only on $|\mathbf{q}_1 - \mathbf{q}_1'|$ and approaches a constant value L when $|\mathbf{q}_1 - \mathbf{q}_1'| \to \infty$. Then the Fourier inverse of (4) yields a divergent integral which may be interpreted as

$$\mathrm{F}(\mathbf{x}, \mathbf{p}) = f(\mathbf{p}) + \mathrm{L}\delta(\mathbf{p}), \quad . \quad . \quad . \quad . \quad . \quad . \quad . \quad (8)$$

where $f(\mathbf{p})$ is a regular function. That is to say, the probability of one particle having zero momentum is the finite fraction $\mathrm{L}/\mathrm{R}_1(\mathbf{x}\, ;\, \mathbf{x})$. Since (8) is in fact an expression for the mean occupation numbers of single-particle levels, L must vanish (and (7) therefore be satisfied) in a Fermi-Dirac system, where the exclusion principle limits the occupation numbers.

§ 3. ASYMPTOTIC BEHAVIOUR OF THE REDUCED DENSITY MATRIX FOR ONE PARTICLE.

In the general case when (7) does not hold we shall consider the behaviour of $R_1(\mathbf{q}_1\,;\,\mathbf{q}_1')$ for values of $|\mathbf{q}_1-\mathbf{q}_1'|$ large compared with both $\hbar(mkT)^{-1/2}$ and the range of U. The integral in (3) may be written, using the Hermitian property of R_2,

$$\int U(\mathbf{r})[R_2(\mathbf{q}_1,\mathbf{q}_1+\mathbf{r}\,;\,\mathbf{q}_1',\mathbf{q}_1+\mathbf{r})-R_2^*(\mathbf{q}_1',\mathbf{q}_1'+\mathbf{r}\,;\,\mathbf{q}_1,\mathbf{q}_1'+\mathbf{r})]\,d\mathbf{r}. \quad . \quad (9)$$

Suppose that the asymptotic form of $R_2(\mathbf{q}_1,\mathbf{q}_1+\mathbf{r}\,;\,\mathbf{q}_1',\mathbf{q}_1+\mathbf{r})$ for large $|\mathbf{q}_1-\mathbf{q}_1'|$ is

$$R_2(\mathbf{q}_1,\mathbf{q}_1+\mathbf{r}\,;\,\mathbf{q}_1',\mathbf{q}_1+\mathbf{r})\sim A(\mathbf{q}_1,\mathbf{r})R_1(\mathbf{q}_1\,;\,\mathbf{q}_1'), \quad . \quad . \quad . \quad (10)$$

just as the neighbour distribution function of a liquid obeys

$$R_2(\mathbf{q}_1,\mathbf{q}_2\,;\,\mathbf{q}_1,\mathbf{q}_2)\sim R_1(\mathbf{q}_1\,;\,\mathbf{q}_1)R_1(\mathbf{q}_2\,;\,\mathbf{q}_2) \quad . \quad . \quad . \quad (11)$$

for large $|\mathbf{q}_1-\mathbf{q}_2|$. For large $|\mathbf{q}_1-\mathbf{q}_1'|$ (3) becomes

$$i\hbar\,\partial R_1(\mathbf{q}_1\,;\,\mathbf{q}_1')/\partial t\sim-(\hbar^2/2m)(\nabla_1^2-\nabla_1'^2)R_1(\mathbf{q}_1\,;\,\mathbf{q}_1')$$
$$+[X(\mathbf{q}_1)-X^*(\mathbf{q}_1')]R_1(\mathbf{q}_1\,;\,\mathbf{q}_1'), \quad . \quad . \quad (12)$$

where $$X(\mathbf{q})=\int A(\mathbf{q},\mathbf{r})U(\mathbf{r})\,d\mathbf{r}=V(\mathbf{q})+iW(\mathbf{q}). \quad . \quad . \quad . \quad . \quad (13)$$

Since the variables in (12) are separable the general solution is a linear combination of expressions of the form

$$\Psi(\mathbf{q}_1)\Psi^*(\mathbf{q}_1'), \quad . \quad . \quad . \quad . \quad . \quad . \quad . \quad . \quad (14)$$

where $$i\hbar\partial\Psi/\partial t=-(\hbar^2/2m)\nabla^2\Psi+X\Psi. \quad . \quad . \quad . \quad . \quad . \quad (15)$$

At equilibrium $D=e^{-\beta H}$, and since the Schrödinger representative of H is real, those of D and the R's are also real. The state of the liquid is uniform, and, therefore, for large enough $|\mathbf{q}_1-\mathbf{q}_1'|$ it may be assumed that

$$R_1(\mathbf{q}_1\,;\,\mathbf{q}_1')\sim\text{const.}$$

This is of the form (14) with $\Psi=\text{const}$. If the density matrix of a non-equilibrium state is sufficiently similar to $e^{-\beta H}$ the required solution of (12) will still be a single expression of the form (14):

$$R_1(\mathbf{q}_1\,;\,\mathbf{q}_1')\sim\Psi(\mathbf{q}_1)\Psi^*(\mathbf{q}_1'). \quad . \quad . \quad . \quad . \quad . \quad (16)$$

The example of a condensed Bose gas may clarify the argument of this section. Equation (16) is true, with Ψ the wave-function of the single-particle state into which condensation has taken place. Husimi's formula (1940)

$$R_2(\mathbf{q}_1,\mathbf{q}_2\,;\,\mathbf{q}_1',\mathbf{q}_2')=R_1(\mathbf{q}_1\,;\,\mathbf{q}_1')R_1(\mathbf{q}_2\,;\,\mathbf{q}_2')+R_1(\mathbf{q}_1\,;\,\mathbf{q}_2')R_1(\mathbf{q}_2\,;\,\mathbf{q}_1')$$

is not valid for a condensed Bose gas; for example, at absolute zero, when all the particles are in the ground state,

$$R_1(\mathbf{q}_1\,;\,\mathbf{q}_1')=\Psi(\mathbf{q}_1)\Psi^*(\mathbf{q}_1'),$$
$$R_2(\mathbf{q}_1,\mathbf{q}_2\,;\,\mathbf{q}_1',\mathbf{q}_2')=\Psi(\mathbf{q}_1)\Psi(\mathbf{q}_2)\Psi^*(\mathbf{q}_1')\Psi^*(\mathbf{q}_2').$$

The correct formula is

$$R_2(\mathbf{q}_1,\mathbf{q}_2\,;\,\mathbf{q}_1',\mathbf{q}_2')=R_1(\mathbf{q}_1\,;\,\mathbf{q}_1')R_1(\mathbf{q}_2\,;\,\mathbf{q}_2')+R_1(\mathbf{q}_1\,;\,\mathbf{q}_2')R_1(\mathbf{q}_2\,;\,\mathbf{q}_1')$$
$$-\Psi(\mathbf{q}_1)\Psi(\mathbf{q}_2)\Psi^*(\mathbf{q}_1')\Psi^*(\mathbf{q}_2') \quad . \quad . \quad . \quad . \quad . \quad (17)$$

(compare London 1943). Assuming that this formula holds for non-equilibrium states, (10) and (11) may be verified, with

$$\mathrm{A}(\mathbf{q}, \mathbf{r})=\mathrm{R}_1(\mathbf{q}+\mathbf{r}\,;\ \mathbf{q}+\mathbf{r})+\mathrm{R}(\mathbf{q}\,;\ \mathbf{q}+\mathbf{r})\Psi(\mathbf{q}+\mathbf{r})/\Psi(\mathbf{q})-\Psi(\mathbf{q}+\mathbf{r})\Psi^*(\mathbf{q}+\mathbf{r}).$$

Madelung's transformation (1927) brings equations (15) and (16) into a form similar to the hydrodynamic equations of motion with velocity potential ϕ, density $|\Psi|^2$, external forces of potential V and a source distribution of strength $2|\Psi|^2\mathrm{W}/\hbar$:

$$\mathrm{R}_1(\mathbf{q}_1\,;\ \mathbf{q}_1')\sim\mathrm{Q}_\infty(\mathbf{q}_1\,;\ \mathbf{q}_1')\exp\{im[\phi(\mathbf{q}_1)-\phi(\mathbf{q}_1')]/\hbar\}, \quad . \quad . \quad (18)$$

where

$$\left.\begin{aligned} \mathrm{Q}_\infty(\mathbf{q}_1\,;\ \mathbf{q}_1')&=|\Psi(\mathbf{q}_1)|\,|\Psi(\mathbf{q}_1')|, \\ \partial|\Psi|^2/\partial t+\nabla\cdot(|\Psi|^2\nabla\phi)&=2|\Psi|^2\mathrm{W}/\hbar, \\ \partial\phi/\partial t+\tfrac{1}{2}(\nabla\phi)^2+\mathrm{V}/m&=\hbar^2\nabla^2|\Psi|/2m^2|\Psi|\simeq 0. \end{aligned}\right\} \quad . \quad . \quad . \quad . \quad (19)$$

At equilibrium Q_∞ depends only on the density and temperature, so that even for non-equilibrium states it is a function of the parameters of the classical description. On the other hand, the velocity $\nabla\phi$ corresponds to no quantity in the classical description; it differs from the classical velocity in its laws of change and in being irrotational.

§ 4. THE TWO-FLUID MODEL OF HELIUM II.

The two-fluid model may be interpreted tentatively as follows: Assume that real functions $\mathrm{Q}_n(\mathbf{q}_1\,;\ \mathbf{q}'_1)$ and $\mathrm{Q}_s(\mathbf{q}_1\,;\ \mathbf{q}_1')$ can be chosen, with $\mathrm{Q}_n\rightarrow 0$ as $|\mathbf{q}_1-\mathbf{q}_1'|\rightarrow\infty$, such that if at one instant

$$\begin{aligned} \mathrm{R}_1(\mathbf{q}_1\,;\ \mathbf{q}_1')=\mathrm{Q}_n(\mathbf{q}_1\,;\ \mathbf{q}_1')&\exp\{im(\mathbf{q}_1-\mathbf{q}_1')\cdot\mathbf{u}(\tfrac{1}{2}[\mathbf{q}_1+\mathbf{q}_1'])/\hbar\} \\ &+\mathrm{Q}_s(\mathbf{q}_1\,;\ \mathbf{q}_1')\exp\{im[\phi(\mathbf{q}_1)-\phi(\mathbf{q}_1')]/\hbar\} \\ &+\mathrm{O}(\nabla\mathbf{u})+\mathrm{O}(\nabla\nabla\phi). \quad . \quad . \quad . \quad . \quad . \quad . \quad . \quad . \quad . \quad (20) \end{aligned}$$

(where the velocities **u** and $\nabla\phi$ do not alter appreciably in a distance $\hbar(mk\mathrm{T})^{-1/2}$), then at later instants it is of the same form, with new real functions Q_n, Q_s, **u**, and ϕ. If $\mathrm{Q}_s=0$ this would describe a system with classical velocity field **u** (Gurov 1948). The density is

$$\begin{aligned} \rho(\mathbf{x})&=m\mathrm{R}(\mathbf{x}\,;\ \mathbf{x})=m\mathrm{Q}_n(\mathbf{x}\,;\ \mathbf{x})+m\mathrm{Q}_s(\mathbf{x}\,;\ \mathbf{x}) \\ &=\rho_n(\mathbf{x})+\rho_s(\mathbf{x}), \quad . \quad . \quad . \quad . \quad . \quad . \quad . \quad . \quad . \quad . \quad . \quad . \quad (21) \end{aligned}$$

and the current density (Born and Green 1948)

$$\begin{aligned} \mathbf{J}(\mathbf{x})&=-(i\hbar/2)(\nabla_1-\nabla_1')\mathrm{R}_1(\mathbf{q}_1\,;\ \mathbf{q}_1') \qquad [\mathbf{q}_1=\mathbf{q}_1'=\mathbf{x}] \\ &=\rho_n(\mathbf{x})\mathbf{u}(\mathbf{x})+\rho_s(\mathbf{x})\nabla\phi(\mathbf{x}). \quad . \quad . \quad . \quad . \quad . \quad . \quad . \quad . \quad . \quad (22) \end{aligned}$$

These two equations are the basis of the two-fluid theory (Landau 1941, Tisza 1947); in Landau's version the superfluid velocity is irrotational.

§ 5. EXAMPLES.

Two examples will illustrate the argument. In a crystal the single-molecule wave-functions are confined to small regions, so that (7) is true and classical ideas should explain its mechanical properties. In a condensed

Bose–Einstein gas with negligible repulsive forces and periodic boundary conditions (Bogoliubov 1947)

$$\left.\begin{aligned} R_1(\mathbf{q}_1\,;\ \mathbf{q}_1')&=B^{-1}\sum_{\mathbf{l}} n_{\mathbf{l}} \exp i\mathbf{l}\cdot(\mathbf{q}_1-\mathbf{q}_1'), \\ Q_\infty(\mathbf{q}_1\,;\ \mathbf{q}_1')&=n_0/B\neq 0, \end{aligned}\right\} \quad . \ . \ . \ . \ . \quad (23)$$

where B is the volume of the container and $n_{\mathbf{l}}$ is the mean occupation number of the single-particle state whose wave-number is **l**, given by

$$\left.\begin{aligned} n_{\mathbf{l}}&=[\exp(\mathbf{l}^2\hbar^2/2mkT)-1]^{-1}, \qquad [\mathbf{l}\neq 0], \\ \sum_{\mathbf{l}} n_{\mathbf{l}}&=N. \end{aligned}\right\} \quad . \ . \ . \quad (24)$$

Bogoliubov claimed that such a system shows superfluidity.

We conclude that (7) is the condition for the classical equations of heat transfer and hydrodynamics to apply, and that when (7) is not satisfied a new quantity enters the equations. This quantity is the potential of a new velocity field superimposed on the classical motion.

ACKNOWLEDGMENTS.

I am very much indebted to Mr. H. N. V. Temperley for supervising this work, to Mr. P. J. Price for discussions, to many of my colleagues for criticizing the manuscript, and to King's College, Cambridge, for awarding me the R. J. Smith Memorial Studentship.

REFERENCES.

BOGOLIUBOV, N. N., 1947, *J. Phys. U.S.S.R.*, **11,** 23.
BORN, M., and GREEN, H. S., 1947, *Proc. Roy. Soc.* A., **190,** 455; 1948, *Ibid.*, **191,** 168.
CHAPMAN, S., and COWLING, T. G., 1939, *The Mathematical Theory of Non-Uniform Gases*, (Cambridge: University Press) p. 117.
DIRAC, P. A. M., 1947, *The Principles of Quantum Mechanics*, 3rd edition, (Oxford: University Press) pp. 131–135.
GUROV, K. P., 1948, *Jour. Exp. and Theor. Phys. U.S.S.R.*, **18,** 110; 1950, *Ibid.*, **20,** 279.
HUSIMI, K., 1940, *Proc. Physico-Math. Soc. Japan*, [3] **22,** 264.
LANDAU, L., 1941, *J. Phys. U.S.S.R.*, **5,** 71.
LONDON, F., 1943, *J. Chem. Phys.*, **11,** 203.
MADELUNG, E., 1927, *Zeit. für Phys.*, **40,** 322.
MOYAL, J., 1949, *Proc. Camb. Phil. Soc.*, **45,** 99.
TISZA, L., 1947, *Phys. Rev.*, **72,** 838.
WIGNER, E. P., 1932, *Phys. Rev.*, **40,** 749.

CXXXVII. *On the Tomonaga Method for Intermediate Coupling in Meson Field Theory.*

By R. H. Dalitz and D. G. Ravenhall,
Department of Mathematical Physics, University of Birmingham.*

[Received August 3, 1951.]

Abstract.

The iteration method of Svartholm (1945) is employed to improve the approximate wave function used by Tomonaga (1947) to describe the scalar meson field of an isolated nucleon. It is found that this wave-function of Tomonaga is surprisingly good, even in the region of intermediate coupling, the change in coupling parameter for given energy being at most 3 per cent after the first iteration.

§ 1.

Comparison of recent experimental data concerning nucleon–nucleon interactions and meson production with the results of perturbation theory calculations, which depend on the smallness of the meson–nucleon interaction, shows that this interaction may not in fact be regarded as " weak ". For the opposite limit of " strong " coupling, Wentzel (1940) has proposed a semi-classical method, and more recently, Tomonaga (1947) has discussed a new approach to the problem, which covers also the intermediate region between these limiting cases. In this work of Wentzel and Tomonaga it was necessary to cut off the high momentum components of the meson field in an arbitrary way in order to obtain finite results. Recently Dyson (1951) has shown how by renormalization of mass and field strength a Hamiltonian can be obtained for which such difficulties do not occur. Accordingly it is of interest to re-examine Tomonaga's method, and it is the purpose of the present work to test the validity of the trial wave-functions proposed by Tomonaga, in the region of intermediate coupling.

§ 2.

Tomonaga investigates the stationary state of a nucleon coupled with a scalar meson field, considering the nucleon as infinitely heavy, so that its recoil and the creation of nucleon pairs are neglected. Here these assumptions are retained.

For charged mesons the Hamiltonian is, in this case,

$$\mathscr{H}=\int \omega(a_k^*a_k+b_k^*b_k)d^3k-l\int \mathrm{G}(\mathbf{k})[(a_k+b_k^*)\tau_++(a_k^*+b_k)\tau_-]d^3k, \quad . \quad (1)$$

---

* Communicated by Professor R. E. Peierls, F.R.S.

where a_k, a_k^* are annihilation and creation operators for the Fourier component $\mathbf{k}$ of the positive meson field, b_k, b_k^* the corresponding operators for negative mesons, and $\omega=\sqrt{(\mu^2+\mathbf{k}^2)}$. With $\mathrm{G}(\mathbf{k})$ as used below, the relation of l to g, the usual coupling constant, is $l=g\sqrt{(4\pi)}$. The divergence difficulties associated with the Hamiltonian (1) are avoided by including in $\mathrm{G}(\mathbf{k})$ a cut-off function $\mathrm{F}(\mathbf{k})$, and in the work below we shall find it convenient to use the expression

$$\mathrm{G}(\mathbf{k})=\mathrm{F}(\mathbf{k})/\sqrt{\omega}=e^{-\omega/\mathrm{M}}/\sqrt{\omega},$$

M being of the order of the nucleon mass. (In fact we have chosen $\mathrm{M}=5\,\mu$.)

Following Fock (1934) we let functions $\chi_{n,\,m}(\mathbf{k}_1\ldots\mathbf{k}_n\,;\;\mathbf{K}_1\ldots\mathbf{K}_m)$ describe the presence of n positive mesons of momenta $\mathbf{k}_1\ldots\mathbf{k}_n$, and m negative mesons of momenta $\mathbf{K}_1\ldots\mathbf{K}_m$. These functions are symmetrical for interchanges within $(\mathbf{k}_1\ldots\mathbf{k}_n)$ and $(\mathbf{K}_1\ldots\mathbf{K}_m)$ separately, and they vanish unless $n=m$, $m+1$ because of the requirement of charge conservation (for the case of a proton). The Schrödinger equation for a stationary state of the system,

$$\mathrm{E}\Psi=\mathscr{H}\Psi, \quad\ldots\ldots\ldots\ldots \quad (2)$$

becomes

$$\left.\begin{aligned}
&\mathrm{E}\chi_{00}=-l\int\mathrm{G}(\mathbf{k}_1)\chi_{10}(\mathbf{k}_1)d^3k_1,\\
&\ldots\ldots\ldots\ldots\ldots\ldots\ldots\ldots\ldots\ldots\ldots\ldots\ldots\ldots\ldots\ldots\ldots\ldots\ldots\ldots\ldots\ldots\ldots\ldots\\
&(\mathrm{E}-\Sigma_k\omega-\Sigma_{\mathrm{K}}\omega)\chi_{n,\,n}\\
&\quad=-l\left\{\frac{1}{\sqrt{n}}\sum_{i=1}^{n}\mathrm{G}(\mathbf{K}_i)\chi_{n,\,n-1}(\mathbf{k}_1\ldots\mathbf{k}_n\,;\,\mathbf{K}_1\ldots\mathbf{K}_{i-1}\,\mathbf{K}_{i+1}\ldots\mathbf{K}_n)\right.\\
&\qquad\left.+\sqrt{(n+1)}\int\mathrm{G}(\mathbf{k}_{n+1})\chi_{n+1,\,n}(\mathbf{k}_1\ldots\mathbf{k}_{n+1}\,;\,\mathbf{K}_1\ldots\mathbf{K}_n)d^3k_{n+1}\right\},\\
&(\mathrm{E}-\Sigma_k\omega-\Sigma_{\mathrm{K}}\omega)\chi_{n+1,\,n}\\
&\quad=-l\left\{\frac{1}{\sqrt{(n+1)}}\sum_{j=1}^{n+1}\mathrm{G}(\mathbf{k}_j)\chi_{n,\,n}(\mathbf{k}_1\ldots\mathbf{k}_{j-1}\,\mathbf{k}_{j+1}\ldots\mathbf{k}_{n+1}\,;\,\mathbf{K}_1\ldots\mathbf{K}_n)\right.\\
&\qquad\left.+\sqrt{(n+1)}\int\mathrm{G}(\mathbf{K}_{n+1})\chi_{n+1,\,n+1}(\mathbf{k}_1\ldots\mathbf{k}_{n+1}\,;\,\mathbf{K}_1\ldots\mathbf{K}_{n+1})d^3\mathrm{K}_{n+1}\right\},\\
&\ldots\ldots\ldots\ldots\ldots\ldots\ldots\ldots\ldots\ldots\ldots\ldots\ldots\ldots\ldots\ldots\ldots\ldots\ldots\ldots\ldots\ldots\ldots\ldots
\end{aligned}\right\}\quad(3)$$

Tomonaga proposed as an approximate solution of (3) the product function

$$\chi_{n,\,m}(\mathbf{k}_1\ldots\mathbf{k}_n\,;\;\mathbf{K}_1\ldots\mathbf{K}_m)=c_{n,m}\phi(\mathbf{k}_1)\ldots\phi(\mathbf{k}_n)\psi(\mathbf{K}_1)\ldots\psi(\mathbf{K}_m), \quad (4)$$

the functions ϕ, ψ being normalized, and the $c_{n,\,m}$ being chosen to minimize the expectation value of the energy of the system. For simplicity ϕ and ψ are taken to be of identical form, the most natural choice being

$$\phi(\mathbf{k})=\psi(\mathbf{k})=\mathrm{G}(\mathbf{k})/(\mathrm{K}_2\omega) \quad\ldots\ldots\ldots \quad (5)$$

where $K_2^2 = \int G^2(\mathbf{k}) d^3k/\omega^2$. A perturbation solution of (3) suggests the suitability of the form (5) for ϕ and ψ, and in fact for neutral mesons such a product form is an exact solution with (5) and suitable coefficients c_n.

It is clear that this is an adequate approximation in the limit of " weak " coupling, where the possibility of having more than one meson present is negligible. In the case of strong coupling Tomonaga shows that this wave-function leads to the same energy value as that given by the more rigorous theory of Wentzel. Physically this is clear, since the correlations between positive and negative mesons are unimportant when only $\chi_{n,m}$ involving many mesons contribute appreciably, and further, a wave-function of the form (4) is an exact solution for neutral mesons. Tomonaga also presents numerical calculations covering the region of intermediate coupling between these well-known limiting cases. It is clearly of interest to investigate to what extent the neglect of the correlation between the mesons, implied in (4), is justifiable in this intermediate region.

§ 3.

As in Svartholm's (1945) treatment of the momentum-space integral equation for the deuteron, we use the fact that the Schrödinger equation (3), which has the form

$$(E-T)\Psi = -lV\Psi, \quad \ldots \ldots \quad (6)$$

may be derived from the variational principle $\delta J = 0$, where

$$J = \langle \Psi^*(E-T)\Psi \rangle / \langle \Psi^* V \Psi \rangle. \quad \ldots \ldots \quad (7)$$

The minimum value $J_{\min}$ is simply the coupling parameter l for the assumed energy value.

In the present work it has been found convenient to restrict the wave-function (4) by requiring $c_{n,m}$ to be of the form

$$c_{n,m} = \alpha^n \beta^m / (n!\, m!\, N^2)^{\frac{1}{2}}, \quad \ldots \ldots \quad (8)$$

where

$$N^2 = \sum_{n=0}^{\infty} \left(\frac{\alpha^{2n}\beta^{2n}}{(n!)^2} + \frac{\alpha^{2n+2}\beta^{2n}}{n!\,(n+1)!} \right) = I_0(2\alpha\beta) + \frac{\alpha}{\beta} I_1(2\alpha\beta),$$

I_0 and I_1, being the Bessel functions of imaginary argument. With the wave-function (4) (referred to as $\chi^{(0)}$) then at once

$$(E-T)_{00} = \langle \chi^{(0)*}(E-T)\chi^{(0)} \rangle = \lambda \left\{ 2\alpha^2 I_0(2\alpha\beta) + \left(2\alpha\beta - \frac{\alpha}{\beta} \right) I_1(2\alpha\beta) \right\}, \quad (9\,a)$$

$$V_{00} = \langle \chi^{(0)*} V \chi^{(0)} \rangle = -2K_2 \lambda\alpha \{ I_0(2\alpha\beta) + I_1(2\alpha\beta) \}, \quad \ldots \ldots \quad (9\,b)$$

where $\lambda = \int \omega \phi^2(\mathbf{k}) d^3k = 2{\cdot}671\,\mu$. The ratio $(E-T)_{00}/V_{00}$ is then minimized by choice of α, β. This may be carried out analytically in the limiting cases of weak and strong coupling. With the notation $\kappa^2 = -E/\lambda$, for weak coupling $\alpha = \kappa + \ldots$, $\beta = \frac{1}{2}\kappa + \ldots$ and $K_2 l = \kappa(1 + \kappa^2/4 + \ldots)$, and for strong coupling $\alpha = \beta = \kappa$ with $K_2 l = \sqrt{2}\kappa(1 - 1/(4\kappa^2) + \ldots)$. Clearly the value of l does not depend critically on the choice of α and β, since

l is stationary. The values given here for l agree thus far with the corresponding expressions obtained from the more rigorous theories in these limits. For the several values of E chosen in the intermediate region it was found that the energy value obtained using the approximation (8) differed by less than 0·2 per cent from that obtained from the best possible choice for $c_{n,\,m}$.

§ 4.

Svartholm (1945) has proposed an iterative method for the solution of eigenvalue problems of the type (6), (7). From an initial function $\Psi^{(0)}$ a sequence of functions $\{\Psi^{(n)}\}$ is defined by the relation

$$(\mathrm{T}-\mathrm{E})\Psi^{(n)}=\mathrm{V}\Psi^{(n-1)}. \qquad (10)$$

Under the conditions that (T−E) and V are positive definite, he has proved that the sequence $l_0, l_{1/2}, l_1, \ldots, l_n, l_{n+1/2}, l_{n+1}, \ldots$ is monotonic decreasing, where $l_n=(\mathrm{T}-\mathrm{E})_{nn}/\mathrm{V}_{nn}$ and $l_{n+1/2}=\mathrm{V}_{nn}/(\mathrm{T}-\mathrm{E})_{n+1,\,n+1}$.

In the weak coupling limit the first steps of this process may be carried out directly. At once

$$\left.\begin{aligned} \chi_{00}^{(1)}&=\mathrm{K}_2\alpha\chi_{00}^{(0)}/\kappa,\\ \chi_{10}^{(1)}&=\mathrm{K}_2\chi_{10}^{(0)}(1+\alpha\beta\lambda/\omega)(1-\lambda\kappa^2/\omega+\ldots),\\ \chi_{11}^{(1)}&=\mathrm{K}_2\chi_{11}^{(0)}\alpha\omega_2/(\omega_1+\omega_2). \end{aligned}\right\} \qquad (11)$$

whence

$$\left.\begin{aligned} (\mathrm{E}-\mathrm{T})_{11}&=2\lambda\mathrm{K}_2^2(1+\mathscr{I}\kappa^2/2+\ldots),\\ \mathrm{V}_{11}&=2\lambda\mathrm{K}_2^3(1+(\mathscr{I}-\tfrac{1}{2})\kappa^2+\ldots), \end{aligned}\right\} \qquad (12)$$

where $\mathscr{I}$ is the definite integral $\iint\omega_2^2\phi^2(\mathbf{k}_1)\phi^2(\mathbf{k}_2)d^3k_1d^3k_2/(\lambda(\omega_1+\omega_2))$. (In fact $\mathscr{I}=0{\cdot}568$.) The sequence $\{l_n\}$ is then

$$\left.\begin{aligned} l_0&=\kappa(1+\kappa^2/4+\ldots)/\mathrm{K}_2,\\ l_{1/2}=l_1&=\kappa(1+(1-\mathscr{I})\kappa^2/2+\ldots)/\mathrm{K}_2. \end{aligned}\right\} \qquad (13)$$

It is apparent from (13) that the important modification of the wave function is that $\chi^{(1)}$ allows to some extent for the correlation between the various mesons. In the same way, $(l_0-l_{\frac{1}{2}})/l_0$ has been calculated as far as terms of order κ^4, as shown in curve (A) of the figure.

§ 5.

In the general case, the iterated functions are given by

$$\chi_{n,n}^{(1)}(\mathbf{k}\,;\ \mathbf{K})=\mathrm{K}_2\chi_{n,n}^{(0)}(\mathbf{k}\,;\ \mathbf{K})\{(\Sigma_{\mathrm{K}}\omega)/\beta+\lambda\alpha\}/(\mathrm{E}-\Sigma_k\omega-\Sigma_{\mathrm{K}}\omega), \qquad (14\,a)$$

$$\chi_{n+1,n}^{(1)}(\mathbf{k}\,;\ \mathbf{K})=\mathrm{K}_2\chi_{n+1,n}^{(0)}(\mathbf{k}\,;\ \mathbf{K})\{(\Sigma_k\omega)/\alpha+\lambda\beta\}/(\mathrm{E}-\Sigma_k\omega-\Sigma_{\mathrm{K}}\omega), \qquad (14\,b)$$

from which $(\mathrm{E}-\mathrm{T})_{11}$ and V_{11} may be calculated. For this the integral representation

$$\frac{\mu}{-\mathrm{E}+\Sigma\omega}=\int_0^\infty e^{(\mathrm{E}-\Sigma\omega)t/\mu}\,dt \qquad (15)$$

is found convenient, and the expression finally obtained is

$$(\mathrm{E}-\mathrm{T})_{11}=-\mathrm{K}_2^2\mu\int_0^{\infty} e^{\mathrm{E}t/\mu}\,dt\left[\left(\mathrm{I}_0+\frac{\alpha}{\beta}\mathrm{I}_1\right)(\mathrm{D}_2+2\lambda\alpha\beta\mathrm{D}_1/\mu)\right.$$
$$\left.+\lambda^2\alpha\beta\left(\frac{\alpha}{\beta}\mathrm{I}_0+\mathrm{I}_1\right)\Big/\mu^2+\mathrm{D}_1^2\alpha\beta\left(\mathrm{I}_1+\frac{\alpha}{\beta}\mathrm{I}_2\right)\right], \quad . \quad . \quad (16)$$

in which $\mathrm{I}_0=\mathrm{I}_0(2\alpha\beta\mathrm{D}_0)$, $\mathrm{I}_1=\mathrm{I}_1(2\alpha\beta\mathrm{D}_0)$, $\mathrm{I}_2=\mathrm{I}_2(2\alpha\beta\mathrm{D}_0)$, D_0, D_1, and D_2 being the integrals $\mathrm{D}_n(t)=\int\omega^n e^{-\omega t/\mu}\phi^2(\mathbf{k})d^3k/\mu^n$, expressible in terms of Bessel functions K_n and their integrals. A similar but more complex expression may also be obtained for V_{11} but this will not be required here.

The expression (16) has been obtained numerically for three energy values, and the coupling constants l_0, $l_{\frac{1}{2}}$ calculated. The results are expressed in the table.

$-\mathrm{E}/\mu$	α	β	$-(\mathrm{E}-\mathrm{T})_{00}/\mu$	$-\mathrm{V}_{00}/\mu$	$-(\mathrm{E}-\mathrm{T})_{11}/\mu$	l_0	$l_{\frac{1}{2}}$
8	1·26	1·04	13·89	16·03	18·88	0·866	0·849
4	0·95	0·675	6·64	11·56	20·65	0·574	0·560
2	0·73	0·455	3·44	8·86	23·86	0·380	0·372

Table of values of α, β, $(\mathrm{E}-\mathrm{T})_{00}$, V_{00}, $(\mathrm{E}-\mathrm{T})_{11}$, l_0, and $l_{\frac{1}{2}}$ for some values of E.

Fig. 1.

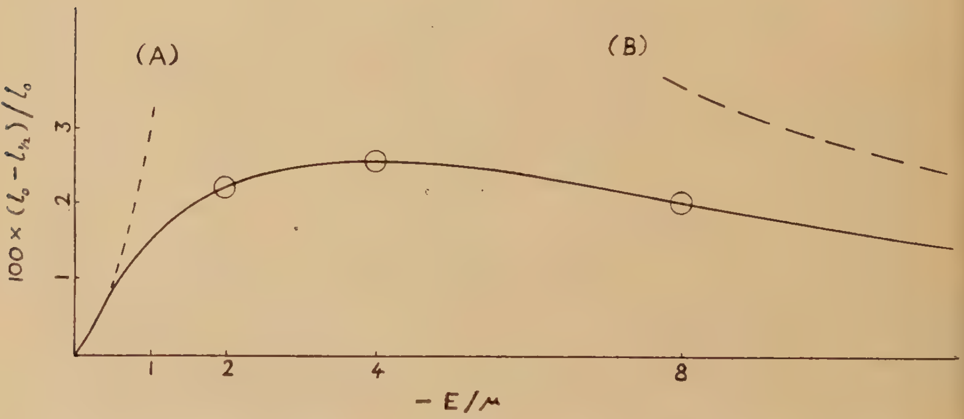

The proportional change produced in l_0 by the first iteration, as a function of the energy.

In the limit of strong coupling, asymptotic expressions for I_0, I_1, I_2 may be used to obtain an analytical expression for $(\mathrm{E}-\mathrm{T})_{11}$. With $\alpha=\beta=\kappa$ this leads finally to

$$(\mathrm{E}-\mathrm{T})_{11}=\frac{e^{2\kappa^2}}{\sqrt{\pi\kappa}}\lambda(1+(2\mu^2\mathrm{D}_2(0)-\lambda^2)/(8\lambda^2\kappa^2)+\ldots),$$

whence $l_{\frac{1}{2}}=\sqrt{2}\kappa(1-\mu^2\mathrm{D}_2(0)/(4\lambda^2\kappa^2)+\ldots)$, in comparison with the value $l_0=\sqrt{2}\kappa(1-1/(4\kappa^2))$. The proportional improvement in the value of l_0 is sketched in the accompanying graph, together with the curves (A) and (B) obtained in the limiting cases.

It should be noted that because of the arbitrariness in the cut-off used in (1) the physically significant quantities are not l_0, $l_{\frac{1}{2}}$, . . . but α and β, which by (8) give a measure of the average number of mesons present in the system.

§ 6.

The eigenvalue equation (6) will have a series of eigenvalues $l^{(0)}$, $l^{(1)}$, . . . $l^{(n)}$, . . . with corresponding eigen-functions ψ_0, . . . ψ_n, . . . satisfying the orthogonality relations $(\psi_n, \mathrm{V}\psi_m)=0$ unless $m=n$. If the initial wave function $\Psi^{(0)}$ for the iteration procedure is

$$\Psi^{(0)}=\sum_n a_n\psi_n,$$

then the rth iterated wave function $\Psi^{(r)}$ is

$$\Psi^{(r)}=\sum_n a_n\psi_n/(l^{(n)})^r,$$

so that if $l^{(1)}$, . . . greatly exceed the lowest eigenvalue $l^{(0)}$, the rate of convergence to the wave function ψ_0 is rapid. The sequence of approximations $\{l^{(0)}_{s/2}\}$ of Svartholm may then be expressed in the form

$$l^{(0)}_{s/2}=\frac{\sum_n |a_n|^2\mathcal{T}_{nn}/(l^{(n)})^s}{\sum_n |a_n|^2\mathcal{T}_{nn}/(l^{(n)})^{s+1}},$$

where $\mathcal{T}_{nn}$ is the expectation value of (T—E) in state ψ_n. Accordingly the first step in the sequence $\{l^{(0)}_{s/2}\}$ should provide the major correction to $l^{(0)}_0$ provided the ratios $l^{(0)}/l^{(n)}$ are sufficiently small, which will be the case if there do not exist any low-lying excited nucleon states—in fact, with this assumption,

$$(l^{(0)}_{1/2}-l^{(0)}_1)/(l^{(0)}_0-l^{(0)}_{1/2})\simeq l^{(0)}/l^{(1)}$$

and

$$(l_0-l_{1/2})/l_0\simeq\sum_{n=1}^{\infty}\left|\frac{a_n}{a_0}\right|^2\mathcal{T}_{nn}/\mathcal{T}_{00},$$

if $\Psi^{(0)}$ is a good approximation to ψ_0. In the present work we have found that $(l_0-l_{\frac{1}{2}})/l_0$ does not exceed 3 per cent so that the wave function of Tomonaga appears to be a surprisingly good approximation to ψ_0, even in the region of intermediate coupling.

We should like to thank Professor Peierls (who suggested this investigation) and Mr. F. J. Dyson for their stimulating interest. One of us (D. G. R.) acknowledges with thanks financial support from the Department of Scientific and Industrial Research.

REFERENCES.

DYSON, F. J., 1951, *Proc. Roy. Soc.*, **207**, 395.
FOCK, V., 1932, *Zeit. f. Phys.*, **75**, 622.
SVARTHOLM, N., 1945, *Univ. Lund* (Thesis Phys. Inst.).
TOMONAGA, S., 1947, *Prog. Theor. Phys.*, **2**, 6.
WENTZEL, G., 1940, *Helv. Phys. Acta*, **13**, (4), 269.

CXXXVIII. *Application of Dislocation Theory to the Polytypism of Silicon Carbide.*

By V. VAND*,
Chemistry Department, The University, Glasgow†.

[Received June 8, 1951. Revised copy received July 14, 1951. Amended copy received August 1, 1951.]

ABSTRACT.

Polytypism of silicon carbide can be understood if the assumption is made that the crystal grows out of the primary nucleus as a single sheet several atomic layers in thickness. The sheet winds itself spirally upwards along a bunch of screw dislocations which are situated at the spiral axis. If there are stacking faults in the original growth layer, they repeat themselves with the periodicity of the pitch of the screw throughout the crystal and thus determine the type and the dimensions of the unit cell. Similar typism occurs in graphite and possibly in diamond and other substances.

AFTER Frank (1951) drew our attention to the existence of spiral growth-steps on carborundum crystals, we examined several hundred well-developed crystals of artificial silicon carbide. The crystal surfaces were not treated in any way and were examined under an optical microscope, using oblique illumination at low magnification. Spiral growth markings, similar to those described by Verma (1951) in the preceding paper, were observed on about 3 per cent of the crystals examined. Some of the steps are obviously many atomic layers in height, whereas some are revealed by preferential deposition or crystal overgrowth of foreign matter, the step acting as a nucleus for overgrowth.

In some cases, preferential etching seemed to take place along the groove of the spiral. In one case a previously invisible spiral has been made plainly visible by smearing and wiping off grease from the crystal face. Some grease deposit remained caught near the spiral step, thus modifying the reflecting power of the crystal surface.

Curved spirals of a type described by Menzies and Sloat (1929) and straight-edged triangular and hexagonal spirals were observed. The outline of the crystal usually bears a close relationship to the shape of the spiral.

We have reached independently similar conclusions regarding the origin of the polytypism of carborundum to those put forward by Frank (1951) in the preceding paper.

---

* I.C.I. Research Fellow.

† Communicated by the Author.

In carborundum crystals the [0001] face, which shows the spiral growth-steps, is the slowest-growing face. If we limit ourselves to the conditions of growth at low supersaturation, then the presence of a primary nucleus initiating a single screw dislocation line would give rise to a needle with the dislocation line as its axis. The cross-section of the needle would remain constant and equal to that of the primary nucleus. Similarly, two straight screw dislocation lines which are not parallel would give rise to a very thin plate of a thickness equal to that of the primary nucleus.

Assuming straight dislocation lines, a crystal can grow in three dimensions only when three screw dislocations are present, not all in the same plane. This rule does not hold for curved dislocation lines, but in general, three-dimensional growth cannot proceed unless there are points of emergence of dislocation lines on at least three different (non-parallel) faces of the crystal.

One can imagine that the first stages of the crystal growth are very thin needles or plates based on one or two straight dislocation lines. However, when dimensions of these exceed certain critical limits, they become very fragile. Depending on the stresses imposed by the environment, deformation and breakage would ultimately occur. If the broken parts carry with them screw dislocations, as needles must do, they can serve as new nuclei (this probably accounts for the hitherto unexplained multiplication of ice nuclei in the high atmosphere), whereas cracks and slip deformations in thin plates, as suggested by Frank in the preceding paper, would give rise to growth-steps having large Burgers (1939) vectors.

It is likely that in carborundum crystals, small steps grow faster than larger ones. The original short screw dislocations, which initiated the plate growth, would in most cases remain unaltered by cracking, so that the plate sides would remain fast-growing. However, if the large face of the plate acquires a screw dislocation with a large Burgers vector, it begins to grow, but remains the slowest-growing face. Even if further dislocations with the small Burgers vector appear on the same face, the large dislocation would tend to remain dominant ; the fast-growing small steps would merge with the large steps when overtaking them.

The crystal can be essentially pictured as a single growth-sheet several atomic layers in thickness, which winds itself upwards spirally using the large Burgers vector as its axis. Provided there is a mistake in the growth-sheet and the dislocation is stable, *i. e.* no new dislocations appear or disappear during growth, the crystal would exhibit periodicity determined by the length of the Burgers vector and the type of the mistake in stacking.

It is most likely that silicon carbide is only one typical example of the occurrence of polytypism by spiral growth from screw dislocations possessing a large Burgers vector. Similar behaviour is to be expected in numerous other substances, the crystals of which grow out by the screw dislocation mechanism. Silicon carbide shows this type of behaviour to a marked extent because of the great stability of its screw dislocation system. Other softer substances probably do not possess such stability and the phenomenon would occur only on a microscopic scale. Graphite behaves in such a manner, as polytypism similar to that of carborundum has been observed by Lipson and Stokes (1942 a, 1942 b) by X-rays and Hoerni (1949) on individual microcrystals by electron diffraction technique. However, the most interesting case might prove to be that of diamond, which should probably behave in the same manner as silicon carbide. Curved faces and edges appear on diamond. Tolansky and Wilcock (1946) have shown that the curved faces are the result of successive stepped growth-sheets. These almost certainly originate as spirals at growth-points located near the centre of the face. It is well known that at least two modifications of diamond, types I. and II., exist. It is therefore to be expected that if not the whole, then at least substantial parts of each crystal of diamond should be all of the same type, as in silicon carbide crystals. Thibault (1944) also mentions the minerals coquimbite and paracoquimbite, both $Fe_2O_3 . 3SO_3 . 9H_2O$ and parisite and synchisite, both $(CeF)_2\ Ca(CO_3)_3$ as displaying polytypism similar to silicon carbide.

I wish to thank Professor J. Monteath Robertson, F.R.S., for his interest, Dr. I. M. Dawson and Dr. F. C. Frank for valuable discussions on the subject of dislocations and Professor M. J. Buerger for pointing out the necessity of three dislocations and Dr. E. D. Currie and Dr. A. Taylor for the loan of carborundum samples.

REFERENCES.

BURGERS, J. M., 1939, *Proc. Kon. Akad. Wet.*, **42,** 294, 378.
FRANK, F. C., 1951, *Phil. Mag.*, **42,** 1014.
HOERNI, J., 1949, *Nature*, **167,** 1045.
LIPSON, H., and STOKES, A. R., 1942 a, *Nature*, **149,** 328 ; 1942 b, *Proc. Roy. Soc.*, **181,** 101.
MENZIES, A. W. C., and SLOAT, C. A., 1929, *Nature*, **123,** 348.
THIBAULT, N. W., 1944, *Amer. Mineralogist*, **29,** 249, 327.
TOLANSKY, S., and WILCOCK, W. L., 1946, *Nature*, **157,** 583.
VERMA, A. R., 1951, *Phil. Mag.*, **42,** 1005.

CXXXIX. *The Fitting of Polynomials to Unequally-Spaced Data.*

By J. G. HAYES and T. VICKERS,
National Physical Laboratory, Middlesex *.

[Received July 10, 1951.]

SUMMARY.

A technique is given for carrying out rapidly the computations involved in fitting a polynomial by least squares to unequally-spaced data. The technique is obtained by adapting the " triangular resolution " methods of solution of linear equations and inversion of matrices given by Fox (1950) and Fox and Hayes (1951) in a way similar to that in which Guest (1950) has adapted a slower method of Doolittle. The method proposed affords the additional advantage of being able to decide, early in the computation, which degree of polynomial curve is appropriate to the data. The theory is presented to establish the validity of the technique and two numerical examples are carried out to deal with two different sets of requirements.

References are made throughout the text to the appropriate sections of the above three papers, but the present paper is intended to be complete in itself, and does not require a prior knowledge of those papers.

§1. INTRODUCTION.

THE use of orthogonal polynomials in the fitting of regression polynomials to equally-spaced observations is now well-known, accounts of it having been given by several authors, *e. g.* Fisher and Yates (1943). In this case the method has considerable advantages over the straightforward method of solving the normal equations derived from the power terms of the regression polynomial, but these advantages are lost in the case of unequally-spaced observations and it is usual to fall back on the straightforward method as the quickest way to carry out the computation.

Guest (1950) has, however, given a method of computation for this case which, while solving the normal equations of the power terms, adapts the solution to keep in view the technique of orthogonal polynomials and thereby preserves many of the advantages of this technique. No work is saved in the calculation of the regression coefficients, but Guest's method does obtain all curves of degree less than p, and their associated residual sums of squares, in the calculation for the curve of degree p, thus enabling the curve of degree best suited to the data to be selected at the end of the calculation. This process has the further important advantage that the calculation of the standard errors of the coefficients of the power terms and of the standard errors of points on the estimated regression curve is considerably simplified.

---

* Communication from the National Physical Laboratory.

The method of solving the normal equations which Guest adapts for this purpose is that of Doolittle, but much of the gain due to using such a systematic method of solution is nullified since he writes down the results of all the multiplications in the computation before summing them instead of, as is usual, accumulating the products on a desk calculating machine and writing down only the sums. Consequently, as Guest states, the arithmetic becomes extremely tiresome in the fitting of curves of degree higher than the third. This extension would, however, be quite straightforward if Doolittle's method were followed rather more closely.

There are now available, however, methods of solution of linear equations and inversion of matrices which are far quicker than this method of Doolittle. Some of these, depending on the technique of "triangular resolution", have been recently presented in papers by Fox (1950) and Fox and Hayes (1951) with particular emphasis on arrangement on the computing sheet. We are concerned here only with those methods for symmetric matrices. The present paper adopts these methods, as Guest has done with Doolittle's method, to the fitting of polynomial curves to unequally-spaced data, preserving, at the same time, the above-mentioned advantages of orthogonal representation.

The major gain in the proposed method, beyond that of the use of a quicker method of inversion, is due to the inclusion of a method of obtaining very early in the computation—in fact, in its first stage—the contribution to the total sum of squares of each of the orthogonal polynomials. With this information, we are able to determine which degree of polynomial is best suited to the data and thus carry out the rest of the calculation for a polynomial of this degree, thereby saving the work of computing, for example, an eighth degree polynomial when a fourth degree one proves to be quite adequate.

Moreover, the elementary matrix theory given by Fox (1950) to develop the "triangular resolution" technique can easily be extended to fulfil our present purpose, and enables the theory underlying our method of fitting polynomials by least squares to be presented very concisely.

The theory of our method is presented in the following sections, but its only purpose is to demonstrate the validity of the computational technique given in the examples, which can easily be carried out by computors having no knowledge of the matrix theory.

Two examples are given which involve slightly different forms of the basic method, designed to meet two different sets of requirements. The data used in the examples are those given by Guest (1950), to enable a direct comparison to be made with his method.

§2. THEORY.

(a) *Fitting of Power Terms.*

The usual algebra for the fitting of the power terms of the regression polynomial by least squares is now outlined in matrix notation. Matrices will be denoted by capital letters in Clarendon type, except for those with only one column, which will be denoted by small letters in Clarendon type.

We have a "dependent" variable y which we take to be related to the "independent" variable x by the equation, of degree q in x,

$$y=\mathbf{x}'\mathbf{b}+\delta, \qquad (1)$$

where $\mathbf{x}'=[1\ x\ x^2\ \ldots\ x^q]$, $\mathbf{b}'=[b_0\ b_1\ \ldots\ b_q]$, the row matrix of the coefficients of corresponding powers of x, and δ is the error term, which, as usual, we take to be normally distributed with mean zero and variance σ^2 independent of x.

Our problem is to estimate the b_r, the standard errors of these estimates, and the standard error of any point on the estimated regression curve.

We make n pairs of observations x_s, y_s $(s=1, \ldots, n)$ of x and y respectively, and our n equations of the form of (1) are represented by

$$\mathbf{y}=\mathbf{X}'\mathbf{b}+\boldsymbol{\delta}, \qquad (2)$$

where $\mathbf{y}'=[y_1\ y_2\ \ldots\ y_n]$, $\mathbf{X}=[\mathbf{x}_1\ \mathbf{x}_2\ \ldots\ \mathbf{x}_n]$ and $\boldsymbol{\delta}$ is the column matrix of the random errors $\delta_1, \delta_2, \ldots, \delta_n$, which are assumed to be statistically independent of each other.

Regression Coefficients.

We then minimize $\Sigma\delta_r^2\equiv\boldsymbol{\delta}'\boldsymbol{\delta}\equiv[\mathbf{y}'-\mathbf{b}'\mathbf{X}][\mathbf{y}-\mathbf{X}'\mathbf{b}]$ with respect to $\mathbf{b}$, obtaining the normal equations

$$\mathbf{X}\mathbf{X}'\hat{\mathbf{b}}=\mathbf{X}\mathbf{y},$$

where $\hat{\mathbf{b}}$ is our estimate of $\mathbf{b}$.

We shall write this as

$$\mathbf{A}\hat{\mathbf{b}}=\mathbf{h}, \qquad (3)$$

where

$$\mathbf{A}=\mathbf{X}\mathbf{X}', \qquad (4)$$

$$\mathbf{h}=\mathbf{X}\mathbf{y}. \qquad (5)$$

Our estimated regression curve is then

$$y=\mathbf{x}'\hat{\mathbf{b}}, \qquad (6)$$

where $\hat{\mathbf{b}}$ is the solution of equation (3).

Residual Mean Square.

The sum of squares of residuals is

$$[\mathbf{y}'-\hat{\mathbf{b}}'\mathbf{X}][\mathbf{y}-\mathbf{X}'\hat{\mathbf{b}}]$$

which reduces to

$$\mathbf{y}'\mathbf{y}-\hat{\mathbf{b}}'\mathbf{h}.$$

The mean square of residuals, which estimates σ^2 is then

$$s_{\mathrm{R}}^2=\frac{1}{n-q-1}(\mathbf{y}'\mathbf{y}-\hat{\mathbf{b}}'\mathbf{h}). \qquad (7)$$

Standard Errors of Regression Coefficients.

We have, from equations (2) and (3),

$$\hat{\mathbf{b}}-\mathbf{b}=\mathbf{A}^{-1}\mathbf{X}\boldsymbol{\delta}.$$

Thus, since $E(\boldsymbol{\delta})=0$,

$$E(\hat{\mathbf{b}})=\mathbf{b}$$

and the sampling covariance matrix of the $\hat{b}_r$ is therefore

$$E(\hat{\mathbf{b}}-\mathbf{b})(\hat{\mathbf{b}}'-\mathbf{b}')=E(\mathbf{A}^{-1}\mathbf{X}\boldsymbol{\delta}\boldsymbol{\delta}'\mathbf{X}'\mathbf{A}^{-1}).$$

But, since further the δ_r are independent and have variance σ^2, we have

$$E(\boldsymbol{\delta}\boldsymbol{\delta}')=\sigma^2\mathbf{I},$$

where $\mathbf{I}$ is the unit matrix of order n, and therefore

$$E(\hat{\mathbf{b}}-\mathbf{b})(\hat{\mathbf{b}}'-\mathbf{b}')=\sigma^2\mathbf{A}^{-1}\mathbf{X}\mathbf{X}'\mathbf{A}^{-1},$$

which, using equation (4),

$$=\sigma^2\mathbf{A}^{-1}, \quad \ldots\ldots\ldots \quad (8)$$

where σ^2 is estimated by s_R^2.

Our estimate of the sampling variance of $\hat{b}_r$ is therefore

$$V(\hat{b}_r)=s_R^2 a^{(r,\,r)}, \quad \ldots\ldots\ldots \quad (9)$$

where $a^{(r,\,r)}$ is the element (r, r) of $\mathbf{A}^{-1}$, $r=0, \ldots, q$.

Standard Error of Estimated y.

If now, for any given value of x, we wish to estimate the corresponding value of y, we use our estimated regression curve

$$y=\mathbf{x}'\hat{\mathbf{b}}$$

and the sampling variance of this estimate is

$$E\{y-E(y)\}^2=E\{\mathbf{x}'(\hat{\mathbf{b}}-\mathbf{b})(\hat{\mathbf{b}}'-\mathbf{b}')\mathbf{x}\},$$

which, by equation (8),

$$=\sigma^2\mathbf{x}'\mathbf{A}^{-1}\mathbf{x}, \quad \ldots\ldots\ldots \quad (10)$$

where s_R^2 is again used to estimate σ^2.

Our estimate of the sampling variance can therefore be written as

$$V(y_e)=s_R^2 \sum_{r=0}^{q} \sum_{s=0}^{q} x^r a^{(r,\,s)} x^s$$

$$=s_R^2 \sum_{r=0}^{q} \sum_{s=0}^{q} x^{r+s} a^{(r,\,s)},$$

giving

$$V(y_e)=s_R^2 \sum_{m=0}^{2q} x^m u_m, \quad \ldots\ldots\ldots \quad (11)$$

where

$$u_m=\sum_{r+s=m} a^{(r,\,s)}, \qquad 0\leqslant r, \quad s\leqslant q.$$

Our computation, therefore, has to provide the solution, $\hat{\mathbf{b}}$, of the equation (3), and also the inverse of the matrix $\mathbf{A}$ so that we can determine $V(\hat{b}_r)$ and $V(y_e)$, our estimates of the sampling variances, from equations (9) and (11).

(b) *Orthogonal Polynomials.*

We shall now give the algebra for the least squares fitting of the regression curve by means of orthogonal polynomials in order to demonstrate how this approach can be of assistance in the fitting of the power terms of the regression polynomial, dealt with in the previous section, particularly with regard to an early decision on which degree of polynomial is best suited to the data. The methods for the solution of linear equations and the inversion of matrices dealt with by Fox (1950) and Fox and Hayes (1951) lend themselves easily to this approach.

The basis of these methods for the symmetric case, in which we are interested, is the resolution of the matrix **A** into the product of a lower triangular matrix **L** and its transpose **L**′. That is, we obtain **L** such that

$$\mathbf{A}=\mathbf{L}\mathbf{L}', \qquad (12)$$

where **L** has zeros above the principal diagonal.

The orthogonal polynomials, p_r, which we shall consider in fitting our polynomial curve are given by

$$p_r=\sum_{s=0}^{r} l^{(r,\,s)}\,.\,x^s, \qquad r=0,\,1,\,\ldots,\,q,$$

where $l^{(r,\,s)}$ is the element $(r,\,s)$ in $\mathbf{L}^{-1}$, also a lower triangular matrix.

In matrix notation these can be written as

$$\mathbf{p}=\mathbf{L}^{-1}\mathbf{x}. \qquad (13)$$

Our n observations, $\mathbf{p}_1,\ldots,\mathbf{p}_n$, of $\mathbf{p}$ are then given by

$$\mathbf{P}=\mathbf{L}^{-1}\mathbf{X},$$

where $\mathbf{P}=[\mathbf{p}_1\,\mathbf{p}_2\cdots\mathbf{p}_n]$.

That these polynomials are, in fact, orthogonal can be seen at once, since

$$\begin{aligned}\mathbf{P}\mathbf{P}'&=\mathbf{L}^{-1}\mathbf{X}\mathbf{X}'(\mathbf{L}^{-1})',\\&=\mathbf{L}^{-1}\mathbf{A}(\mathbf{L}^{-1})' &&\text{from (4)},\\&=\mathbf{L}^{-1}\mathbf{L}\mathbf{L}'(\mathbf{L}^{-1})' &&\text{from (12)},\end{aligned}$$

giving

$$\mathbf{P}\mathbf{P}'=\mathbf{I}, \qquad (14)$$

where **I** is the unit matrix of order $(q+1)$.

These orthogonal polynomials are not the ones used by Guest (1950), but are multiples of them. One coefficient in each of the $(q+1)$ polynomials can be chosen arbitrarily: Guest has made the coefficient of the highest power of x in each polynomial equal to unity, whereas we have chosen the polynomials which produce equation (14).

In fitting to our observations a regression curve in the form of a sum of these orthogonal polynomials, we write the fundamental equation (1) in the form

$$y=\mathbf{p}'\mathbf{c}+\delta, \qquad (1')$$

where

$$\mathbf{p}'\mathbf{c}\equiv\mathbf{x}'\mathbf{b}.$$

Similarly, in place of equation (2), we have

$$\mathbf{y}=\mathbf{P}'\mathbf{c}+\boldsymbol{\delta} \quad . \quad . \quad . \quad . \quad . \quad . \quad . \quad . \quad (2')$$

and we estimate $\mathbf{c}$ by $\hat{\mathbf{c}}$, obtained by minimizing $\boldsymbol{\delta}'\boldsymbol{\delta}$ with respect to $\mathbf{c}$.

The algebra is then exactly the same as in the previous section with $\mathbf{X}$ replaced by $\mathbf{P}$ and $\hat{\mathbf{b}}$ replaced by $\hat{\mathbf{c}}$.

Also, therefore,

$\mathbf{A}(\equiv\mathbf{XX}')$ is replaced by $\mathbf{PP}'$, which is equal to $\mathbf{I}$,

and

$\mathbf{h}(\equiv\mathbf{Xy})$ is replaced by $\mathbf{Py}$, which is equal to $\mathbf{L}^{-1}\mathbf{h}$.

Our estimate $\hat{\mathbf{c}}$ is therefore given by the equation (corresponding to equation (3))

$$\hat{\mathbf{c}}=\mathbf{L}^{-1}\mathbf{h}, \quad . \quad . \quad . \quad . \quad . \quad . \quad . \quad . \quad (3')$$

and our estimated regression curve is

$$y=\mathbf{p}'\hat{\mathbf{c}}. \quad . \quad . \quad . \quad . \quad . \quad . \quad . \quad . \quad (6')$$

This curve is, of course, identical with that of the previous section (equation (6)), as can easily be shown algebraically using equations (3′), (13), (12) and (3).

Similarly, equation (7) becomes the equivalent equation

$$s_{\mathrm{R}}^2=\frac{1}{n-q-1}(\mathbf{y}'\mathbf{y}-\hat{\mathbf{c}}'\mathbf{L}^{-1}\mathbf{h}),$$

or, in a more usual form, from equation (3′),

$$\left.\begin{aligned} s_{\mathrm{R}}^2&=\frac{1}{n-q-1}(\mathbf{y}'\mathbf{y}-\hat{\mathbf{c}}'\hat{\mathbf{c}}),\\ \text{or}\qquad & \\ s_{\mathrm{R}}^2&=\frac{1}{n-q-1}\left(\sum_{r=1}^{n}y_r^2-\sum_{r=0}^{q}\hat{c}_r^2\right). \end{aligned}\right\} \quad . \quad . \quad . \quad . \quad . \quad (7')$$

Finally, equation (9) becomes,

$$\mathrm{V}(\hat{c}_i)=s_{\mathrm{R}}^2, \quad . \quad . \quad . \quad . \quad . \quad . \quad . \quad . \quad (9')$$

which is not usually of any interest to us, and equation (11), written in the form of equation (10), becomes the equivalent equation

$$\mathrm{V}(y_e)=s_{\mathrm{R}}^2\cdot\mathbf{p}'\mathbf{p}. \quad . \quad . \quad . \quad . \quad . \quad . \quad . \quad . \quad (11')$$

It is equation (3′), together with equation (7′), which proves to be of value in obtaining the standard errors associated with the regression curve. We know that $\hat{c}_r^2$ is the reduction in the total sum of squares due to fitting the orthogonal polynomial of degree r, and, therefore, what is equivalent, $\hat{c}_r^2$ is the extra amount removed from the total sum of squares when a power series of degree r is fitted instead of a power series of degree $(r-1)$. (It may be noted, incidentally, that this latter fact can easily be established as an algebraic identity without reference to orthogonal polynomials, $\hat{\mathbf{c}}$ then being *defined* by equation (3′). The use of these polynomials, however, allows a better understanding of the computational procedure and of the meaning of the numbers that occur in the calculations.)

The coefficients $\hat{c}_r$ are, in fact, produced as by-products in the first stage of the solution of linear equations for the symmetric case, as given by Fox (1950) in his Example 4: **L** is produced a column at a time, and as column r is produced so also is the element r of a row matrix $\mathbf{z}'$, which is the solution of the equation

$$\mathbf{Lz}=\mathbf{h}.$$

(In Fox's notation this is $\mathbf{Ly}=\mathbf{b}$.) That is,

$$\mathbf{z}=\mathbf{L}^{-1}\mathbf{h}.$$

$\mathbf{z}$ is, therefore, from equation (3′), our column of coefficients $\hat{c}_r$. By considering the reduction in the total sum of squares due to each $\hat{c}_r$ in turn as it is produced at the end of column r of **L**, we can decide which degree of power series is most appropriate to our data, and can complete our computation for this degree. We thus save the waste of labour which is consequent on calculating a regression series which proves to be either too short or too long.

§3. DETAILS OF COMPUTATION.

A decision has to be taken as to what degree of polynomial curve is to be considered at the start, that is, what is the highest power of x we are going to use in calculating the sums of squares and products (the elements of **A** and **h**). Since, however, we shall know very early in the subsequent calculation which degree of polynomial is, in fact, appropriate to our data, this decision is of only minor importance: if we find that we have used too high a power we merely delete the unnecessary elements of **A**, **L**, etc.; if we find that we have used too low a power we calculate the further sums of powers and products and elements of **L** as required, incurring no unnecessary calculation other than the trivial adjustment of the row and column sums, $\mathbf{s}_2$ and $\mathbf{s}_3$, referred to below.

To facilitate comparison between the method here presented and that given by Guest (1950), we shall not concern ourselves with this question, but shall carry out the computation exactly corresponding to that of his example, the fitting of a cubic curve to the sixteen pairs of observations he gives. These are

x	y	x	y
−9·0	0·40	0·8	2·30
−7·3	0·53	2·8	2·85
−6·4	1·09	3·5	3·62
−5·5	0·76	4·8	4·50
−4·4	0·80	6·1	6·40
−3·65	1·17	6·25	5·08
−2·2	1·16	7·2	6·85
−1·25	1·45	7·9	8·10

Also following Guest, we shall not concern ourselves with the calculation of the power sums of the x_r or the sums of products of the y_r with the powers of the x_r, but shall assume these to have been obtained by the method he suggests. In other words, we shall start our computation having already obtained the matrix **A** (the element (r, s) of which is given by $a_{rs}=\sum_{i=1}^{n} x_i^{r+s}$, $r, s=0, \ldots, q$) and the column **h** (the element r of which is given by $h_r=\sum_{i=1}^{n} y_i x_i^r$).

We shall, however, work in terms of $x/10$ instead of x, since this makes all the diagonal elements of **A** of roughly the same size and order unity, permitting the advantage of keeping a fixed number of decimals throughout the calculation.

Method I.

In outline, this method obtains the regression coefficients, $\hat{b}_r$ of the power terms from equation (3) by the technique given by Fox (1950) in his Example 4, the first stage of which produces **L** and $\hat{\mathbf{c}}$. The latter enables the residual mean square to be calculated from equation (7′), and the decision to be taken as to the degree of polynomial appropriate to the data. The inverse of **A** is then computed from **L** by Method II. of the paper by Fox and Hayes (1951), and so we are able to obtain the standard errors of the regression coefficients by using equation (9) and of points on the regression curve by using equation (11).

The computation is set out in Example I. below.

A and **h** are placed side by side on the computing sheet. For checking purposes, the column sums of **A** and the sum of the elements of **h** are entered in the next row as $\mathbf{s}'_2$, and the row sums of **A** and **h** together are entered in the next column as $\mathbf{s}_1$.

We then calculate **L′** and $\hat{\mathbf{c}}$ (this is a slight variant of Fox's technique, which deals with **L** and $\hat{\mathbf{c}}'$) a row at a time from the equations

$$\mathbf{LL}'=\mathbf{A} \quad . \quad . \quad . \quad . \quad . \quad . \quad . \quad . \quad . \quad (12)\text{ bis}$$

and

$$\mathbf{L}\hat{\mathbf{c}}=\mathbf{h}, \quad . \quad . \quad (\text{alternative form of } (3'))$$

in the form

$$\text{column } r \text{ of } \mathbf{L}' \times \text{column } s \text{ of } \mathbf{L}'=\text{element } (r, s) \text{ of } \mathbf{A}. \quad . \quad (15)$$

Here s takes the values r up to $(q+1)$ in turn for each r from 0 up to q in turn, where the column $(q+1)$ of **L′** is to be read as $\hat{\mathbf{c}}$ and the element $(r, q+1)$ should be read as the element r of **h**, $r=0, \ldots, q$. At each stage, every element in equation (15) is known, except the element (r, s) of **L′**, or the element r of $\hat{\mathbf{c}}$, which can therefore be obtained.

When row r of **L′** and $\hat{\mathbf{c}}$ has been thus produced, the elements in this row are summed to give element r of $\mathbf{s}_3$. The computation of the row is then checked by

$$\text{column } r \text{ of } \mathbf{L}' \times \text{the column } \mathbf{s}_3=\text{element } r \text{ of } \mathbf{s}_1, \quad . \quad . \quad (16)$$

in which all the elements are known except for those in $\mathbf{s}_3$ which are multiplied by zeros in $\mathbf{L}'$.

It is at this stage that we can decide whether or not a polynomial of degree r is sufficient for fitting our data, and so whether or not we need compute any more rows of $\mathbf{L}'$ and $\hat{\mathbf{c}}$. We enter $\hat{c}_r^2$ in position r of the column " sums of squares due to orthogonal polynomials " and subtract this from the entry $(r-1)$ in the column " residual sum of squares " to obtain the entry r in the latter column. (For $r=0$, we subtract $\hat{c}_0^2$ from Σy^2.) In the next column we enter the appropriate number of degrees of freedom $(=n-r-1$, for $r=0, 1, 2, \ldots)$ and so obtain the residual mean square. These last four columns could be entered beside $\hat{\mathbf{c}}$, but to save computing columns have been entered as a separate table at the end of the main calculation. We can then test the hypothesis $\hat{c}_r$ (and coefficients of all higher degree polynomials)$=0$ by an F test on the ratio of the sum of squares due to the orthogonal polynomial of degree r to the residual sum of squares in the same row, since, under that hypothesis, these are independently distributed as $\chi^2\sigma^2$, on 1 and $(n-r-1)$ degrees of freedom respectively.

We proceed in this way until we obtain a $\hat{c}_r$, say $\hat{c}_k$, which does not reduce the sum of squares significantly. We then delete row k of $\mathbf{L}'$ $\hat{\mathbf{c}}$, $\mathbf{A}$ and $\mathbf{h}$ and column k of $\mathbf{L}'$ and $\mathbf{A}$, and all subsequent rows and columns as appropriate, adjust $\mathbf{s}'_2$ and $\mathbf{s}_3$ accordingly, and proceed to the next stage of the calculation using the remainder of $\mathbf{L}'$ and $\hat{\mathbf{c}}$.

If, on the other hand, we complete the calculation of $\mathbf{L}'$ and $\hat{\mathbf{c}}$ without obtaining a $\hat{c}_r$ which does not reduce the sum of squares significantly, we must compute further rows and columns of $\mathbf{A}$ and $\mathbf{h}$ and, from them, further rows and columns of $\mathbf{L}'$ and $\hat{\mathbf{c}}$ until we do obtain such a $\hat{c}_r$, and then we proceed as before. It should be noted that such an increase in the size of $\mathbf{A}$ and $\mathbf{h}$, or the final decrease in their size, does not affect the elements of $\mathbf{L}'$ and $\hat{\mathbf{c}}$ already obtained, the only alteration required being to the row and column sums $\mathbf{s}_2'$ and $\mathbf{s}_3$.

As stated earlier, however, we shall not concern ourselves in our example with this problem of deciding on the appropriate degree of polynomial to use, but shall carry out the straightforward calculation for fitting the cubic. We are assuming, in effect, that we have carried out our computation so far with five rows and columns $(q=4)$ in $\mathbf{A}$ etc., found that $\hat{c}_4$ does not reduce the sum of squares significantly, and consequently deleted row 4 and column 4 of $\mathbf{A}$ etc. and adjusted s_2' and $\mathbf{s}_3$, leaving ourselves with the elements given in the example.

The next stage is the computation of $\hat{\mathbf{b}}$.

We have, from equations (3) and (12),

$$\mathbf{L}\mathbf{L}'\hat{\mathbf{b}}=\mathbf{h},$$

and, therefore,

$$\mathbf{L}'\hat{\mathbf{b}}=\mathbf{L}^{-1}\mathbf{h},$$

which, by equation (3′), gives

$$\mathbf{L}'\mathbf{b}=\hat{\mathbf{c}}. \quad \ldots\ldots\ldots\ldots \quad (17)$$

To obtain $\hat{\mathbf{b}}$ we use equation (17) in the form

$$\text{row } r \text{ of } \mathbf{L}' \times \text{the row } \hat{\mathbf{b}}' = \text{element } r \text{ of } \hat{\mathbf{c}},$$

allowing r to take the values q down to zero in turn, so obtaining $\hat{b}_q, \ldots, \hat{b}_0$ in turn.

$\hat{\mathbf{b}}$ is then checked by the equation

$$\text{the row } \mathbf{s}_2' \times \text{the row } \hat{\mathbf{b}}' = \text{total of column } \mathbf{h}.$$

Finally, we compute $\mathbf{A}^{-1}$ from $\mathbf{L}'$ by Method II. in the paper by Fox and Hayes (1951). From equation (12) we can obtain

$$\mathbf{L}'\mathbf{A}^{-1} = \mathbf{L}^{-1},$$

and use this, to obtain $\mathbf{A}^{-1}$ without needing the unknown part of $\mathbf{L}^{-1}$, in the form

$$\left.\begin{aligned} \text{row } r \text{ of } \mathbf{L}' \times \text{row } s \text{ of } \mathbf{A}^{-1} &= \text{element } (r, s) \text{ of } \mathbf{L}^{-1} \\ &= 0, \qquad \text{when } r<s \\ &= 1/l_{rr}, \quad \text{when } r=s, \end{aligned}\right\} \quad . \quad (18)$$

where l_{rr} is the diagonal element r of $\mathbf{L}'$, $r=0, \ldots, q$.

For this purpose the quantities $1/l_{rr}$ are recorded in a row beneath $\hat{\mathbf{b}}$.

By letting s take the values $q, q-1, \ldots, r$ in turn for each r from q down to zero, we obtain from equation (18) the elements of $\mathbf{A}^{-1}$ row by row, and in each row from right to left in turn.

When row r has been thus obtained, it is copied into column r and checked by the equation

$$\text{row } r \text{ of } \mathbf{A}^{-1} \times \text{the row } \mathbf{s}_2' = \text{unity}.$$

Having obtained $\mathbf{A}^{-1}$, we can calculate the sampling variances of the $\hat{b}_r$ using equation (9), and of points on the regression curve, using equation (11), in the form

$$\mathrm{V}(y_e) = s_{\mathrm{R}}^2(u_0 + u_1x + u_2x^2 + \ldots + u_{2q}x^{2q}),$$

where the u_r are the sums of the elements of $\mathbf{A}^{-1}$ in the appropriate backward diagonals. For example, u_2 is the sum of the elements underlined in $\mathbf{A}^{-1}$ of example I. and u_4 is the sum of the elements marked by an asterisk.

Example I.

	A				**h**	$\mathbf{s}_1$
	16·00000	−0·03500	4·78877	−0·17961	47·06000	67·63416
	−0·03500	4·78877	−0·17961	2·28074	19·74100	26·59590
	4·78877	−0·17961	2·28074	−0·26553	16·36283	22·98720
	−0·17961	2·28074	−0·26553	1·29699	8·90970	12·04229
$\mathbf{s}_2'$	20·57416	6·85490	6·62437	3·13259	92·07353	

	$\mathbf{L}'$				$\hat{\mathbf{c}}$	$\mathbf{s}_3$
	4·00000	−0·00875	1·19719	−0·04490	11·76500	16·90854
		2·18831	−0·07729	1·04206	9·06816	12·22124
			0·91733	−0·14306	3·24722	4·02149
				0·43430	1·04289	1·47719
$\hat{\mathbf{b}}'$	1·80352	3·13867	3·91435	2·40131		
l_{rr}^{-1}	0·25000	0·45697	1·09012	2·30256		

	$\mathbf{A}^{-1}$			
	0·17596	0·07893	−0·38575	−0·19341
	0·07893	1·38489	$-\overline{0{\cdot}34720}$	−2·49547*
	−0·38575	$-\overline{0{\cdot}34720}$	1·31731*	0·82682
	$-\overline{0{\cdot}19341}$	−2·49547*	0·82682	5·30177
$V(\hat{b}_r)$	0·0213	0·1673	0·1591	0·6405

$\Sigma y^2 = 233{\cdot}729$

r	$\hat{c}_r^2$=sum of squares due to poly. degree r	Residual sum of squares	Degrees of freedom	Residual mean square
0	138·415	95·314	15	
1	82·232	13·082	14	0·9344
2	10·544	2·538	13	0·1952
3	1·088	1·450	12	0·1208

$$V(y_e) = 0{\cdot}1208\left[0{\cdot}1760 + 0{\cdot}1579\left(\frac{x}{10}\right) + 0{\cdot}6134\left(\frac{x}{10}\right)^2 - 1{\cdot}0812\left(\frac{x}{10}\right)^3 - 3{\cdot}6736\left(\frac{x}{10}\right)^4 + 1{\cdot}6536\left(\frac{x}{10}\right)^5 + 5{\cdot}3018\left(\frac{x}{10}\right)^6\right]$$

E. g., for $x=10$, $V(y_e)=0{\cdot}3803$,
for $x=5$, $V(y_e)=0{\cdot}0215$.

Method II.

It often happens that we are not interested in the sampling variances of points on the regression curve, and are required to find only the regression coefficients and their sampling variances. In this case (from equation (9)) we need only the diagonal coefficients of $\mathbf{A}^{-1}$ and it is quicker to compute $\mathbf{L}^{-1}$ instead of $\mathbf{A}^{-1}$ and to obtain the diagonal coefficients of $\mathbf{A}^{-1}$ from this. Our method of computing $\mathbf{L}^{-1}$ is that of Example 2 in the paper by Fox (1950).

The computation for this case is given in our Example II. It proceeds as in our method I. as far as the production of $\mathbf{L}'$ and $\hat{\mathbf{c}}$ and the decision as to the appropriate degree of polynomial except that $\mathbf{L}$, $\hat{\mathbf{c}}'$ and $\mathbf{s}_3'$ are recorded, exactly as in Fox's Example 4, instead of their transposes, as in our Example I. That is, equations (15) and (16) are replaced respectively by the equivalent equations

$$\text{row } r \text{ of } \mathbf{L} \times \text{row } s \text{ of } \mathbf{L} = \text{element } (r, s) \text{ of } \mathbf{A},$$

and

$$\text{row } r \text{ of } \mathbf{L} \times \text{the row } \mathbf{s}_3' = \text{element } r \text{ of } \mathbf{s}_1.$$

$\mathbf{L}$ and $\hat{\mathbf{c}}'$ are thereby obtained column by column.

Having obtained $\mathbf{L}$, we compute $(\mathbf{L}^{-1})'$ a column at a time by means of the equation

$$\mathbf{L}\mathbf{L}^{-1} = \mathbf{I},$$

in the form

$$\begin{aligned} \text{row } r \text{ of } \mathbf{L} \times \text{row } s \text{ of } (\mathbf{L}^{-1})' &= 1, \qquad \text{when } r = s, \\ &= 0, \qquad \text{when } r \neq s, \end{aligned}$$

where we let s take the values $0, 1, \ldots, q$ in turn for each r from 0 to q. In practice, s takes only the values $0, 1, \ldots, r$, because of the zeros in $\mathbf{L}$ and $(\mathbf{L}^{-1})'$, the latter having zeros below the principal diagonal. When column r of $(\mathbf{L}^{-1})'$ has been obtained, its elements are summed to give element r of $\mathbf{s}_4'$, and the column is checked by means of the equation

$$\text{row } r \text{ of } \mathbf{L} \times \text{the row } \mathbf{s}_4' = \text{unity}.$$

In passing, it will be remembered from equation (13) that element (r, s) of $(\mathbf{L}^{-1})'$ is the coefficient of x^r in the orthogonal polynomial of degree s.

From equation (17), we have

$$\hat{\mathbf{b}} = (\mathbf{L}^{-1})'\hat{\mathbf{c}},$$

which can be used, to obtain the coefficient $\hat{b}_r$, in the form

$$\hat{b}_r = \text{row } r \text{ of } (\mathbf{L}^{-1})' \times \text{the row } \hat{\mathbf{c}}'. \qquad (19)$$

When all the $\hat{b}_r$ have been obtained, their computation is checked, as in Method I., by

$$\text{the row } \hat{\mathbf{b}}' \times \text{the row } \mathbf{s}_2' = \text{sum of elements of } \mathbf{h}.$$

To obtain the diagonal coefficients, $a^{(r,r)}$, of $\mathbf{A}^{-1}$ we have from equation (12)

$$(\mathbf{L}^{-1})'\mathbf{L}^{-1} = \mathbf{A}^{-1}, \qquad (20)$$

which can be used for this purpose in the form

$$\text{row } r \text{ of } (\mathbf{L}^{-1})' \times \text{row } r \text{ of } (\mathbf{L}^{-1})' = a^{(r,r)}.$$

The $a^{(r,r)}$ yield the sampling variances of the $\hat{b}_i$ by using equation (9).

EXAMPLE II.

	A				**h**	$\mathbf{s}_1$
	16·00000	−0·03500	4·78877	−0·17961	47·06000	67·63416
	−0·03500	4·78877	−0·17961	2·28074	19·74100	26·59590
	4·78877	−0·17961	2·28074	−0·26553	16·36283	22·98720
	−0·17961	2·28074	−0·26553	1·29699	8·90970	12·04229
$\mathbf{s}_2'$	20·57416	6·85490	6·62437	3·13259	92·07353	

		L		
	4·00000			
	−0·00875	2·18831		
	1·19719	−0·07729	0·91733	
	−0·04490	1·04206	−0·14306	0·43430
$\hat{\mathbf{c}}'$	11·76500	9·06816	3·24722	1·04289
$\mathbf{s}_3'$	16·90854	12·22124	4·02149	1·47719
		$(\mathbf{L}^{-1})'$		
	0·25000	0·00100	−0·32619	−0·08400
		0·45697	0·03850	−1·08377
			1·09012	0·35909
				2·30256
$\mathbf{s}_4'$	0·25000	0·45797	0·80243	1·49388
$\hat{\mathbf{b}}'$	1·80350	3·13864	3·91435	2·40132
$V(\hat{b}_r)$	0·0213	0·1673	0·1591	0·6405

Table of Sums of Squares, etc. as in Example I.

As has been pointed out, Method II. is suggested for the case where the sampling variances, $V(y_e)$, of points on the regression curve are not required. If, however, after carrying out Method II. we desire to calculate $V(y_e)$, the inverse of **A** can be obtained row by row for this purpose from $(\mathbf{L}^{-1})'$ by means of equation (20) in the form

$$\text{row } r \text{ of } (\mathbf{L}^{-1})' \times \text{row } s \text{ of } (\mathbf{L}^{-1})' = \text{element } (r, s) \text{ of } \mathbf{A}^{-1},$$

the check being the same as in Method I.

Method I. is, however, the quicker method if it is intended from the start to obtain $\mathbf{A}^{-1}$.

It may be seen further that it is possible, in using Method II., to obtain the regression coefficients for a fitted power series of every degree up to q in the process of obtaining those for degree q. This merely requires the writing down of all the sub-totals of the summations involved in calculating the $\hat{b}_r$ from equation (19) since the coefficient, $\hat{b}_{rs}$ say, of x^r in the regression power series of degree s is given by the equation

$$\hat{b}_{rs} = \sum_{t=0}^{s} l^{(t,r)} \times \hat{c}_i, \quad . \quad . \quad . \quad . \quad . \quad . \quad . \quad . \quad (21)$$

where $l^{(t,r)}$ is the element (t, r) of $(\mathbf{L}^{-1})'$.

Thus, for example, the coefficient of x (that is, when $r=1$) in the fitted series of degree 1 is $0·45697 \times 9·06816 = 4·14388$; the coefficient of x in the series of degree 2 is this quantity added to $0·03850 \times 3·24722$, giving 4·26890; and that in the series of degree 3, which is $\hat{b}_3$ in Examples I. and II., is this latter quantity added to $-1·08377 \times 1·04289$, giving 3·13864.

All the coefficients obtained from equation (21) are given in the appended table.

TABLE I.

Degree of power series	Coefficient of			
	1	$x/10$	$x^2/100$	$x^3/1000$
0	2·94125			
1	2·95032	4·14388		
2	1·89111	4·26890	3·53986	
3	1·80350	3·13864	3·91435	2·40132

ACKNOWLEDGMENT.

The work described above has been carried out as part of the research programme of the National Physical Laboratory, and this paper is published by permission of the Director of the Laboratory.

REFERENCES.

FISHER, R. A., and YATES, F., 1943, *Statistical Tables for Biological, Agricultural and Medical Research* (London : Oliver and Boyd Ltd.), 2nd edition.
FOX, L., 1950, *J. R. Statist. Soc. Ser.* B., **12,** 120.
FOX, L., and HAYES, J. G., 1951, *J. R. Statist. Soc. Ser.* B (in press).
GUEST, P. G., 1950, *Phil. Mag.*, [7] **41,** 124.

CXL. *Dislocations in Thin Plates.*

By J. D. ESHELBY and A. N. STROH,
H. H. Wills Physical Laboratory, University of Bristol*.

[Received August 15, 1951.]

ABSTRACT.

The stress due to a screw dislocation passing normally through an infinite plate or a disc is largely confined to the neighbourhood of the dislocation line, in contrast to the case of a dislocation in an infinite medium. Two screw dislocations in a plate attract or repel one another with a short-range force in place of the inverse first power law for infinite parallel dislocations. The stress due to an edge dislocation is not essentially different in the plate and infinite body so long as the plate remains flat, but in some circumstances the stress may be largely relieved by buckling of the plate.

§ 1. INTRODUCTION.

FORTY (1951) has studied the growth of tabular crystals containing one or more dislocations. Dawson and Vand (1950, 1951) have published photographs of thin crystals with growth spirals terminating on dislocations. It seems worth while, therefore, to contrast the properties of a dislocation in a thin plate and in an infinite body.

We discuss in detail the following configurations of a straight screw dislocation: (i.) meeting normally the surface of a semi-infinite body, (ii.) running normally through an infinite plate and (iii.) along the axis of a disc, with or without a stress-free hole excluding the core of the dislocation. Case (i.) may be of interest in connection with the detailed topography of the surface near the point of emergence of a dislocation (Frank 1951). Fig. 25 of Forty's (1951) paper corresponds almost exactly to case (iii.).

The corresponding problem for an edge dislocation is only briefly touched on.

It is interesting to note that the steps in Forty's growth spirals may be an arbitrary number of lattice spacings (of the order of 100), so that we have to deal with effectively the classical Volterra dislocation with arbitrary Burgers vector, in contrast with the theory of metals where the Burgers vector is assumed to be limited to one of a few simple lattice displacements.

---

* Communicated by Professor N. F. Mott, F.R.S.

§ 2. A SCREW DISLOCATION NORMAL TO THE SURFACE OF A SEMI-INFINITE BODY.

For a screw dislocation in an infinite body along the z-axis of cylindrical coordinates (r, θ, z) the non-vanishing components of displacement and stress are

$$u_z = \frac{b}{2\pi}\theta, \qquad \tau_{\theta z} = \frac{\mu b}{2\pi}\frac{1}{r}. \quad \ldots \ldots \quad (1)$$

The elastic image field which annuls the traction due to the dislocation on the plane $z=0$ is

$$u_\theta = -\frac{b}{2\pi}\frac{r}{R+z}, \quad \tau_{\theta z} = -\frac{\mu b}{2\pi}\frac{r}{R(R+z)}, \quad \tau_{r\theta} = \frac{\mu b}{2\pi}\left(\frac{z^2}{R^3}+\frac{1}{R+z}\right), \quad (2)$$

with $R^2 = r^2 + z^2$ and the other components zero. It is produced by a distribution of couples along the negative z-axis, twisting about the z-axis and with density proportional to distance from the origin. This may be verified by integrating twice with respect to z the expression given by Love (1927, p. 187) for a point-couple. The sum of the states (1) and (2) thus gives the elastic field about a screw dislocation perpendicular to the free surface of the semi-infinite solid $z>0$.

§ 3. A SCREW DISLOCATION IN A PLATE OR DISC.

To solve the problem of a screw dislocation in an infinite plate we must annul the traction on the planes $z = \pm d$. It is easy to see that this can be done by introducing an infinite series of images of the type (2). A useful expression is, however, more easily found as follows. We take from the image representation the fact that only u_θ, $\tau_{\theta z}$ and $\tau_{r\theta}$ do not vanish. Then

$$\tau_{\theta z} = \mu \partial u_\theta/\partial z, \qquad \tau_{r\theta} = \mu(\partial u_\theta/\partial r - u_\theta/r)$$

and the equilibrium condition is

$$\frac{\partial^2 u_\theta}{\partial r^2} + \frac{1}{r}\frac{\partial u_\theta}{\partial r} - \frac{u_\theta}{r^2} + \frac{\partial^2 u_\theta}{\partial z^2} = 0.$$

A simple solution is $u_\theta = \exp(\pm kz) J_1(kr)$. Multiplication by a function of k and integration yields a more general solution. The solution of our problem is easily found to be

$$u_\theta = -\frac{b}{2\pi}\int_0^\infty \frac{\sinh kz}{\cosh kd} J_1(kr)\frac{dk}{k}, \quad \ldots \ldots \quad (3)$$

for then

$$(\tau_{\theta z})_{z=\pm d} = -\frac{\mu b}{2\pi}\int_0^\infty J_1(kr)\,dk = -\frac{\mu b}{2\pi}\frac{1}{r}.$$

Since

$$\operatorname{sech} x = 2\sum_0^\infty (-1)^n \exp\{-(2n+1)x\}$$

and

$$\int_0^\infty e^{-kx} J_1(kr)\frac{dk}{k} = \frac{r}{x+\sqrt{(x^2+r^2)}}$$

(3) becomes, with $d_n=(2n+1)\,d$,

$$u_\theta=-\frac{b}{2\pi}\sum_{n=0}^{\infty}(-1)^n\left\{\frac{r}{d_n-z+\sqrt{[(d_n-z)^2+r^2]}}-\frac{r}{d_n+z+\sqrt{[(d_n+z)^2+r^2]}}\right\},$$

exhibiting u_θ as the sum of a set of images of the type (2). Returning to (3), u_θ can be expressed as a series of modified Bessel functions K_1 by contour integration or by following the analysis of Riemann (1855) in a similar problem. In this way the elastic field of a screw dislocation passing perpendicularly through an infinite plate of thickness $2d$ is found to be

$$\left.\begin{aligned}
&u_z=\frac{b}{2\pi}\,\theta,\quad u_\theta=-\frac{b}{2\pi}\,\frac{z}{r}+\frac{b}{\pi}\,\Sigma\,(\sin\tfrac{1}{2}n\pi)\,\frac{2}{n\pi}\,\mathrm{K}_1\left(\frac{n\pi r}{2d}\right)\sin\frac{n\pi z}{2d},\\
&\tau_{\theta z}=\frac{\mu b}{\pi d}\,\Sigma\,(\sin\tfrac{1}{2}n\pi)\,\mathrm{K}_1\left(\frac{n\pi r}{2d}\right)\cos\frac{n\pi z}{2d},\\
&\tau_{r\theta}=\frac{\mu b}{\pi}\,\frac{z}{r^2}-\frac{\mu b}{\pi d}\,\Sigma\,(\sin\tfrac{1}{2}n\pi)\,\mathrm{K}_2\left(\frac{n\pi r}{2d}\right)\sin\frac{n\pi z}{2d},\\
&u_r=0,\qquad \tau_{rr}=\tau_{\theta\theta}=\tau_{zz}=\tau_{rz}=0.
\end{aligned}\right\}\qquad (4)$$

with summation over integral n.

The case of a screw dislocation in the annular disc bounded by the surfaces $z=\pm d$, $r=r_i$, r_o $(r_i<r_o)$ can be treated by replacing each K_1 in the u_θ of (4) by a linear combination of K_1 and I_1 and adjusting the constants to annul the traction on the cylindrical surfaces. The result is

$$\left.\begin{aligned}
&u_z=\frac{b}{2\pi}\,\theta,\quad u_\theta=-\frac{b}{2\pi}\,\frac{z}{r}+\Sigma\left\{\mathrm{A}_n\mathrm{I}_1\left(\frac{n\pi r}{2d}\right)+\mathrm{B}_n\mathrm{K}_1\left(\frac{n\pi r}{2d}\right)\right\}\sin\frac{n\pi z}{2d},\\
&\tau_{\theta z}=\frac{\mu\pi}{2d}\,\Sigma n\left\{\mathrm{A}_n\mathrm{I}_1\left(\frac{n\pi r}{2d}\right)+\mathrm{B}_n\mathrm{K}_1\left(\frac{n\pi r}{2d}\right)\right\}\cos\frac{n\pi z}{2d},\\
&\tau_{r\theta}=\frac{\mu b}{\pi}\,\frac{z}{r^2}+\frac{\mu\pi}{2d}\,\Sigma n\left\{\mathrm{A}_n\mathrm{I}_2\left(\frac{n\pi r}{2d}\right)-\mathrm{B}_n\mathrm{K}_2\left(\frac{n\pi r}{2d}\right)\right\}\sin\frac{n\pi z}{2d},\\
&u_r=0,\quad \tau_{rr}=\tau_{\theta\theta}=\tau_{zz}=\tau_{rz}=0,
\end{aligned}\right\}\quad (5$$

where

$$\mathrm{A}_n=\frac{4b}{\pi^2}\,\frac{1}{n^3}\sin\tfrac{1}{2}n\pi\,\frac{(2d/n\pi r_i)^2\mathrm{K}_2(n\pi r_o/2d)-(2d/n\pi r_o)^2\mathrm{K}_2(n\pi r_i/2d)}{\mathrm{I}_2(n\pi r_o/2d)\mathrm{K}_2(n\pi r_i/2d)-\mathrm{I}_2(n\pi r_i/2d)\mathrm{K}_2(n\pi r_o/2d)}$$

and B_n is obtained from A_n by writing I_2 for K_2 in the numerator.

The energy required to form the dislocation in the annulus is

$$\mathrm{W}=\tfrac{1}{2}b\int_{-d}^{d}dz\int_{r_i}^{r_o}dr\,\tau_{\theta z}.\quad .\ .\ .\ .\ .\ .\ .\ .\ .\quad (6)$$

When the outer radius r_o is infinite

$$\begin{aligned}
\mathrm{W}&=\frac{8\mu b^2 d}{\pi^3}\sum_{n\ \mathrm{odd}}\frac{\mathrm{K}_0(n\pi r_i/2d)}{n^2(n\pi r_i/2d)^2\mathrm{K}_2(n\pi r_i/2d)},\\
&=\frac{\mu b^2}{4\pi}\,.\,2d\,.\,\frac{2}{3}\left(\frac{d}{r_i}\right)^2,\qquad r_i\gg d,\\
&=\frac{\mu b^2}{4\pi}\,.\,2d\,.\,\ln\left(\frac{d}{2{\cdot}24r_i}\right);\qquad r_i\ll d.\quad .\ .\ .\ .\ .\quad (7)
\end{aligned}$$

When $r_i=0$, $r_o=\infty$ the dislocation at the origin exerts a force

$$\mathrm{F}=b'\int_{-d}^{d}\tau_{\theta z}\,dz=\frac{4bb'\mu}{\pi^2}\sum_{n\,\mathrm{odd}}n^{-1}\mathrm{K}_1\left(\frac{n\pi r}{2d}\right) \quad . \quad . \quad . \quad . \quad . \quad (8)$$

on another screw dislocation with Burgers vector b' distant r from it.

Since when $x>1$ $\mathrm{I}_m(x)$ and $\mathrm{K}_m(x)$ respectively increase and decrease exponentially with x the elastic state is given closely by

$$u_z=\frac{b}{2\pi}\theta, \qquad u_\theta=-\frac{b}{2\pi}\frac{z}{r}, \qquad \tau_{r\theta}=\frac{\mu b}{\pi}\frac{z}{r^2}, \qquad \tau_{\theta z}=0, \quad . \quad (9)$$

if the point r is a few multiples of d away from both the inner and outer edges of the annulus. (9) represents exactly the combined effect of (1) together with (2) and its reflection in the plane $z=0$, with couples of opposite hand. In (4) the terms in K annul the effect of that part of the couple distribution which would lie inside the plate.

§ 4. SCREW DISLOCATION : DISCUSSION.

It will be seen that the elastic state of the plate (equations (4)) is quite different from that of a slab of width $2d$ marked out perpendicular to a screw dislocation in an infinite body (equations (1)). The shear stress $\tau_{\theta z}$ is confined to the neighbourhood of the dislocation. That this must be so is clear : $\tau_{\theta z}$ vanishes at the surface of the plate, and far from the dislocation this state of affairs must persist throughout the thickness of the plate. The energy of a screw dislocation in an infinite plate, with its core excluded by a stress-free hole, is finite, while for a dislocation in an infinite cylinder the integral (6), $(\mu b^2/4\pi)\,.\,2d.\,\ln\,(r_o/r_i)$, diverges as $r_o\rightarrow\infty$. Again, in an infinite body two parallel screw dislocations attract like electrostatic line-charges, with a force $(\mu bb'/2\pi)\,.\,2d/r$ per length $2d$, whilst each term in (8) is the force due to a line-charge made up of particles attracting with the Yukawa potential const. $r^{-1}\exp\{-n\pi r/2d\}$. Because $\tau_{r\theta}$ does not vanish the screw dislocation will also interact with an edge dislocation running parallel to the z-axis. Since $\tau_{r\theta}$ is an odd function of z there will be no net force between them, but only a couple. It is also clear that the image-force attracting the dislocation towards the edge of a lamina will be very small unless the dislocation is only a few multiples of d from the edge. In the simple case where the dislocation is distant D from the edge of a semi-infinite plate this force is given by (8) with $b'=b$, $r=2\mathrm{D}$. For comparison the image force on a length $2d$ of a screw dislocation running at a distance D parallel to the free surface of a semi-infinite solid is $\mu b^2 d/\mathrm{D}$.

§ 5. EDGE DISLOCATIONS.

The stresses τ_{rr}, $\tau_{\theta\theta}$, $\tau_{r\theta}$ produced by an edge dislocation along the z-axis in an infinite body are derived from the Airy function $\chi=\mathrm{const.}\,r\ln r\sin\theta$, while $\tau_{zz}=\nu(\tau_{rr}+\tau_{\theta\theta})$ and the remaining components are zero. To solve the problem of an edge dislocation traversing a plate we must find an image stress system giving $\tau_{rz}=0$ and $\tau_{zz}=\text{const.}\sin\theta/r$ on the planes $z=\pm d$. The necessary analysis would be similar to that of Sneddon (1946). We should have to evaluate integrals like those in his § 5, but with Bessel functions of higher order on account of the angular dependence. The results would not be simple, and the case of an edge dislocation in an annular disc would be quite intractable. The general nature of the result can, however, be made out quite simply. If in the solution (Love, *op. cit.* p. 225) for an infinite hollow cylinder with an edge dislocation we replace λ by $2\lambda\mu/(\lambda+2\mu)$ the resulting expressions give the stresses and displacements averaged across the thickness of a disc cut from the cylinder and having surfaces free of stress (generalized plane stress: Love, *op. cit.*, p. 207). The average stresses will fall off as $1/r$ and the elastic state will not be very different from what it was when the disc formed part of the infinite cylinder.

As long as the plate containing the edge dislocation remains flat there is thus no widespread relaxation of stress, as there is for the screw dislocation. However, the energy may be reduced by buckling of the plate. Take a sheet of paper with a hole in it and make a tuck of constant width b (small compared with the size of the hole) running from the hole to the edge of the sheet. The paper will form a surface given roughly by the equation $z=(b\sqrt{2}\sin\theta)/2\pi$. If the paper is flattened out to form a plane dislocated lamina a large amount of strain-energy will be introduced. On the other hand we should not expect buckling to occur in a thick dislocated disc.

To find out the relations between the Burgers vector and the thickness and inner and outer radii of the annular disc for which buckling is energetically favourable we should have to use the theory of plates with strain in the middle surface (v. Kármán (1910)), modified to take account of initial stress. These equations are non-linear and it is difficult to solve them with the necessary boundary conditions. It seems clear, however, that in certain circumstances an edge dislocation will be able to relieve most of its stress by slight buckling of the plate, except within a few multiples of d from its centre, leading to a state of affairs similar to that discussed for the screw dislocation.

REFERENCES.

DAWSON, I. M., and VAND, V., 1950, *Nature*, **165,** 295 ; 1951, *Proc. Roy. Soc.* **206A** 555.

FORTY, A. J., 1951, *Phil. Mag.*, [7], **42,** 670.

FRANK, F. C., 1951, *Acta Cryst.* In the press.

V. KÁRMÁN, TH., 1910, *Ency. der Math. Wiss. IV*, [4], 348, (Leipzig: Teubner).

LOVE, A. E. H., 1927, *Mathematical Theory of Elasticity*, (Cambridge : University Press).

RIEMANN, B., 1855, *Ann. der Phys.*, **95,** 130.

SNEDDON, I. N., 1946, *Proc. Camb. Phil. Soc.*, **42,** 260.

CXLI. *The Influence of Deviations from the Debye Spectrum on the Electrical Conductivity of Metals.*

By F. H. J. Cornish and D. K. C. MacDonald,
Clarendon Laboratory, Oxford*.

[Received August 3, 1951.]

In the modern theory of the electrical resistance of metals, as originally developed by Bloch (1928, 1930) and Wilson (1936), (see also Mott and Jones (1936)), the assumptions made about the thermal vibrations of the crystalline lattice are essentially those which lead to the Debye spectrum familiar in the theory of specific heats. Bloch himself derived rigorous formulæ valid for low $(T \ll \Theta)$ and high $(T \gg \Theta)$ temperatures, and Grüneisen (1933) suggested a general interpolation formula for all temperatures :

$$\rho \sim \frac{T^5}{\Theta^6} \int_0^{\Theta/T} \frac{z^5\,dz}{(e^z-1)(1-e^{-z})}, \quad \ldots \ldots \quad (1)$$

based on Bloch's work, which agrees with the rigorous expressions at both limits of T. More recently Sondheimer (1950) and Rhodes (1950) have extended Bloch's analysis to deal rigorously with the intermediate temperature region and it appears that the Grüneisen formula differs nowhere by more than ∼10 per cent. Since in our work we have been concerned with trying to interpret experimental deviations from the simple Bloch–Grüneisen theory of several hundreds per cent at low temperatures, we shall accept (1) as an adequate representation of the resistance of an ideal metal with a pure Debye lattice spectrum.

The work of Born and Blackman (1935) on specific heats has shown that the Debye spectrum can only be regarded in general as a rather rough approximation to the actual vibration spectrum of specific crystals. Thus several detailed calculations have been made, based on crystal dynamics, of the actual frequency spectrum (*e. g.* Helen Smith (1948), Kellerman (1940)), and these reveal that the frequency spectrum has several peaks. This has the consequence that experimental specific heat data tend in general at low temperatures to give an apparent fall in the Debye temperature.

It is therefore somewhat surprising that, as far as we are aware, no attempt has yet been made to extend the theory of metallic conduction to allow for a vibrational spectrum of more arbitrary form. This is probably due to the fact that a direct generalization is not immediately obvious as in the case of internal energy and therefore specific heats, and also possibly because it might be expected that the electrical resistance

---

* Communicated by the Authors.

would depend less critically on the particular vibration spectrum. Thus, for example perhaps, one might look for a crude dependence on lattice entropy (*e. g. cf.* Simon 1924, Mott 1934).

From the fundamental theory of metallic resistance (*e. g.* Wilson, *loc. cit.*) it is quite straightforward to derive the following expression for the resistance as the corresponding generalization of (1) above :

$$\rho \sim \frac{1}{\mathrm{T}} \int_0^{\hat{q}} \frac{q^5\, dq}{(\exp[h\nu/k\mathrm{T}]-1)(1-\exp[-h\nu/k\mathrm{T}])}, \quad . \quad . \quad . \quad (2)$$

where q is the lattice wave number, ν is the frequency and $\nu=uq/2\pi$, u being the wave velocity. $\hat{q}$ is the upper limit of wave number determined by the total number of normal modes of the lattice. The Debye temperature is then defined in terms of q by $k\Theta=\hbar\hat{u}\hat{q}$.

1. If then u is set $=u_0$ (constant for all q), corresponding to the Debye spectrum, then (2) above reduces immediately to (1) as expected.

2. If $\nu=\nu_0$ (constant for all q) corresponding to an " Einstein Model " then we have

$$\rho \sim \frac{1}{\mathrm{T}} \cdot \frac{1}{(\exp[h\nu_0/k\mathrm{T}]-1)(1-\exp[-h\nu_0/k\mathrm{T}])}$$

or, setting $h\nu_0=k\Theta_{\mathrm{E}}$,

$$\rho \sim \frac{1}{\mathrm{T}} \cdot \frac{1}{(\exp[\Theta_{\mathrm{E}}/\mathrm{T}]-1)(1-\exp[-\Theta_{\mathrm{E}}/\mathrm{T}])}, \quad . \quad . \quad . \quad (3)$$

reducing to $\rho\sim\mathrm{T}/\Theta_{\mathrm{E}}^2$ for $\mathrm{T}\gg\Theta_{\mathrm{E}}$ and $\rho\sim 1/\mathrm{T}\exp(-\Theta_{\mathrm{E}}/\mathrm{T})$ for $\mathrm{T}\ll\Theta_{\mathrm{E}}$. Since, as Born has pointed out, the highly dispersive optical branches of the lattice spectrum may be approximated closely by Einstein oscillators it is clear from the latter formula that for T appreciably less than Θ_{E} the contribution to the resistance from these branches is negligible.

We have turned our attention initially to the case of the monovalent alkali metal Lithium which would be expected *a priori* to conform most closely to the ideal free electron model on which the Bloch theory is based. However it is evident from the specific heat measurements of Simon and Swain (1935) that there is considerable deviation from the simple Debye spectrum, and the experimental Θ value drops from $\sim$380° K. at 60° K. to $\sim$330° K. at 15° K. At the same time electrical resistance measurements (*cf.* Meissner and Voigt 1930, MacDonald and Mendelssohn 1950) have shown that down to $\sim$70° K. equation (1) fits the experimental results quite well with $\Theta\doteqdot 360$° K., but that at low temperatures there is very strong divergence.

In order to apply equation (2) to a metal with a spectrum departing to some extent from the simple Debye model, we have considered the $\nu-q$ function as made up of linear portions. The three such basic types involving a single discontinuity are sketched in the accompanying figure together with the resulting N$-\nu$ spectra. In our numerical work thus far we have limited ourselves to Case (a), *i. e.* explicitly :

$$\left.\begin{array}{lll} \nu=u_1\,\dfrac{q}{2\pi} & 0\leqslant\nu\leqslant\nu_1 & 0\leqslant q\leqslant q_1, \\[2ex] \nu=u_2\,\dfrac{q}{2\pi} & \nu_2\leqslant\nu\leqslant\nu_3 & q_1=q_2\leqslant q\leqslant q_3. \end{array}\right\} \quad . \quad . \quad . \quad (4)$$

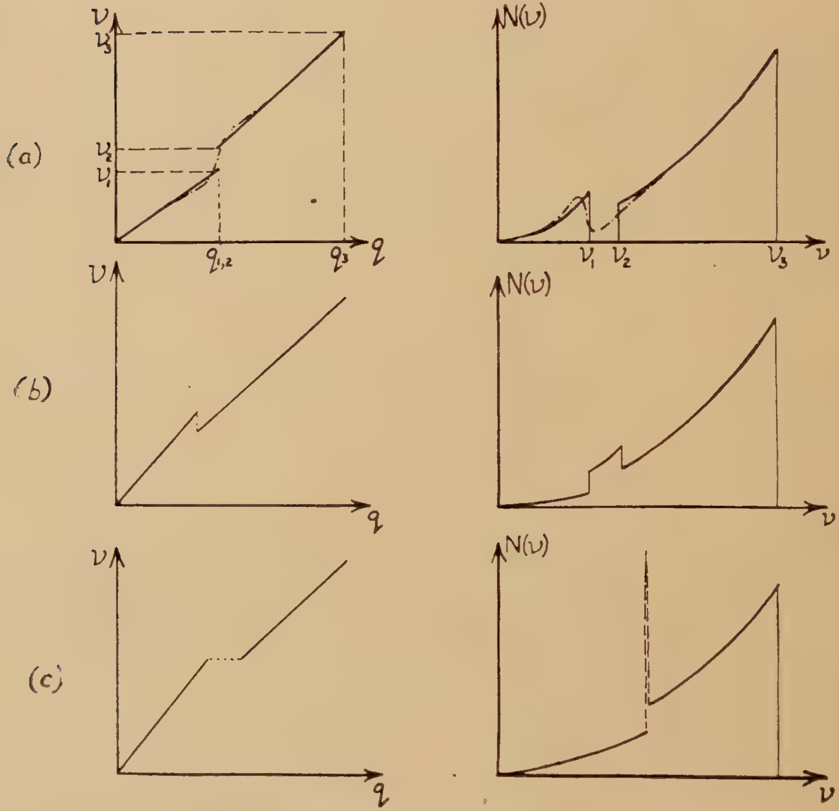

$\nu-q$ and N$-\nu$ curves for lattices deviating from simple Debye model.

[*Note.*—The direct complement to model (c) has been here omitted because a retrogression of wave-number, q, is involved leading to a negative value of N(ν) at the discontinuity.]

This leads to the following expression for the resistance :

$$\rho\sim\mathrm{T}\left[\frac{\alpha^6}{\beta^4}\,\mathrm{G}\left(\frac{\Theta_1}{\mathrm{T}}\right)+\mathrm{G}\left(\frac{\Theta_3}{\mathrm{T}}\right)-\left(\frac{\alpha}{\beta}\right)^4\mathrm{G}\left(\frac{\Theta_2}{\mathrm{T}}\right)\right], \quad . \quad . \quad . \quad (5)$$

where $\alpha u_1=u_2 \;:\; \beta\nu_1=\nu_3 \;:\; \nu_1/u_1=\nu_2/u_2 \;:\; k\Theta_r=h\nu_r$

and

$$G\left(\frac{\Theta}{T}\right)=\left(\frac{T}{\Theta}\right)^4\int_0^{\Theta/T}\frac{z^5\,dz}{(e^z-1)(1-e^{-z})},$$

i. e. G is the function tabulated by Grüneisen (1933). Two sets of (α, β) values have been used and they lead to the results (normalized at 273° K.) tabulated below. There is clearly improved agreement with experiment over the Grüneisen formula in the temperature range $T<70°$ K. This does suggest that a major part of the apparent discrepancy with theory may be attributed to the departure of the lattice spectrum, or rather the $\nu-q$ curve, from the simple Debye model. It is, however, quite probable that part is still due to deviation of the electron characteristics from those of an ideal electron gas.

Table of Comparative Results.

T (° K.) :	374·5	273	80·1	20·4	11·4	6·0
Observed resistance*	1·443	1·000	0·1252	0·0013	0·00009	0·000007
Grüneisen Eq. (1) ($\Theta=360°$ K.)	1·433	1·000	0·125	0·00042	0·000022	0·0000009
New model :						
1. $\alpha=1{\cdot}3, \beta=2$	1·434	1·000	0·144	$0{\cdot}0015_8$	$0{\cdot}00009_7$	0·000004
2. $\alpha=1{\cdot}3. \beta=3$	1·435	1·000	0·129	0·00118	$0{\cdot}00010_3$	$0{\cdot}000004_3$

* With residual resistance subtracted, and normalized to unity at 273° K.

The abrupt gap in the frequency spectrum in the model we have chosen may appear somewhat surprising at first sight. Physically, however, one might rather expect to have $\nu-q$ and $N-\nu$ curves somewhat as shown by the broken curves in fig. 1 (*a*).

The specific heat for the model chosen is given by

$$C_v=\left(\frac{\alpha}{\beta}\right)^3(D_1-D_2)+D_3, \quad . \quad . \quad . \quad . \quad . \quad . \quad . \quad (6)$$

where (α, β) are as before in (5) and $D_r=D(\Theta_r/T)$, where D is the specific heat for the simple Debye model. The apparent Θ values for a specific heat based on this model with $\alpha=1{\cdot}3$, $\beta=3$ are : at 60° K., $\Theta=354°$ K., and at 15° K., $\Theta=286{\cdot}5°$ K. This then compares quite favourably with the relative variation of Θ observed by Simon and Swain, although the absolute values are not in agreement. In any case, of course, as Blackman (1951) has emphasized again, the effective spectrum will be different for the specific heat and the electrical resistivity, since in an ideal metal only the longitudinal vibrations produce significant electron scattering.

We intend to extend this work to other metals and to consider also the electronic thermal conductivity and we hope to publish in more detail later.

References.

BLACKMAN, M., 1935, *Proc. Roy. Soc.* A, **148,** 365, 384 ; 1951, *Proc. Phys. Soc.* A, **64,** 681.

BLOCH, F., 1928, *Z. f. Phys.*, **52,** 555 ; 1930, *Ibid.*, **59,** 208.

GRÜNEISEN, E., 1933, *Ann. d. Phys.*, **16,** 530.

KELLERMAN, E. W., 1940, *Phil. Trans. Roy. Soc.*, **238,** 513, 548.

MACDONALD, D. K. C., and MENDELSSOHN, K., 1950, *Proc. Roy. Soc.* A, **202,** 103.

MEISSNER, W., and VOIGT, B., 1930, *Ann. d. Phys.*, **7,** 761, 892.

MOTT, N. F., and JONES, H., 1936, *Theory of the properties of metals and alloys.* (Oxford : University Press.)

MOTT, N. F., 1934, *Proc. Roy. Soc.* A, **146,** 465.

RHODES, P., 1950, *Proc. Roy. Soc.* A, **202,** 466.

SIMON, F. E., 1924, *Z. Phys.*, **27,** 157.

SIMON, F. E.. and SWAIN, R. C., 1935, *Z. phys. Chem.* B, **28,** 189.

SMITH, HELEN, 1948, *Phil. Trans. Roy. Soc.*, **241,** 105, 145.

SONDHEIMER, E. H., 1950, *Proc. Roy. Soc.* A, **203,** 75.

WILSON, A. H., 1936, *The Theory of Metals*, (Cambridge : University Press).

CXLII. *Effects of the Recoil on Allowed β-Transitions.*

By O. KOFOED-HANSEN,
Institute for Theoretical Physics, University of Copenhagen*.

[Received July 9, 1951.]

SUMMARY.

The recoil corrections to the shape of the Fermi distribution for the β-spectrum are calculated, and it is concluded that they are of the same order of magnitude as other effects, which are usually neglected. Furthermore it is shown that the observed half-life and shape of the β-spectrum of the neutron excludes any coupling in β-decay depending on nuclear v./c. terms only.

§ 1. INTRODUCTION.

WHEN the shape of the β-spectrum is calculated one considers the β-decaying nucleus as infinitely heavy, and one neglects the kinetic energy of the recoil in the conservation of energy since it is small compared with the energy of the β-particle and the neutrino.

In that approximation, where the neutrino rest mass is neglected, the maximum value of the kinetic energy of the recoil, $T_R^{\max}$, occurs when the β-particle is emitted with its maximum energy. $T_R^{\max}$ is given by

$$T_R^{\max}=\frac{533}{A}(T_\beta^{\max^2}+1{\cdot}022T_\beta^{\max})10^{-6} \quad . \quad . \quad . \quad . \quad . \quad (1)$$

where $T_R^{\max}$ and $T_\beta^{\max}$ are given in MeV. A is the mass number of the isobars in question. For the β-decay of the neutron one finds $T_R^{\max}\cong 0{\cdot}1$ per cent of $T_\beta^{\max}$ and for He^6 and B^{12} $T_R^{\max}\cong 0{\cdot}05$ per cent of $T_\beta^{\max}$.

The effect on the shape of the β-spectrum is somewhat larger as will be shown in a following section. Although it is not necessary for this calculation to apply so general methods we shall first give an exact relativistic treatment of the phase space calculation for a general three particle process in the next section, and in the following section we shall apply the results of this calculation to the special case of nuclear β-decay.

The effects from the recoil will partly enter in the phase space calculation and partly in the determination of the square of the matrix element for the transition. In the special case of the β-decay of the neutron some particular effects from the recoil appear in the matrix element and give rise to the exclusions of the pseudoscalar coupling case as responsible for the β-decay of the neutron. This special case will be treated in the last section of this paper.

---

* Communicated by Professor C. Møller.

§ 2. EXACT RELATIVISTIC PHASE SPACE CALCULATION.

The probability of a process where a particle at rest disintegrates into three individual particles is proportional to the integral

$$P=(4\pi)^{-2}\int|\mathcal{M}|^2\,d\mathbf{p}_1\,d\mathbf{p}_2\,d\mathbf{p}_3\,\delta(\mathbf{p}_1+\mathbf{p}_2+\mathbf{p}_3)\,\delta(M-E_1-E_2-E_3)\quad . \; . \; . \quad (2)$$

where $\mathcal{M}$ is the matrix element for the process, p_i is the momentum of the ith particle, and E_i is the corresponding energy including the rest mass m_i. The abbreviation $d\mathbf{p}$ means $dp_x\,dp_y\,dp_z$ and the function $\delta(\mathbf{x})$ is the product of the three delta functions in each of the ocordinates of the vector $\mathbf{x}$. M is the mass of the original particle, and $c=1$. The two delta functions express the conservation of momentum and of energy.

If we assume a random orientation in the space of the original particles the process is completely described by two parameters in the momentum triangle, and we can average (2) over all parameters besides such two variables.

Three of the integrations in (2) take away the momentum delta function. This means, however, that we have to take into account the momentum conservation in the form

$$p_3{}^2=p_1{}^2+p_2{}^2+2p_1p_2\cos\theta_{12}\quad . \; . \; . \; . \; . \; . \; . \quad (3)$$

in the delta function for the energy. Here θ_{12} is the angle between the vectors $\mathbf{p}_1$ and $\mathbf{p}_2$. By a well-known transformation (see Bethe 1933) we get

$$P=\tfrac{1}{2}\int E_1\,dE_1\,E_2\,dE_2\,E_3\,dE_3\,|\mathcal{M}|^2\,\delta(M-E_1-E_2-E_3).\quad . \; . \quad (4)$$

One further integration leads to

$$\begin{aligned}P&=\int P(E_1E_2)\,dE_1\,dE_2\\&=\tfrac{1}{2}\int|\mathcal{M}|^2\,(M-E_1-E_2)E_1\,dE_1\,E_2\,dE_2.\quad . \; . \; . \; . \quad (5)\end{aligned}$$

$P(E_1E_2)$ is the distribution function for the two variables E_1 and E_2. These two variables determine the process completely. It must be remembered that for a fixed value of E_1 the variable E_2 cannot assume any value between m_2 and $E_2^{\max}$. It follows from the laws of conservation of energy and momentum that for a fixed value of E_1 the variable E_2 must lie in the interval between the two limits

$$\left.\begin{matrix}E_2'\\E_2''\end{matrix}\right\}=[(M-E_1)(M^2-2ME_1+m_1{}^2+m_2{}^2-m_3{}^2)$$
$$\pm p_1\{(M^2-2ME_1+m_1{}^2-m_2{}^2-m_3{}^2)^2-4m_2{}^2m_3{}^2\}^{\frac{1}{2}}]/[2(M^2-2ME_1+m_1{}^2)].$$
$$. \; . \; . \quad (6)$$

This expression can be verified *e. g.* by means of the geometrical picture of the conservation laws of energy and momentum given by Blaton (1950). Fig. 1 shows as an illustration to (6) the area in an E_1E_2 plane inside which these parameters may vary in the special case $m_1=m_3=0{\cdot}3M$ and $m_2=0{\cdot}2M$.

Any one of the particles obtains its maximum energy when the two others travel in the same direction and with the same velocity. This is easily seen by a simple extremum consideration. From this result we find

$$E_1^{\max}=[M^2+m_1^2-(m_2+m_3)^2]/(2M). \quad . \quad . \quad . \quad . \quad . \quad . \qquad (7)$$

Let us consider a certain process in which $|\mathscr{M}|^2$ is substantially constant. Then we find the probability distribution of one of the energies simply by an integration of (5) where $|\mathscr{M}|^2$ is taken outside the integral. The integration must be carried out inside the limits given by (6). We find

$$\begin{aligned}P_{E1}=\tfrac{1}{24}p_1E_1\{(M^2-2ME_1+m_1^2-m_2^2-m_3^2)^2-4m_2^2m_3^2\}^{\frac{1}{2}}\{3(M-E_1)^2\\ \cdot[(M^2-2ME_1+m_1^2)^2-(m_2^2-m_3^2)^2]-(E_1^2-m_1^2)[(M^2-2ME_1+m_1^2\\ -m_2^2-m_3^2)^2-4m_2^2m_3^2]\}/(M^2-2ME_1+m_1^2)^3 \quad . \quad . \quad . \quad . \quad . \qquad (8)\end{aligned}$$

Fig. 1.

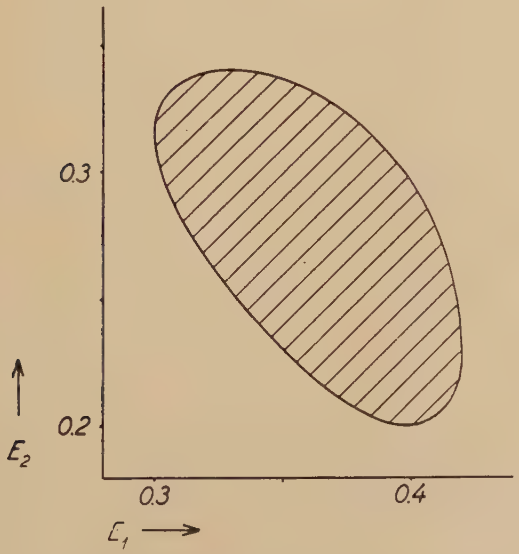

The hatched area is the area in the E_1E_2 plane inside which E_1 and E_2 may vary in the special case $m_1=m_3=0{\cdot}3M$ and $m_2=0{\cdot}2M$.

If one wants to determine the total probability for a disintegration one has to carry out one further integration over E_1, where the integral is taken between the limits m_1 and $E_1^{\max}$. This integral is the complete relativistic analogue to the Fermi integral in β-decay. The integral can be expressed in terms of complete elliptic integrals of the first, second and third kind in the general case. Only when all three particles may be treated non-relativistically or when one of the particles has zero rest mass can the integral be expressed in terms of simple functions. Fig. 2 shows the value of the integral of (8) in the special case $m_1 = m_2 = m_3$. The figure gives this integral divided by $7M^5/3840$ and as a function of m/M where m is the common mass for the three particles. The dotted curve is the non-relativistic approximation. The curve illustrates the validity of the non-relativistic approximation.

§ 3. RECOIL EFFECTS ON THE PHASE SPACE CALCULATION IN β-DECAY.

In the β-deacy the square of the matrix element for the transition is given by an expression of the type (Hamilton 1947)

$$|\mathcal{M}|^2 = |\mathcal{M}_K|^2 (1 + a(p_\beta/E_\beta)\cos\theta_{\beta\nu}) \quad . \quad . \quad . \quad . \quad . \quad (9)$$

Fig. 2.

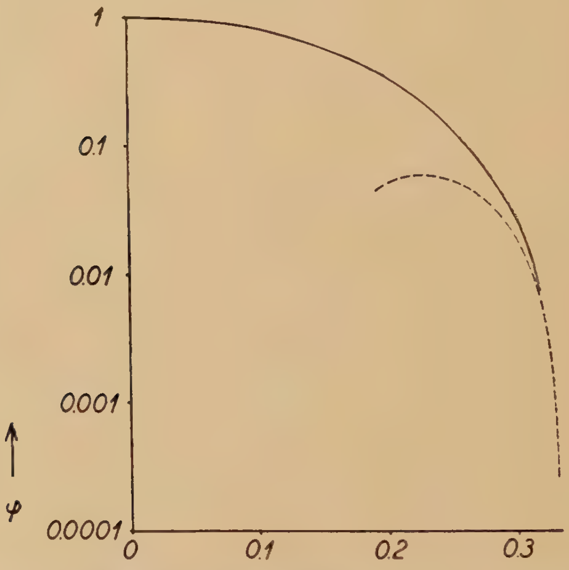

The figure shows the generalized Fermi integral divided by $7M^5/3840$ as a function of m in the special case $|\mathcal{M}| = 1$ and $m_1 = m_2 = m_3 = m$. The dotted curve is the non-relativistic approximation.

where we have neglected the neutrino rest mass. $|\mathcal{M}_K|^2$ is the square of the nuclear matrix element, which we shall consider as a constant in this section. In the derivation of (9) one has neglected all nuclear v./c. terms and all higher order terms in the expansion of the lepton wave-functions over the finite extension of the nucleus *i. e.* one has neglected terms of the order R/λ or of higher order where R is the nuclear radius, and where λ is the wavelength of the leptons.

Integrations of the type leading from (5) to (8) are easily performed also when matrix elements such as (9) are taken into account. The resulting expression is in many respects similar to (8) but of course it is somewhat more involved. If the result is expanded in a series in E_β/M one finds

$$P(E_\beta)=p_\beta E_\beta(E_\beta^{\max}-E_\beta)^2[1+3E_\beta/M-E_\beta^{\max}/M+a(m_\beta^2/(ME_\beta)-3E_\beta/M)]. \quad \ldots \quad (10)$$

This expression is identical with the usual Fermi β-spectrum apart from the extra factor contained in the square bracket.

The deviation is small since the extra factor is very close to unity. The maximum correction amounts to 0·2 per cent for He^6, 0·5 per cent for the neutron and 0·6 per cent for B^{12} with the choice $a=-1$. The effect is larger for Li^8, but due to the complicated structure of the Be^8 daughter nucleus this β-spectrum is not directly comparable with the simple Fermi spectrum. In any case higher order effects may influence the shape of the β-spectrum to the same order of magnitude. We shall mention that v./c. terms and R/λ terms may change the allowed shape to the same order of magnitude, namely about 0·1 per cent.

Thus we may conclude that the effects from the neglect of T_R in the energy conservation is of the same order of magnitude as other effects which are usually neglected in the discussion of allowed β-decay.

§ 4. β-DECAY OF THE NEUTRON.

Usually the nuclear matrix element $\mathscr{M}_K$ cannot be calculated since so far no satisfactory theory of nuclei exist. In the case of the β-decay of the neutron, however, one may assume that a satisfactory treatment of the behaviour of the neutron and the recoil proton is obtained when these particles are described by a Dirac equation. In this case it is a simple problem to determine $\mathscr{M}_K$.

In the scalar coupling case one finds

$$\begin{aligned}|\mathscr{M}_K|^2&=\tfrac{1}{2}(E_PM+Mm_P)/(E_PM)\\&=1 \quad \ldots \quad (11)\end{aligned}$$

where the index P refers to the recoil proton. In the pseudoscalar coupling case one finds

$$\begin{aligned}|\mathscr{M}_K|^2&=\tfrac{1}{2}(E_PM-Mm_P)/(E_PM)\\&=\tfrac{1}{4}v_P^2. \quad \ldots \quad (12)\end{aligned}$$

We remember that we have put $c=1$.

In case of β-decay of other nuclei than the neutron one would still find in the pseudoscalar coupling case that $|\mathscr{M}_K|^2$ is of the order of v_P^2 but now v_P means the velocity of the nucleon in a bound state, and thus $|\mathscr{M}_K|^2$ would be $\sim 10^4$ as large as for the neutron (see also Marshak 1949) in contradiction to experimental results (Robson 1950, 1951, Snell, Pleasonton and McCord 1950). Thus we may conclude that the experimental detection of the β-decay of the neutron has ruled out the possibility that the pseudoscalar coupling case can be responsible for the β-decay of the neutron.

Also in case of a pseudoscalar coupling the β-spectrum of the neutron would not be the same as for normal allowed β-spectra, since the variation of (12) with E_β is proportional to

$$|\mathbf{p}_\beta + \mathbf{p}_\nu|^2 \qquad (13)$$

In other words the shape of the β-spectrum of the neutron would be of the same type as for first forbidden spectra. This result is also in contradiction with experimental results (Snell 1951).

I wish to thank Professor N. Bohr and Professor C. Møller for their interest in this work.

References.

Bethe, H., 1933, *Handbuch der Physik*, **24,** 1, 354.
Blaton, J., 1950, *Dan. Mat. Fys. Medd.*, **24,** no. 20.
Hamilton, D. R., 1947, *Phys. Rev.*, **71,** 456.
Marshak, R. E., 1949, *Phys. Rev.*, **75,** 513.
Robson, J. M., 1950, *Phys. Rev.*, **78,** 311 ; 1951, *Ibid.*, **81,** 297.
Snell, A. H., 1951, *Nucleonics*, **8,** 3.
Snell, A. H., Pleasonton, F., and McCord, R. V., 1950, *Phys. Rev.*, **78,** 310.

CXLIII. *Thermal Convection in a Magnetic Field**.

By W. B. THOMPSON †,
University of Toronto ‡.

[Received August 13, 1951.]

SUMMARY.

The modifications produced in the Rayleigh-Jeffreys theory of slow thermal convection by magneto-hydrodynamic effects in a conducting fluid placed in a magnetic field are examined.

Even for a non-viscous fluid, a critical temperature gradient β_0 must be exceeded in order that convection occur. In this, the place of viscosity η occurring in the Rayleigh-Jeffreys formula is taken by a quantity η_H depending on the conductivity of the fluid, the magnetic field strength H and depth of fluid d, thus $\eta_H=(4/27)(d^2/\pi^2)(\sigma\mu^2 H^2/c^2)$. If the fluid is viscous a multiple of the normal viscosity depending on H must be added to η_H.

An estimate of the critical gradient is made for somewhat artificial boundary conditions and it is found large enough to be experimentally detectable.

The applicability of Jeffreys' method of marginal stability is discussed and the nature of possible oscillations investigated.

INTRODUCTION.

THE interaction between the flow of electrically conducting fluids and magnetic fields has been considered by Alfven (1950) and Walen (1944) in discussing processes in the sun, by Fermi (1949), Richtmeyer and Teller (1949) in a theory of the origin of cosmic rays, and by Elsasser (1946) and Bullard (1949) in an explanation of terrestrial magnetism. Bullard (1949) has proposed a reasonably simple scheme of thermal convection currents and magnetic fields within the core of the earth which might be able to maintain the observed field at the surface by the self-inductive mechanism originally proposed by Larmor. He also showed that the magnetic field is of prime importance in determining the flow.

As a first step toward investigating the hydrodynamical aspects of this process a study has been made of the slow thermal convection currents set up in a plane layer of conducting fluid placed in a homogeneous magnetic field and heated from below. The motion occurring when no field is present has been studied experimentally by Bénard (1901) and by Sutton (1951) and examined theoretically by Rayleigh (1917) and Jeffreys (1926).

---

* An extract from a thesis submitted in partial fulfilment of the requirements for the degree of Doctor of Philosophy at the University of Toronto.

† Communicated by the Author.

‡ Now at the Atomic Energy Research Establishment, Harwell.

The stream lines form a system of horizontal vortex rings dividing the plane into cells with fluid flowing up in the centre and down at the edges. Rayleigh's theory described this system, predicted the temperature gradient needed to produce it, and made statements about the shape of the cells. Here the analysis of Rayleigh and Jeffreys will be modified by including the ponderomotive effects of the magnetic field, which involves adding to the hydrodynamic and heat flow equations Maxwell's equations for the electromagnetic fields.

§ 1. MATHEMATICAL FORMULATION OF THE PROBLEM.

We shall consider an infinite horizontal layer of depth d of an incompressible fluid with electrical conductivity σ placed in a homogeneous magnetic field $\boldsymbol{H}_0$ and heated from below. At first viscosity will be neglected and Euler's equation for the velocity $\boldsymbol{V}=(u, v, w)$ written as

$$\rho\left[\frac{\partial \boldsymbol{V}}{\partial t}+(\boldsymbol{V}\cdot\nabla)\boldsymbol{V}\right]=-\nabla p+\rho\boldsymbol{g}+\frac{\mu}{c}\,\boldsymbol{j}\times\boldsymbol{H}, \quad . \quad . \quad . \quad (1.1)$$

where ρ is the density of the fluid, p the pressure, $\boldsymbol{g}$ the gravitational acceleration, and $\boldsymbol{j}\times\boldsymbol{H}$ the ponderomotive force due to the magnetic field $\boldsymbol{H}$, $\boldsymbol{j}$ being the electric current density.

The motion arises because of the temperature dependence of the density, ρ. This dependence may be taken in a form appropriate to an incompressible fluid with a coefficient of thermal expansion α,

$$\rho=\rho_0(1-\alpha T). \quad . \quad . \quad . \quad . \quad . \quad . \quad . \quad . \quad . \quad (1.2)$$

The temperature distribution is determined by Fourier's equation modified by the motion to read

$$\frac{\partial T}{\partial t}+\boldsymbol{V}\cdot\nabla T=K\nabla^2 T, \quad . \quad . \quad . \quad . \quad . \quad . \quad . \quad (1.3)$$

where K is the thermal diffusivity.

In addition, the motion is subject to the equation of continuity

$$\operatorname{div}\rho\boldsymbol{V}=-\frac{\partial\rho}{\partial t}. \quad . \quad . \quad . \quad . \quad . \quad . \quad . \quad . \quad . \quad (1.4)$$

The current $\boldsymbol{j}$ is given in Gaussian units by

$$\boldsymbol{j}=\sigma\left(\boldsymbol{E}+\mu\frac{\boldsymbol{V}}{c}\times\boldsymbol{H}\right), \quad . \quad . \quad . \quad . \quad . \quad . \quad . \quad . \quad (1.5)$$

where σ is the electrical conductivity, and the fields $\boldsymbol{E}$ and $\boldsymbol{H}$ satisfy Maxwell's equations with a dielectric constant ϵ, and permeability μ.

$$\left.\begin{aligned} \operatorname{curl} \boldsymbol{H} &= \frac{4\pi}{c}\boldsymbol{j} + \frac{\epsilon}{c}\frac{\partial \boldsymbol{E}}{\partial t}, \\ \operatorname{curl} \boldsymbol{E} &= -\frac{\mu}{c}\frac{\partial \boldsymbol{H}}{\partial t}, \\ \operatorname{div} \boldsymbol{H} &= 0, \\ \operatorname{div} \boldsymbol{E} &= 4\pi\frac{q}{\epsilon}, \\ \operatorname{div} \boldsymbol{j} &= -\frac{\partial q}{\partial t}. \end{aligned}\right\} \quad \ldots\ldots \quad (1.6)$$

Here q is the electric charge density and c is the velocity of light in vacuum.

To render the problem tractable a number of assumptions must be made. First, the equations must be linearized by considering departures from equilibrium so small that their squares can be neglected. By expanding all functions in powers of a constant $\lambda = \bar{v}/v_0$ where $\bar{v}$ represents the mean velocity and v_0 is defined by $\frac{1}{2}\rho v_0{}^2 = \mu/(8\pi)\mathrm{H}_0{}^2$ one can show that the neglect of terms of higher order than the first leads to small errors in the solution provided that λ is small. That is, the linearization can be justified if the kinetic energy per unit volume of fluid is small compared to the magnetic energy density.

A second assumption is that the fractional variation in the density is small and that the continuity equation (1.4) may be replaced by (Hales 1937)

$$\operatorname{div} \boldsymbol{V} = 0. \quad \ldots\ldots\ldots\ldots \quad (1.7)$$

The third assumption is that a physically meaningful result, can be obtained by solving the time independent problem. Jeffreys (1926) gives an argument justifying this procedure derived from the principle of marginal stability. In a later section the modifications produced in this argument by consideration of the magnetic field are discussed and it is shown that Jeffreys' argument remains valid provided $c^2/4\pi\mu\mathrm{K}\sigma < 1$.

With these assumptions the zero'th approximation yields the condition of static equilibrium. If a Cartesian coordinate system with the origin in the lower surface of the fluid and the positive $0z$ axis directed vertically upwards is introduced, the relevant quantities can be written :

$$p_0 = \rho_0 g(z-d) + \rho_0 \alpha g \beta (z^2 - d^2), \quad \ldots\ldots \quad (1.8)$$

$$\mathrm{T}_0 = -\beta z, \quad \ldots\ldots\ldots\ldots \quad (1.9)$$

where β is the negative temperature gradient, and ρ_0 is the density at the lower surface of the fluid, where the temperature is considered as zero.

If the static terms are removed, the equations determining the first approximation to the velocity, and the first order corrections p, and T' to the pressure and temperature are

$$0=-\nabla p-\rho_0\alpha \boldsymbol{g}T'+\frac{\mu}{c}(\boldsymbol{j}\times\boldsymbol{H}_0)\quad . \quad . \quad . \quad . \quad . \qquad (1.10)$$

$$-\beta w=K\nabla^2 T'\quad . \quad . \quad . \quad . \quad . \quad . \quad . \quad . \quad . \quad . \quad . \qquad (1.11)$$

to which must be added Maxwell's equations for the approximations to the field, and the equation of continuity for velocities.

§ 2. DEDUCTION OF THE FUNDAMENTAL DIFFERENTIAL EQUATION.

From (1.10) and (1.11), the static form of Maxwell's equations, and the continuity equation it is possible to deduce a differential equation for T'. This is done by first applying the operator curl to (1.10) obtaining

$$0=-\operatorname{curl}(\rho_0\alpha\boldsymbol{g}T')+\frac{\mu}{c}\operatorname{curl}(\boldsymbol{j}\times\boldsymbol{H}_0).\quad . \quad . \quad . \quad . \qquad (2.1)$$

The second term may be developed as

$$(\boldsymbol{H}_0\cdot\nabla)\boldsymbol{j}-\boldsymbol{H}_0(\nabla\cdot\boldsymbol{j})$$

which, in view of (1.5) and (1.6) becomes

$$(\boldsymbol{H}_0\cdot\nabla)\sigma(\boldsymbol{E}+\frac{\mu}{c}\boldsymbol{V}\times\boldsymbol{H}_0).$$

When this replacement has been made the curl operator may be applied to (2.1) yielding

$$0=-\operatorname{curl}\operatorname{curl}(\rho_0\alpha\boldsymbol{g}T')+\frac{\sigma\mu}{c}\boldsymbol{H}_0\cdot\nabla\left[\operatorname{curl}\boldsymbol{E}+\frac{\mu}{c}\operatorname{curl}(\boldsymbol{V}\times\boldsymbol{H}_0)\right].\quad . \quad . \qquad (2.2)$$

From this equation curl $\boldsymbol{E}$ vanishes by (1.6 *b*), curl $(\boldsymbol{V}\times\boldsymbol{H}_0)$ reduces to $(\boldsymbol{H}_0\cdot\nabla)\boldsymbol{V}$ from (1.7) and curl curl $(\rho_0\alpha g T')$ can be expanded to leave

$$0=\nabla^2(\rho_0\alpha\boldsymbol{g}T')-\operatorname{grad}(\rho_0\alpha\boldsymbol{g}\cdot\nabla T')+\frac{\sigma\mu^2}{c^2}(\boldsymbol{H}_0\cdot\nabla)^2\boldsymbol{V}.\quad . \quad . \qquad (2.3)$$

Since $\rho_0\alpha\boldsymbol{g}$ is a constant vector directed along the negative $0z$ axis, the $0z$ component of (2.3) may be written

$$-\rho_0\alpha g\left(\nabla^2-\frac{\partial^2}{\partial z^2}\right)T'+\frac{\sigma\mu^2}{c^2}(\boldsymbol{H}_0\cdot\nabla)^2 w=0.\quad . \quad . \quad . \qquad (2.4)$$

Finally, w can be eliminated with the help of (1.11) leaving the desired equation

$$\rho_0\alpha g\left(\nabla^2-\frac{\partial^2}{\partial z^2}\right)T'+\frac{K}{\beta}\frac{\sigma\mu^2}{c^2}(\boldsymbol{H}_0\cdot\nabla)\nabla^2 T'=0.\quad . \quad . \quad . \qquad (2.5)$$

It proves convenient to write this in dimensionless form introducing as a unit of length the depth d of the fluid, and writing the inducing field $\boldsymbol{H}_0=\mathrm{H}\mathbf{U}$ where $\mathbf{U}$ is a unit vector. Then (2.5) becomes

$$\left[(\mathbf{U}\cdot\nabla)^2\nabla^2+\Lambda\left(\nabla^2-\frac{\partial^2}{\partial z^2}\right)\right]\mathrm{T}'=0, \quad . \quad . \quad . \quad . \quad (2.6)$$

where

$$\Lambda=d^2\frac{\rho_0\alpha g}{\mathrm{K}}\,\frac{\beta . c^2}{\sigma\mu^2\mathrm{H}^2}. \quad . \quad . \quad . \quad . \quad . \quad . \quad . \quad . \quad . \quad (2.7)$$

This differential equation with its boundary conditions forms an eigenvalue problem for Λ and its solution determines the minimum temperature gradient required for the onset of any convective mode, and the form of the temperature perturbation produced. From this, the remaining variables can be determined.

§ 3. SOLUTION TO THE FUNDAMENTAL DIFFERENTIAL EQUATION.

The solution ot (2.6) is obtained by the method used by Rayleigh for the analogous problem in the absence of a field. This involves considering, not the close packed hexagonal cells observed experimentally but hypothetical rectangular cells. If the plane layer is infinite we write

$$\mathrm{T}'=\mathrm{T}'(z)\exp(ilx+imy)+\text{complex conjugate} \quad . \quad . \quad . \quad (3.1)$$

where $\pi d/l$, $\pi d/m$ are the dimensions of the cell considered and x and y are coordinates measured horizontally.

Suitable boundary conditions are those suggested by Rayleigh (1917), the vanishing of the temperature perturbation T′, and of the vertical component of velocity w, corresponding to rigid conducting walls.

(1.11) implies that these boundary conditions are

$$\mathrm{T}'(0)=\mathrm{T}'(1)=\frac{d^2\mathrm{T}'(0)}{dz^2}=\frac{d^2\mathrm{T}'(1)}{dz^2}=0.$$

Since (2.6) is homogeneous with constant coefficients we may write

$$\mathrm{T}'(z)\sim\exp isz$$

where s is a root of the quartic,

$$(s^2+l^2+m^2)(s\sin\phi+l\cos\phi)^2=\Lambda(l^2+m^2). \quad . \quad . \quad . \quad (3.2)$$

Here, the unit vector $\mathbf{U}=(\cos\phi,\ 0,\ \sin\phi)$ making ϕ the inclination of the magnetic field $\boldsymbol{H}_0$ to the horizontal. For $\phi=\pi/2$ the field is directed vertically upwards and for $\phi=0$ along the positive OX axis.

Any solution is a linear combination of four fundamental solutions involving the roots s_1, s_2, s_3, and s_4, of (3.2),

$$\mathrm{T}'(z)=\sum_{j=1}^{4}\mathrm{A}_j\exp is_jz.$$

The boundary conditions put four homogeneous conditions on the constants A_j, whose consistency restricts the roots of (3.2) to those satisfying

$$\Delta=\begin{vmatrix} 1 & 1 & 1 & 1 \\ s_1^2 & s_2^2 & s_3^2 & s_4^2 \\ \exp is_1 & \exp is_2 & \exp is_3 & \exp is_4 \\ s_1^2\exp is_1 & s_2^2\exp is_2 & s_3^2\exp is_3 & s_4^2\exp is_4 \end{vmatrix}=0. \quad . \quad (3.3)$$

Equations (3.3) and (3.2) define Δ as a function of the parameters l, m. The minimum value of $\Delta(l, m)$ determines the temperature gradient needed to start convection, and the corresponding values of l and m determine the nature of the initial motion. The good agreement between Rayleigh's and Jeffreys' results and the measurements of Bénard and Chandra (1938) show that this cell size is preserved for finite values of the velocities.

§ 4. Existence of a Minimum Temperature Gradient.

It is possible to show that unless the field is horizontal ($\sin\phi=0$) the negative temperature gradient must exceed a certain critical value before Bénard–Rayleigh convection can occur. With $\Delta=0$ (3.2) becomes

$$(s^2+l^2+m^2)(s\sin\phi+l\cos\phi)^2=0 \quad . \quad . \quad . \quad . \quad . \quad (4.1)$$

which for $\sin\phi\neq0$ has roots,

$$s_1=i\sqrt{(l^2+m^2)}, \qquad s_2=-i\sqrt{(l^2+m^2)}, \qquad s_3=s_4=-l\cot\phi.$$

Since the characteristic equation has a repeated root the solution can be written

$$T'(z)=A_1\exp is_1z+A_2\exp is_2z+(A_3+A_4z)\exp is_3z$$

and (3.3) must be replaced by

$$\Delta=\begin{vmatrix} 1 & 1 & 1 & 0 \\ s_1^2 & s_2^2 & s_3^2 & -2is_3 \\ \exp is_1 & \exp is_2 & \exp is_3 & \exp is_3 \\ s_1^2\exp is_1 & s_2^2\exp is_2 & s_3^2\exp is_3 & (s_3^2-2is_3)\exp is_3 \end{vmatrix}=0. \quad (4.2)$$

or

$$(2s^2y^2+y^4+s^4)\sinh y=(y^2+s^2)^2\sinh y=0 \quad . \quad . \quad . \quad (4.3)$$

where $y=\sqrt{(l^2+m^2)}$ and $s=l\cot\phi$ are both real. Hence the only possible solution is $l=m=0$; and unless $\sin\phi=0$, Δ and consequently β must attain some positive value before convection begins. Physically this means that convection cannot occur until the temperature gradient attains some negative value, as would be expected. However, it is possible to prove a stronger statement than this, namely: for a non-horizontal field ($\phi \neq 0$) solutions do not exist unless Λ exceeds some definite positive quantity, and hence that convective motions only occur when the negative temperature gradient exceeds a definite critical value β_0.

In order to do this we must show that not only is there no solution for $\Lambda=0$ but that it is not possible to obtain solutions for arbitrarily small positive values of Λ. To inspect solutions for small values of Λ it is easiest to expand the roots s in a series of powers of Λ and consider only the first terms. For convenience (3.2) is written

$$(s^2+b^2)(s+a)^2=c^2b^2 \quad . \quad . \quad . \quad . \quad . \quad . \quad . \quad . \quad (4.4)$$

where $a=l \cot \phi$, $b^2=l^2+m^2$ and $c^2=\Lambda \operatorname{cosec}^2 \phi$. For $c=0$ the roots are $s_1=ib$, $s_2=-ib$, $s_3=s_4=-a$.

We expand s as a Taylor's series in c, thus

$$s=s(0)+c\left(\frac{\partial s}{\partial c}\right)_{c=0}+\ldots$$

and from (4.4)

$$\frac{\partial s}{\partial c}=\frac{cb^2}{(s+a)[s(s+a)+s^2+b^2]},$$

and for $s_1=-s_2=ib$, $c=0$; $\partial s/\partial c=0$, while for $s=-a$

$$\frac{\partial s}{\partial c}=\frac{b^2}{a^2+b^2}\lim_{c\to 0}\left(\frac{c}{s+a}\right),$$

$$\left(\frac{\partial s}{\partial c}\right)=\pm\frac{b}{\sqrt{(a^2+b^2)}}.$$

To first powers of c the four roots may be written

$$s_1=ib, \quad s_2=-ib, \quad s_3=-\left(a+\frac{bc}{\sqrt{(a^2+b^2)}}\right), \quad s_4=-\left(a-\frac{bc}{\sqrt{(a^2+b^2)}}\right). \quad . \quad . \quad . \quad (4.5)$$

The determinant Δ which must vanish if the boundary conditions are to be satisfied may be expanded to read,

$$\Delta=\left[b^4+\left(a^2-\frac{b^2c^2}{a^2+b^2}\right)^2+b^2\left(a^2+\frac{b^2c^2}{a^2+b^2}\right)\right]\sinh b \sin \frac{bc}{\sqrt{(a^2+b^2)}}. \qquad (4.6)$$

The only zeroes of these yielding non-trivial solutions are

$$\frac{bc}{\sqrt{(a^2+b^2)}}=n\pi\,;$$

or

$$c=n\pi\sqrt{\left(1+\frac{a^2}{b^2}\right)};$$

and since a and b are real, $c \geqslant \pi$ and $\Lambda \geqslant \pi^2 \sin^2 \phi$.

This establishes that solutions do not exist for arbitrary small values of Λ, but, in view of the approximations used cannot be considered as establishing the actual minimum value for Λ; however it will be shown below that this value is in fact a good approximation.

§ 5. SOLUTION FOR SPECIAL CASES.

For certain orientations of the inducing field $\boldsymbol{H}_0$ it is possible to write down exact solutions to the problem.

(a) *Vertical Field.*

(3.2) becomes

$$(s^2+l^2+m^2)s^2=\Lambda(l^2+m^2) \quad . \quad . \quad . \quad . \quad . \quad . \quad . \quad (5.1)$$

with roots

$$s=\pm\left[\frac{l^2+m^2}{2}\left\{\sqrt{\left(1+\frac{4\Lambda}{l^2+m^2}\right)}-1\right\}\right]^{1/2}$$

$$=\pm i\left[\frac{l^2+m^2}{2}\left\{\sqrt{\left(1+\frac{4\Lambda}{l^2+m^2}\right)}+1\right\}\right]^{1/2} \quad . \quad . \quad . \quad (5.2)$$

and (3.3) may be written

$$0=\sinh\left[\frac{l^2+m^2}{2}\left\{\sqrt{\left(1+\frac{4\Lambda}{l^2+m^2}\right)}+1\right\}\right]^{1/2}$$

$$\times\sin\left[\frac{l^2+m^2}{2}\left\{\sqrt{\left(1+\frac{4\Lambda}{l^2+m^2}\right)}-1\right\}\right]^{1/2} . \quad . \quad . \quad . \quad (5.3)$$

Therefore for a non-trivial solution

$$\Lambda=\pi^2\left(1+\frac{\pi^2}{l^2+m^2}\right) . \quad . \quad . \quad . \quad . \quad . \quad . \quad . \quad (5.4)$$

This has its minimum value π^2 at $1/(l^2+m^2)=0$ which implies that in at least one direction the convection cells must be very small; the size in the other direction is indeterminate.

The critical gradient needed for convection is from (2.7)

$$\beta_{\mathrm{H}}=\frac{\pi^2}{d^2}\frac{\mathrm{K}}{\rho_0\alpha g}\frac{\sigma\mu^2\mathrm{H}^2}{c^2} . \quad . \quad . \quad . \quad . \quad . \quad . \quad . \quad . \quad (5.5)$$

For thermal convection in a viscous fluid with the boundary conditions imposed here, Rayleigh (1917) found the critical gradient

$$\beta_\eta=\frac{27}{4}\frac{\pi^4}{d^4}\frac{\mathrm{K}}{\rho_0\alpha g}\eta . \quad . \quad . \quad . \quad . \quad . \quad . \quad . \quad (5.6)$$

where η=coefficient of viscosity.

This suggests introducing a " magnetic-viscosity "

$$\eta_{\mathrm{H}}=\frac{4}{27}\frac{d^2}{\pi^2}\frac{\sigma\mu^2\mathrm{H}^2}{c^2} \quad . \quad . \quad . \quad . \quad . \quad . \quad . \quad . \quad . \quad (5.7)$$

which depends on the scale of the system. This need not be small; in a one-centimetre layer of mercury a field of 300 gauss produces one centipoise magnetic viscosity. Hence, for conducting fluids magnetic forces should be of considerable importance in the process of thermal convection.

(b) *Horizontal Field, Convection Rolls.*

If the field is horizontal (3.2) becomes

$$(s^2+l^2+m^2)l^2=\Lambda(l^2+m^2), \quad . \quad . \quad . \quad . \quad . \quad . \quad . \qquad (5.8)$$

or

$$s=\pm\sqrt{\left(\Lambda\left(\frac{l^2+m^2}{l^2}\right)-(l^2+m^2)\right)}.$$

The boundary conditions are satisfied if $s=\pm\pi$, i.e. if

$$\Lambda=l^2\left(\frac{\pi^2}{l^2+m^2}+1\right), \quad . \quad . \quad . \quad . \quad . \quad . \quad . \quad . \qquad (5.9)$$

which is zero for $l=0$; hence in a horizontal field there is a stable mode of convection for arbitrarily small gradients, in the form of rolls with their axes along the field direction. This type of motion has been observed in the absence of a magnetic field by Chandra (1938) when convection occurs in a gas in non-uniform horizontal motion.

(c) *Convection Rolls in an Arbitrary Field.*

There is an exact solution to the fundamental equation corresponding to Chandra rolls with their axes along the direction of the horizontal component of the field. This is obtained by setting $l=0$ in (3.2) which becomes

$$\sin^2\phi\,.\,s^2(s^2+m^2)=m^2\Lambda \quad . \quad . \quad . \quad . \quad . \quad . \qquad (5.10)$$

with roots

$$s=\pm\frac{m}{\sqrt{2}}\left[\sqrt{\left(1+\frac{4\Lambda}{m^2\sin^2\phi}-1\right)}\right]^{1/2},$$
$$\pm\frac{im}{\sqrt{2}}\left[\sqrt{\left(1+\frac{4\Lambda}{m^2\sin^2\phi}\right)}+1\right]^{1/2}.$$

As in (*a*) the boundary conditions demand

$$\Lambda=\pi^2\sin^2\phi\left(1+\frac{\pi^2}{m^2}\right). \quad . \quad . \quad . \quad . \quad . \quad . \quad . \qquad (5.11)$$

which has its minimum $\Lambda=\pi^2\sin^2\phi$ at infinite m, yielding two finite values for s. This value of Λ is not, of course, necessarily the minimum possible one as l has been arbitrarily set equal to zero.

§ 6. APPROXIMATE SOLUTIONS FOR ARBITRARY FIELD.

Although the special solutions described above were easily obtained only an approximate solution has been secured for an arbitrary field. One obvious approximation procedure is to use the solution for a vertical field as starting points for an expansion in powers of $l\cot\phi$.

For $\sin\phi\neq 0$, (3.2) can be written again as

$$(s^2+b^2)(s+a)^2=c^2b^2. \quad . \quad . \quad . \quad . \quad . \quad . \quad . \quad . \qquad (6.1)$$

This equation has at least two real roots, the intersections of the curves

$$y=s^2+b^2 \quad \text{and} \quad y=\frac{c^2b^2}{(s+a)^2}.$$

The four roots can be written s_1, s_2, $x+iy$, $x+iy$, where all quantities are real with the exception of y which may be purely imaginary.

The determinant Δ becomes

$$\Delta=2xy(s_1^2-s_2^2)\left[\cos\,(a+s_1+s_2)-\cosh y\cos\frac{(s_2-s_1)}{2}\right]$$
$$+[(x^2+y^2)^2+s_1^2s_2^2-(s_1^2+s_2^2)(x^2-y^2)]\sinh y\sin\frac{(s_2-s_1)}{2}. \quad . \quad (6.2)$$

From (6.1) and (6.2) roots s can be eliminated leaving c as a function of a and b, which can then be minimized to determine the critical gradient and the conditions at the onset of convection. In fact, however, algebraic complexity prohibits this programme, and an expansion in powers of a about $a=0$ must be used, by writing :

$$\left.\begin{aligned} s&=s(0)+a\frac{\partial s}{\partial a}(0)+\frac{a^2}{2}\frac{\partial s^2}{\partial a^2}(0)+\ldots\\ c^2&=c^2(0)\qquad\qquad\quad+\frac{a^2}{2}\frac{\partial^2 c^2}{\partial a^2}(0)+\ldots\\ \Delta&=\Delta(0)+a\frac{\partial\Delta}{\partial a}(0)+\ldots.\end{aligned}\right\} \quad . \quad . \quad . \quad (6.3)$$

Since Δ is not an explicit function of a we must use

$$\frac{\partial\Delta}{\partial a}=\sum_{i}^{i=4}\frac{\partial\Delta}{\partial s_i}\frac{\partial s_i}{\partial a}.$$

It will be noticed that $\partial c^2/\partial a\sim\partial\Lambda/\partial a$ has been equated to zero, the condition for a maximum or minimum of Λ with respect to a.

The values of the partial derivatives of Δ are calculated in terms of b and c with aid of the known values of $s_i(0)$. Requiring that successive terms in the expansion for Δ vanish yields a system of equations for c^2 and its derivatives, and hence to an expression for $\Lambda(a, b)$ which to second order in a is

$$\frac{\Lambda}{\sin^2\phi}=\pi^2\left(1+\frac{\pi^2}{b^2}\right)+\frac{\pi^2}{b^2}a^2\left[4\left(\frac{\pi^2+b^2}{2\pi^2+b^2}\right)^2+3\left(\frac{\pi^2+b^2}{2\pi^2+b^2}\right)\right]. \quad . \quad (6.4)$$

Since a and b are necessarily real, this has its least value at $a=0$, that is, at $l=0$, corresponding to the convection rolls described in § 5. A slight inclination of the field therefore removes the ambiguity encountered in § 5 (a).

The corresponding temperature gradient is

$$\beta_{\mathrm{H}}=\frac{\pi^2}{d^2}\frac{\mathrm{K}}{\rho_0\alpha g}\frac{\sigma\mu^2\mathrm{H}^2}{c^2}\sin^2\phi. \quad . \quad . \quad . \quad . \quad . \quad . \quad . \quad . \quad (6.5)$$

This suggests that only the vertical component of the field should be included in the definition of the " magnetic viscosity ".

§ 7. THE EFFECT OF VISCOSITY.

It will be noted that in all the solutions discussed the minimum eigenvalue Λ occurs when one of the cell parameters becomes infinite, corresponding to a cell of vanishing dimensions. This obviously arises from neglect of viscosity, which leaves the possible velocity shears unlimited, and in order to obtain physically meaningful flow patterns it is necessary to consider viscous effects. The viscous stress adds to the hydrodynamic equation of motion a force $\boldsymbol{F}\eta=-\eta$ curl curl $\boldsymbol{V}$ which for an incompressible fluid reduces to

$$\boldsymbol{F}\eta=\eta\nabla^2\boldsymbol{V}. \qquad (7.1)$$

This addition calls for no change in the procedure used to get the fundamental equation (2.6) which is now modified to read

$$\Lambda\left(\nabla^2-\frac{\partial^2}{\partial z^2}\right)\mathrm{T}'+(\mathbf{U}\cdot\nabla)^2\nabla^2\mathrm{T}'-\Gamma\nabla^6\mathrm{T}'=0, \qquad (7.2)$$

where $$\Gamma=\frac{c^2\eta}{\sigma\mu^2\mathrm{H}^2d^2}=\frac{27}{4}\pi^2\frac{\eta}{\eta_{\mathrm{H}}}\sin^2\phi.$$

This equation may be solved as was (2.6), and if the same boundary conditions are used (although these have admittedly become somewhat artificial) the solution presents no great difficulties for the special cases studied in § 5. In particular, for convection rolls of width $\pi d/m$

$$\frac{\Lambda}{\pi^2\sin^2\phi}=1+\frac{\pi^2}{m^2}+\Gamma\frac{\pi^4}{m^4}\left(1+\frac{m^2}{\pi^2}\right)^3. \qquad (7.3)$$

Minimizing this yields an equation determining m which is most neatly written by introducing a variable χ such that

$$\pi^2+m^2=3/2\pi^2\chi$$

whereupon the condition that Λ be a minimum becomes

$$\chi^2(\chi-1)=\frac{\eta_{\mathrm{H}}}{\eta}. \qquad (7.4)$$

The corresponding critical temperature gradient is

$$\beta=\frac{27}{4}\frac{\mathrm{K}}{\alpha g\rho_0}\frac{\pi^4}{d^4}(\chi^2\eta+\eta_{\mathrm{H}})=\chi^2\beta_\eta+\beta_{\mathrm{H}}. \qquad (7.5)$$

For $\eta_{\mathrm{H}}=0$, $\chi=1$ and β reduces to the value given by Rayleigh. Identical results hold in a vertical field with m^2 replaced by $b^2=l^2+m^2$.

The width f of the roll is given by

$$f=\frac{\pi d}{m}=\sqrt{\left(\frac{2}{3\chi-2}\right)}\,d. \qquad (7.6)$$

For square cells occurring in a vertical field this is multiplied by $\sqrt{2}$.

The formula determining the width f of the cell renders (7.5) intelligible. The effect of the magnetic field is to establish a resistance to flow across the lines of force, hence the cell width is reduced, thus diminishing the excursion of any element of fluid across the field lines. This squeezing up of the cells increases the velocity gradients, hence increasing the viscous stresses. The effect of a field then, is to add a term β_H due to the magnetic viscosity, and a multiple $\chi^2>1$ of the normal viscous term β_η.

The effects here described are of sufficient magnitude to be easily detected. For example, for a layer of mercury one centimetre in depth placed in a vertical field of 1000 gauss the relevant quantities are

$$\begin{array}{ll} \eta=0{\cdot}014 \text{ poise}, & \beta_\eta=0{\cdot}162^\circ \text{ C./cm.}, \\ \eta_H=0{\cdot}152 \text{ poise}, & \beta=2{\cdot}86^\circ \text{ C./cm.}, \\ \chi=2{\cdot}6, & f=0{\cdot}69 \text{ cm.}, \\ & f_\eta=1{\cdot}41 \text{ cm.} \end{array}$$

§ 8. The Nature of the Solutions.

Once the cell parameters have been fixed the remaining dynamical quantities can be determined in terms of the temperature perturbation T′. Unfortunately, the theory is linear and homogeneous in the dependent variable, and the solution is only obtained to within a multiplicative factor. This means that in common with existing analytical theories of thermal convection it does not predict the heat transported.

If now, we remove the convention that displacement be measured in units of d, the depth of the layer, the temperature perturbation for the two-dimensional roll solution becomes

$$T'=A\cos\frac{my}{d}\sin\frac{sz}{d}. \qquad (8.1)$$

From (1.11) the $0z$ component of velocity can be written

$$w=-\frac{K}{\beta}\nabla^2 T'=\frac{K}{\beta d^2}(m^2+s^2)A\cos\frac{my}{d}\sin\frac{sz}{d}. \qquad (8.2)$$

The second velocity component v is determined from the equation of continuity as

$$v=-\frac{s}{m}\frac{K}{\beta d^2}(m^2+s^2)A\sin\frac{my}{d}\cos\frac{sz}{d}. \qquad (8.3)$$

The electric charge density q is obtained from the continuity equation for the current

$$0=\operatorname{div}\boldsymbol{j}=\sigma\left(\operatorname{div}\boldsymbol{E}+\operatorname{div}\frac{\mu}{c}\boldsymbol{V}\times\boldsymbol{H}\right),$$

whence

$$q=\frac{\epsilon}{4\pi}\operatorname{div}\boldsymbol{E}=-\frac{\epsilon\mu}{4\pi c}\boldsymbol{H}\,.\,\operatorname{curl}\boldsymbol{V}=-\frac{\epsilon\mu}{4\pi c}H\cos\phi\left(\frac{\partial w}{\partial y}-\frac{\partial v}{\partial z}\right). \qquad (8.4)$$

The electric field can be written

$$\boldsymbol{E}=\left(0,\ -\frac{\mu Hw}{c}\cos\phi,\ \frac{\mu Hv}{c}\cos\phi\right). \qquad (8.5)$$

This satisfies $E_{\tan}=0$ at the boundaries which are assumed perfectly conducting, although the normal component does not vanish but gives a surface charge Σ

$$\Sigma=\frac{\epsilon\mu}{4\pi c}\frac{K}{\beta}\frac{m^2+s^2}{d^2}\frac{s}{m}H\cos\phi\,.\,A\sin my. \qquad (8.6)$$

The current density $\boldsymbol{j}$ is given when $\boldsymbol{E}$ and $\boldsymbol{V}$ are specifid as

$$\boldsymbol{j}=\left(\frac{\sigma\mu\mathrm{H}}{c}\sin\phi\,.\,v,\ 0,\ 0\right). \qquad \qquad (8.7)$$

The induced magnetic field can now be determined since the vector potential within the fluid, a solution of $\nabla^2\mathbf{A}=(4\pi/c)\boldsymbol{j}$ can be written

$$\mathbf{A}=\left(-4\pi\frac{\sigma\mu\mathrm{H}}{c^2}\frac{\mathrm{K}}{\beta}\frac{s}{m}\mathrm{A}\sin\frac{my}{d}\cos\frac{sz}{d},\ 0,\ 0\right),$$

and the field $\boldsymbol{h}$ within the fluid

$$\boldsymbol{h}=\left(0,\ \frac{4\pi\mu\sigma\mathrm{H}}{c^2d}\frac{\mathrm{K}}{\beta}\frac{s^2}{m}\mathrm{A}\sin\frac{my}{d}\sin\frac{sz}{d},\ \frac{4\pi\mu\sigma\mathrm{H}}{c^2d}\frac{\mathrm{K}}{\beta}s\mathrm{A}\cos\frac{my}{d}\cos\frac{sz}{d}\right). \qquad (8.8)$$

Outside the fluid $\boldsymbol{h}$ is most easily determined by noting that the boundary conditions at the surface are satisfied if $\boldsymbol{h}=-\nabla\psi$ where ψ is the magnetostatic potential due to a surface pole distribution

$$\frac{\mu\sigma}{c^2}\frac{\mathrm{H}}{d}\frac{\mathrm{K}}{\beta}s\mathrm{A}\cos\frac{my}{d}$$

on the surface $z=0$ and a similar distribution with opposite sign on $z=d$. The field then has the form

$$\boldsymbol{h}=\left(0,\ 4\pi\frac{\mu\sigma}{c^2}\frac{\mathrm{K}}{\beta}\frac{\mathrm{H}}{d^2}s\mathrm{A}\sin\frac{my}{d}\exp\frac{mz}{d},\ 4\pi\frac{\mu\sigma}{c^2}\frac{\mathrm{H}}{d}\frac{\mathrm{K}}{\beta}s\mathrm{A}\cos\frac{my}{d}\exp\frac{mz}{d}\right) \qquad (8.9)$$

for $z<0$ and a corresponding quantity varying as $\exp m\left(1-\frac{z}{d}\right)$ for $z>d$.

Finally, the pressure perturbation is given from the hydrodynamical equations

$$\frac{\partial p}{\partial x}=0\,; \qquad \frac{\partial p}{\partial y}=-\frac{\sigma\mu^2\mathrm{H}^2}{c^2}\sin^2\phi\,.\,v, \qquad \frac{\partial p}{\partial z}=-\rho_0\alpha g\mathrm{T}'.$$

The integrebility condition is seen to be equivalent to the equation for T' and the pressure perturbation may be written

$$p'=\rho_0\alpha g\frac{d}{m}\,.\,A\cos\frac{my}{d}\cos\frac{sz}{d}. \qquad \qquad (8.10)$$

§ 9. Stability Conditions.

An important assumption has yet to be considered, the condition for the existence of stable convection currents. The argument used by Jeffreys to justify treating the time independent problem was as follows. Consider a solution with time dependence in the form $\exp\gamma t$, where γ is a function of β the temperature gradient. As β is increased γ moves from negative to positive values, negative values corresponding to static equilibrium and positive ones to instability and the establishing of convection currents. The condition for marginal stability, the case separating these two regions, is that γ vanish. It is however, necessary that γ be real, and Jeffreys appeals to experiment to show that undamped convective oscillations do not occur as they would if γ had a pure imaginary value at marginal stability. Such an appeal cannot be made for the magneto-hydrodynamic problem, and it has been suggested (Walen 1944) that oscillations do occur, therefore to determine the significance of the solutions for marginal stability it is necessary to examine the time dependent problem. We shall seek a solution to the time dependent problem in the form $f(x, y, z) \exp \gamma t$ where γ will be found to satisfy a cubic equation with coefficients depending on the constants of the material, and flow pattern, and the negative temperature gradient β. For low enough values of β, γ has a negative real part indicating that small motions are damped out, and the conduction of heat through the resting fluid is a stable process. If β is larger the real part of γ is positive and any motion increases with time until limited by non-linear effects. We will find that γ is real if this latter condition holds unless the constants of the material satisfy very stringent conditions, and therefore that steady currents and not oscillations are to be expected.

Again, the linearizing procedure is carried out, but the time independent assumption is not made. The first order equations can be written to determine the significance of the solutions for marginal stability,

$$\frac{\partial \boldsymbol{V}}{\partial t} = -\frac{1}{\rho_0}\nabla p - \alpha \mathrm{T}'\boldsymbol{g} + \frac{\mu}{\rho_0 c}\boldsymbol{j}\times\boldsymbol{H}_0, \quad . \quad . \quad . \quad (9.1)$$

$$\frac{\partial \mathrm{T}'}{\partial t} - w\beta = \mathrm{K}\nabla^2\mathrm{T}', \quad . \quad . \quad . \quad . \quad . \quad . \quad . \quad . \quad . \quad . \quad . \quad (9.2)$$

$$\operatorname{div} \boldsymbol{V} = 0. \quad . \quad . \quad . \quad . \quad . \quad . \quad . \quad . \quad . \quad . \quad . \quad . \quad . \quad (9.3)$$

Again, it has been assumed that variations in ρ are small, and moreover that the time variation is slow. Then, the displacement current can be omitted from Maxwell's equations,

$$\operatorname{curl} \boldsymbol{h} = \frac{4\pi}{c}\boldsymbol{j}, \quad . \quad . \quad . \quad . \quad . \quad . \quad . \quad . \quad . \quad . \quad (9.4)$$

$$\operatorname{curl} \boldsymbol{E} = -\frac{\mu}{c}\frac{\partial \boldsymbol{h}}{\partial t}, \quad . \quad . \quad . \quad . \quad . \quad . \quad . \quad . \quad . \quad (9.5)$$

$$\operatorname{div} \boldsymbol{E} = 4\pi q, \quad . \quad . \quad . \quad . \quad . \quad . \quad . \quad . \quad . \quad . \quad (9.6)$$

$$\operatorname{div} \boldsymbol{h} = 0, \quad . \quad . \quad . \quad . \quad . \quad . \quad . \quad . \quad . \quad . \quad . \quad (9.7)$$

$$\operatorname{div} \boldsymbol{j} = \frac{\partial q}{\partial t}, \quad . \quad . \quad . \quad . \quad . \quad . \quad . \quad . \quad . \quad . \quad (9.8)$$

$$\boldsymbol{j} = \sigma\left[\boldsymbol{E} + \frac{\mu}{c}\boldsymbol{V}\times\boldsymbol{H}\right]. \quad . \quad . \quad . \quad . \quad . \quad (9.9)$$

From (9.4), (9.5) and (9.9)

$$\left[\frac{\partial}{\partial t} - \frac{c^2}{4\pi\mu\sigma}\nabla^2\right]\boldsymbol{h} = (\boldsymbol{H}\,.\,\nabla)\boldsymbol{V}. \quad . \quad . \quad . \quad . \quad . \quad (9.10)$$

And from (9.1)

$$\frac{\partial}{\partial t}(-\nabla^2\boldsymbol{V}) + \frac{\mu}{4\pi\rho_0}(\boldsymbol{H}_0\,.\,\nabla)\nabla^2\boldsymbol{h} = -\operatorname{curl}\operatorname{curl}(\alpha\mathrm{T}'\boldsymbol{g}). \quad . \quad (9.11)$$

Using (9.10) to eliminate ***h***, and (9.2) to eliminate the $0z$ component of velocity leaves the fundamental equations for T' in the form

$$\left(\frac{\partial}{\partial t}-\frac{c^2}{4\pi\mu\sigma}\nabla^2\right)\left(\frac{\partial}{\partial t}-K\nabla^2\right)\frac{\partial}{\partial t}\nabla^2 T'-\frac{\mu}{4\pi\rho_0}(\boldsymbol{H}_0\,.\,\nabla)^2\left(\frac{\partial}{\partial t}-K\nabla^2\right)\nabla^2 T'$$
$$-\alpha g\beta\left(\frac{\partial}{\partial t}-\frac{c^2}{4\pi\mu\sigma}\nabla^2\right)\left(\nabla^2-\frac{\partial^2}{\partial z^2}\right)T'=0. \quad . \quad . \quad (9.12)$$

If we consider a vertical field and use the Rayleigh boundary conditions the appropriate solution can be written as

$$T'\sim\exp\,(ilx+imy+\gamma t)\sin sz$$

where the parameters satisfy the characteristic equation

$$k^2\gamma^3+\left(\frac{c^2}{4\pi\mu\sigma}k^2+Kk^2\right)k^2\gamma^2+\left[\frac{\mu}{4\pi\rho_0}H^2s^2k^2-\alpha g\beta(k^2-s^2)+\frac{Kc^2k^6}{4\pi\mu\sigma}\right]\gamma$$
$$+\frac{\mu}{4\pi\rho_0}H^2Ks^2k^4-\frac{c^2}{4\pi\mu\sigma}\alpha g\beta(k^2-s^2)k^2=0, \quad . \quad . \quad . \quad (9.13)$$

where $k^2=l^2+m^2+s^2$. This equation can be written

$$\gamma^3+A\gamma^2+\beta\gamma+C=0$$

and in order that steady convection currents appear $C<0$.

If the equation is to have a complex root with positive real part x, a condition for instability to oscillations, x must satisfy

$$x^3+2Ax^2+(A^2+B)x+(AB-C)=0$$

hence the condition that oscillations, not steady motion should occur is

$$C>0>AB-C.$$

This in turn, is a condition on the negative temperature gradient

$$\frac{\mu^2\sigma}{\rho_0 c^2}KH^2k^2s^2>\alpha g\beta(k^2-s^2)>\frac{c^2}{16\pi^2}\frac{H^2s^2k^2}{\rho_0 K\sigma}+\frac{k^6c^2}{4\pi\mu\sigma}\left[\frac{c^2}{4\pi\mu\sigma}+K\right], \quad . \quad (9.14)$$

and the condition for oscillation

$$(\mu K\sigma)^2>\frac{c^4}{16\pi^2}+\left[\left(\frac{c^2}{4\pi\mu\sigma}\right)^2+\frac{c^2K}{4\pi\mu\sigma}\right]\frac{\rho_0 c^2}{H^2}K\sigma\frac{k^4}{s^2}. \quad . \quad . \quad (9.15)$$

Hence a necessary condition on the material involved is

$$\frac{c^2}{4\pi\mu K\sigma}=\theta<1. \quad . \quad . \quad . \quad . \quad . \quad . \quad . \quad . \quad (9.16)$$

The values of μ, K, σ for solid copper give $\theta=0{\cdot}7$, hence the condition is not easily satisfied in the laboratory.

A necessary condition on θ for oscillation is obtained by substitution in (9.15)

$$\theta<[\sqrt{5}-1]\frac{H^2}{8\pi\rho K^2}\frac{s^2}{k^4}. \quad . \quad . \quad . \quad . \quad . \quad . \quad . \quad (9.17)$$

If such oscillations do occur it is possible also to determine the gradient required for the onset of convection, and the frequency of the oscillations at marginal stability,

$$\alpha g\beta_0=\frac{c^2}{16\pi^2}\frac{H^2s^2}{\rho K\sigma}+\frac{3}{4}\frac{k^4c^2}{\pi\mu\sigma}\left[\frac{c^2}{4\pi\mu\sigma}+K\right], \quad . \quad . \quad . \quad (9.18)$$

which with (9.14) gives for the cell parameter $k^2=3/2\chi s^2$ and χ a root of

$$\chi^2(\chi-1)=\frac{8}{27}\frac{\mu H^2}{8\pi\rho\kappa^2}\frac{s^2}{\theta+1}. \qquad (9.19)$$

The corresponding frequency obtained from (9.13) is

$$\omega=i\gamma=\sqrt{2s}\sqrt{\left(\frac{\mu H^2}{8\pi\rho}\right)\theta}\sqrt{\left(\frac{1-\theta}{\theta^2}-\frac{8\pi\chi^2 s^2}{\mu H^2}\right)}. \qquad (9.20)$$

Introducing the magnetic energy per unit mass $\mathscr{E}=(\mu H^2)/(8\pi\rho)$ and $s=\pi/d$ this is

$$\omega=\sqrt{\left(2-\frac{\pi}{d}\right)\theta}\sqrt{\left(\frac{1-\theta}{\theta^2}\mathscr{E}-\kappa\chi^2\frac{\pi^2}{d^2}\right)}. \qquad (9.21)$$

§ 10. CONCLUSION.

We have examined the modifications produced in the Rayleigh-Jeffreys theory of slow thermal convection by the addition of magnetic forces acting on induced currents. It has been shown that for most materials the flow is steady, although oscillations seem possible in principle. An approximate value for the critical gradient has been found, but as was the case for Rayleigh's analysis this is probably somewhat in error due to improper choice of boundary conditions. A numerical analysis similar to that given by Jeffreys (1926) for ordinary convection would improve the estimate of A. On the other hand, the present analysis is a great deal simplified and the proper dependence of on depth and field strength has probably been deduced. This predicted dependence could be tested experimentally by determining the temperature gradient for which the thermal conductivity law ceases to hold for a thin layer of fluid heated from below as was done by Schmidt and Saunders (1938) for ordinary convection in water.

Finally, the author wishes to express his thanks to Dr. E. C. Bullard who suggested the problem and gave valuable advice and encouragement.

REFERENCES.

ALFVEN, H., 1950, *Cosmical Electrodynamics* (Oxford : Clarendon Press).
BÉNARD, H., 1901, *Ann. de Chemie et de Physique*, **23**, 62.
BULLARD, E. C., 1949 a, *Proc. Roy. Soc.* A, **197**, 433 ; 1949 b, *Ibid.*, **199**, 413.
CHANDRA, K., 1938, *Proc. Roy. Soc.* A, **164**, 231.
ELSASSER, W. M., 1946, *Phys. Rev.*, **67**, 106.
FERMI, E., 1949, *Phys. Rev.*, **75**, 1169.
HALES, A. L., 1937, *M.N. R.Ast.Soc. Geo. Sup.*, **4**, 132.
JEFFREYS, H., 1926, *Phil. Mag.*, **2**, 833.
RAYLEIGH, 1917, *Phil. Mag.*, **32**, 529.
RICHTMEYER, R. D., and TELLER, E., 1949, *Phys. Rev.*, **75**, 1729.
SCHMIDT, R. J., and SAUNDERS, O. A., 1938, *Proc. Roy. Soc.* A, **165**, 216.
SUTTON, O. G., 1951, *Proc. Roy. Soc.* A, **204**, 297.
WALEN, C., 1944, *Ark. f. mat. astr. o. fysik*, **30***A*, No. 15.

CXLIV. *The Boundary Layer in Three Dimensional Flow.*—Part II. *The Flow near a Stagnation Point**.

By L. Howarth, F.R.S.,
Department of Mathematics, University of Bristol†.

[Received August 16, 1951.]

Summary.

The equations of boundary layer flow in the vicinity of a stagnation point on a general (three dimensional) surface are discussed and shown to be reducible to a pair of simultaneous ordinary third-order differential equations containing a single parameter c which is determined by the mainstream flow. The variation of c can be effectively limited to the range from 0 (corresponding to two dimensional flow) to 1 (corresponding to the axial flow past a body of revolution), and solutions have been computed for the cases $c=0{\cdot}25$, $0{\cdot}50$, $0{\cdot}75$ and are tabulated below. A series expansion useful for small c is also given.

Introduction.

In Part I. (Howarth 1951) the equations of flow in the boundary layer along a general curved surface were derived using an orthogonal coordinate system ξ, η, ζ comprising respectively the surfaces generated by the normals along the lines of curvature and the parallel surfaces. The equations for steady flow were found to be

$$\frac{u}{h_1}\frac{\partial u}{\partial \xi}+\frac{v}{h_2}\frac{\partial u}{\partial \eta}+w\frac{\partial u}{\partial \zeta}-\mathrm{K}_2uv+\mathrm{K}_1v^2=-\frac{1}{\rho h_1}\frac{\partial p}{\partial \xi}+\nu\frac{\partial^2 u}{\partial \zeta^2}, \quad . \quad . \quad (1)$$

$$\frac{u}{h_1}\frac{\partial v}{\partial \xi}+\frac{v}{h_2}\frac{\partial v}{\partial \eta}+w\frac{\partial v}{\partial \zeta}+\mathrm{K}_2u^2-\mathrm{K}_1uv=-\frac{1}{\rho h_2}\frac{\partial p}{\partial \eta}+\nu\frac{\partial^2 v}{\partial \zeta^2}, \quad . \quad . \quad (2)$$

$$\frac{1}{h_1}\frac{\partial u}{\partial \xi}+\frac{1}{h_2}\frac{\partial v}{\partial \eta}+\frac{\partial w}{\partial \zeta}-\mathrm{K}_1u-\mathrm{K}_2v=0, \quad . \quad . \quad . \quad . \quad . \quad . \quad . \quad (3)$$

where h_1, h_2, h_3 are the length elements and

$$\mathrm{K}_1=-\frac{1}{h_1h_2}\frac{\partial h_2}{\partial \xi}, \qquad \mathrm{K}_2=-\frac{1}{h_1h_2}\frac{\partial h_1}{\partial \eta}. \quad . \quad . \quad . \quad . \quad (4)$$

The purpose of this paper is to discuss the flow in the neighbourhood of a stagnation point S on the surface. We shall suppose that S is the point $\xi=0$, $\eta=0$, $\zeta=0$, that the surface is regular at S and in particular that $\left(\frac{\partial h_1}{\partial \xi}\right)_0$, $\left(\frac{\partial h_1}{\partial \eta}\right)_0$, $\left(\frac{\partial h_1}{\partial \zeta}\right)_0$, $\left(\frac{\partial h_2}{\partial \xi}\right)_0$, $\left(\frac{\partial h_2}{\partial \eta}\right)_0$, $\left(\frac{\partial h_2}{\partial \zeta}\right)_0$ are bounded. We may, without loss of generality, suppose that ξ and η are so defined in magnitude that at S $h_1 = h_2 = 1$. Then, in the vicinity of S,

---

* This paper forms part of one of the essays for which the Adams Prize was awarded in 1951.

† Communicated by the Author.

$$h_1 = 1 + \left(\frac{\partial h_1}{\partial \xi}\right)_0 \xi + \left(\frac{\partial h_1}{\partial \eta}\right)_0 \eta + \left(\frac{\partial h_1}{\partial \zeta}\right)_0 \zeta, \quad \ldots \quad (5)$$

$$h_2 = 1 + \left(\frac{\partial h_2}{\partial \xi}\right)_0 \xi + \left(\frac{\partial h_2}{\partial \eta}\right)_0 \eta + \left(\frac{\partial h_2}{\partial \zeta}\right)_0 \zeta \quad \ldots \quad (6)$$

approximately.

The Nature of the Solution.

We shall suppose that the flow in the mainstream outside the boundary layer is irrotational, so that, if we denote by U, V its component velocities in the directions ξ, η increasing respectively,

$$h_2 \frac{\partial V}{\partial \xi} - h_1 \frac{\partial U}{\partial \eta} + V \frac{\partial h_2}{\partial \xi} - U \frac{\partial h_1}{\partial \eta} = 0^*. \quad \ldots \quad (7)$$

At S, by definition, U and V vanish and since S is a regular point of the surface, we shall have in its vicinity

$$U = A\xi + B\eta, \quad \ldots \quad (8)$$

$$V = D\xi + C\eta, \quad \ldots \quad (9)$$

where A, B, C, D are constants. Hence we see from the leading terms in (7) that

$$D = B.$$

Since the velocities in the boundary layer will be dominated by U, V, it is evident that the curvature terms in equations (1), (2), (3) may be neglected and that h_1 and h_2 may each be replaced by unity in determining the leading terms near S†. As we might have anticipated on physical grounds, we see that the equations of flow and the condition of irrotationality of the main flow are to this order exactly the same as if the surface were plane, ζ measured normal to it and ξ and η along two axes at right angles in the surface. We are at this stage, therefore, free to rotate our ξ, η axes about Sζ to any convenient position whilst at the same time maintaining the form of our equations.

Now, by the irrotational condition, the tensor

$$\begin{bmatrix} \left(\frac{\partial U}{\partial \xi}\right)_0 & \left(\frac{\partial V}{\partial \xi}\right)_0 \\ \left(\frac{\partial U}{\partial \eta}\right)_0 & \left(\frac{\partial V}{\partial \eta}\right)_0 \end{bmatrix}$$

is symmetric and by suitable rotation of the axes Sξ, Sη to Sx, Sy, say, we may express it in its principal form. In other words we may take the mainflow outside the boundary layer to have components (ax, by)

---

[*] It may perhaps be mentioned here that, just as in the corresponding two dimensional problem, we do not suppose that U, V in themselves satisfy the equation of continuity, but only after due account is taken of the outflow from the boundary layer.

[†] These assertions may be justified *a posteriori*.

and proceed with the solution as an immediate extension of the standard two dimensional solution. We may assume, without loss of generality, that a is positive.

We find, now using u, v, w for the velocity components referred to our new axes S(x, y, ζ), that

$$\begin{aligned} u&=axf'(z),\\ v&=byg'(z),\\ w&=-\frac{\nu^{1/2}}{a^{1/2}}[af(z)+bg(z)], \end{aligned} \qquad (10)$$

where

$$z=\frac{a^{1/2}\zeta}{\nu^{1/2}}, \qquad (11)$$

and

$$f'^2-ff''-cgf''=1+f''', \qquad (12)$$

$$g'^2-gg''-\frac{1}{c}fg''=1+\frac{1}{c}g''' \qquad (13)$$

and

$$c=b/a. \qquad (14)$$

The boundary conditions for (12) and (13) are

$$\begin{aligned} &f=g=f'=g'=0 \quad \text{at} \quad z=0,\\ &f'\to 1, \qquad g'\to 1 \quad \text{as} \quad z\to\infty. \end{aligned}$$

This slightly asymmetric form of the equations is advantageous for discussing conditions when c is small.

The skin friction components $\tau_{\zeta x}$, $\tau_{\zeta y}$ are given by

$$\begin{aligned} \tau_{\zeta x}&=\rho\nu^{1/2}a^{3/2}xf''(0),\\ \tau_{\zeta y}&=\rho\nu^{1/2}a^{3/2}cyg''(0). \end{aligned}$$

The following special cases have previously been discussed :—

(i.) $c=0$, which corresponds to two dimensional flow,

(ii.) $c=1$, which corresponds to flow round a body of revolution placed symmetrically in a stream. Here we have obviously $g=f$, so that

$$f'^2-2ff''=1+f''' \qquad (15)$$

and this is Homann's (1936) equation.

We may confine attention to the range $c=0$ to $c=1$ since it can readily be verified that

$$\left.\begin{aligned} f(z,-c)&=f(z,c), & f'(z,-c)&=f'(z,c),\\ g(z,-c)&=-g(z,c), & g'(z,-c)&=-g'(z,c) \end{aligned}\right\} \qquad (16)$$

and

$$\left.\begin{aligned} f\left(z,\frac{1}{c}\right)&=c^{1/2}g\left(\frac{z}{c^{1/2}},c\right), & f'\left(z,\frac{1}{c}\right)&=g'\left(\frac{z}{c^{1/2}},c\right),\\ g\left(z,\frac{1}{c}\right)&=c^{1/2}f\left(\frac{z}{c^{1/2}},c\right), & g'\left(z,\frac{1}{c}\right)&=f'\left(\frac{z}{c^{1/2}},c\right). \end{aligned}\right\} \qquad (17)$$

In any event it is simply a matter of notation to ensure that in any given case $0\leqslant c\leqslant 1$.

Numerical solution.

The solutions of equations (12) and (13) may be obtained by standard numerical methods, but before embarking on them it is convenient to have expansions when c is small, for it is here that conditions change most rapidly with c. To obtain these expansions we write

$$\left.\begin{aligned} f&=f_0+cf_1+c^2f_2+\ldots, \\ g&=g_0+cg_0+c^2g^2+\ldots, \end{aligned}\right\} \qquad (18)$$

substitute in equations (12) and (13), equate coefficient of powers of c, and obtain the following equations :—

$$f_0'''+f_0f_0''-f_0'^2=1, \qquad (19)$$

$$f_1'''+f_0f_1''-2f_0'f_1'+f_0''f_1=-g_0f_0'', \qquad (20)$$

$$f_2'''+f_0f_2''-2f_0'f_2'+f_0''f_2=f_1'^2-f_1f_1''+(g_0f_1''+g_1f_0''), \qquad (21)$$

$$g_0'''+f_0g_0''=0, \qquad (22)$$

$$g_1'''+f_0g_1''=-f_1g_0''-g_0g_0''+g_0'^2-1, \qquad (23)$$

$$g_2'''+f_0g_2''=-f_2g_0''-f_1g_1''+2g_0'g_1'-g_0g_1''-g_0''g_1. \qquad (24)$$

The boundary conditions are $f_r=g_r=f_r'=g_r'=0$ at $z=0$ $(r=0, 1, 2, \ldots)$ and

$$f_0'=g_0'=1, \qquad f_r'=g_r'=0 \quad (r=1, 2, 3, \ldots) \quad \text{at} \quad z=\infty.$$

Equation (19) is the standard two dimensional equation (see Howarth 1934 for the solution) and equation (22) has previously been integrated by Prandtl (1945) and by Sears (1948). Equations (20), (21), (23), (24) have been integrated numerically and the results for the first derivatives are given in Table I. They enable velocity distributions to be evaluated for small values of c. For completeness, values of f_0' and g_0' have been included in the table. The corresponding results for the skin friction components are determined by

$$f_0''(0)=1{\cdot}2326, \qquad f_1''(0)=0{\cdot}0478, \qquad f_2''(0)=0{\cdot}059,$$
$$g_0''(0)=0{\cdot}5705, \qquad g_1''(0)=1{\cdot}0535, \qquad g_2''(0)=-0{\cdot}537.$$

These results, although insufficient for accurate computation as far as $c=1$, were found to give, in conjunction with the known solution when $c=1$, useful starting points for the detailed numerical solution of equations (12) and (13), which has been undertaken for $c=0{\cdot}25$, $0{\cdot}50$, $0{\cdot}75$ by the Adams method. The results for the first derivatives are shown in Table II. and include the results for $c=1$ computed in the course of an interesting investigation by Miss Hannah (1947) from Homann's equation. (The values of f_0', g_0' in Table I. are, of course, the results for $c=0$.) The skin friction is determined by the values in Table III., and a few values of f and g are contained in Table IV.

It may perhaps be remarked that, throughout the range $c=0$ to 1, f varies very slowly—in fact $f''(0)$ only changes from 1·233 to 1·312—whereas in g the changes are much more rapid, the corresponding

TABLE I.

z	f'_0	f'_1	f'_2	g'_0	g'_1	g'_2
0·0	0·000	0·000	0·000	0·000	0·000	0·000
0·1	0·118	0·005	0·006	0·057	0·100	−0·054
0·2	0·227	0·010	0·012	0·114	0·191	−0·107
0·3	0·325	0·014	0·018	0·171	0·271	−0·160
0·4	0·415	0·019	0·023	0·228	0·341	−0·213
0·5	0·495	0·023	0·027	0·284	0·400	−0·264
0·6	0·566	0·027	0·031	0·339	0·450	−0·314
0·7	0·630	0·030	0·035	0·393	0·488	−0·360
0·8	0·686	0·033	0·037	0·446	0·517	−0·404
0·9	0·735	0·035	0·038	0·498	0·536	−0·444
1·0	0·778	0·036	0·039	0·547	0·546	−0·478
1·1	0·815	0·037	0·038	0·594	0·547	−0·507
1·2	0·847	0·037	0·036	0·639	0·540	−0·530
1·3	0·874	0·036	0·034	0·681	0·527	−0·547
1·4	0·897	0·035	0·032	0·720	0·507	−0·557
1·5	0·916	0·033	0·028	0·756	0·481	−0·561
1·6	0·932	0·031	0·025	0·789	0·452	−0·557
1·7	0·946	0·029	0·022	0·819	0·420	−0·548
1·8	0·957	0·026	0·018	0·846	0·385	−0·532
1·9	0·966	0·024	0·015	0·870	0·350	−0·510
2·0	0·973	0·021	0·012	0·891	0·314	−0·484
2·1	0·979	0·019	0·009	0·910	0·279	−0·454
2·2	0·984	0·016	0·007	0·926	0·246	−0·422
2·3	0·988	0·014	0·005	0·939	0·214	−0·387
2·4	0·991	0·012	0·003	0·951	0·184	−0·351
2·5	0·993	0·010	0·002	0·961	0·157	−0·315
2·6	0·995	0·008	0·001	0·969	0·132	−0·279
2·7	0·996	0·007	0·001	0·975	0·111	−0·245
2·8	0·997	0·005	0·000	0·981	0·092	−0·212
2·9	0·998	0·004		0·985	0·075	−0·182
3·0	0·998	0·003		0·988	0·061	−0·154
3·1	0·999	0·003		0·991	0·049	−0·128
3·2	0·999	0·002		0·993	0·039	−0·106
3·3	0·999	0·002		0·995	0·031	−0·086
3·4	1·000	0·001		0·996	0·024	−0·069
3·5		0·001		0·997	0·018	−0·055
3·6		0·001		0·998	0·014	−0·042
3·7		0·000		0·999	0·011	−0·032
3·8				0·999	0·008	−0·024
3·9				0·999	0·006	−0·017
4·0				1·000	0·004	−0·012

variation being from 0·570 to 1·312. These changes are reflected in the series solution in the much larger coefficients, after the first, in the g series as compared with the f.

CONCLUSIONS.

The main conclusions are embodied in Tables I. to IV., but some of the general trends may, however, be worthy of special note.

TABLE II.

	$c=0{\cdot}25$		$c=0{\cdot}50$		$c=0{\cdot}75$		$c=1{\cdot}0$
z	f'	g'	f'	g'	f'	g'	$f'=g'$
0·0	0·000	0·000	0·000	0·000	0·000	0·000	0·000
0·1	0·120	0·079	0·122	0·097	0·124	0·113	0·126
0·2	0·230	0·156	0·233	0·190	0·238	0·218	0·242
0·3	0·330	0·230	0·335	0·277	0·342	0·315	0·349
0·4	0·420	0·301	0·428	0·359	0·436	0·405	0·445
0·5	0·502	0·369	0·511	0·435	0·521	0·488	0·532
0·6	0·574	0·434	0·585	0·506	0·596	0·562	0·609
0·7	0·639	0·496	0·650	0·572	0·663	0·630	0·677
0·8	0·696	0·554	0·708	0·631	0·722	0·690	0·736
0·9	0·746	0·608	0·758	0·686	0·772	0·742	0·787
1·0	0·789	0·658	0·802	0·734	0·816	0·789	0·830
1·1	0·826	0·704	0·839	0·777	0·852	0·828	0·865
1·2	0·858	0·746	0·870	0·815	0·883	0·862	0·896
1·3	0·884	0·784	0·896	0·848	0·909	0·891	0·920
1·4	0·907	0·817	0·918	0·877	0·929	0·914	0·940
1·5	0·926	0·847	0·936	0·901	0·946	0·934	0·955
1·6	0·941	0·873	0·951	0·921	0·959	0·949	0·967
1·7	0·954	0·896	0·962	0·938	0·970	0·962	0·975
1·8	0·964	0·915	0·971	0·952	0·978	0·971	0·983
1·9	0·972	0·932	0·979	0·963	0·984	0·979	0·988
2·0	0·979	0·946	0·984	0·972	0·988	0·984	0·992
2·1	0·984	0·957	0·988	0·979	0·992	0·989	0·995
2·2	0·988	0·966	0·992	0·984	0·994	0·992	0·997
2·3	0·991	0·974	0·994	0·988	0·996	0·994	0·998
2·4	0·993	0·980	0·996	0·991	0·997	0·996	0·999
2·5	0·995	0·985	0·997	0·994	0·998	0·997	0·999
2·6	0·996	0·988	0·998	0·996	0·998	0·998	
2·7	0·997	0·991	0·998	0·997	0·999	0·998	
2·8	0·998	0·993	0·999	0·998	0·999	0·999	
2·9	0·998	0·995	0·999	0·998	0·999	0·999	
3·0	0·999	0·997	0·999	0·999	1·000	0·999	

TABLE III.

c	0·00	0·25	0·50	0·75	1·00
$f''(0)$	1·233	1·247	1·267	1·288	1·312
$g''(0)$	0·570	0·805	0·998	1·164	1·312

As a matter of notation, since we have restricted attention effectively to $0\leqslant c\leqslant 1$, we may call the axes Sx, Sy respectively, the major and minor principal axes of the mainflow. We may remark first of all that the changes with c in this range are then relatively small for the velocity component in the major direction, though marked in the minor direction.

Secondly, the direction of the velocity vector at a particular station (that is for given x, y) may undergo appreciable changes as we move through the layer. The velocity is zero at the surface, but there is a limiting direction of flow there (which is also the direction of the resultant skin friction), and this direction is inclined to the mainflow direction at an angle

$$\tan^{-1}\left(\frac{g''(0)}{f''(0)}\right)\frac{cy}{x}-\tan^{-1}\frac{cy}{x}.$$

It appears from an examination of Table II. that, as we pass from the mainstream towards the surface, the angular deviation of the velocity vector steadily changes towards this value, the sense of the change being from the mainflow towards the major principal direction. For $c=0{\cdot}00$, 0·25, 0·50, 0·75, 1·00, $g''(0)/f''(0)$ takes the values 0·463, 0·645, 0·788, 0·903, 1·0, and the maximum values of the corresponding changes in direction are then 21°*, 14°, 6°, 3°, 0° respectively; the first four occur respectively when cy/x takes the values 1·47*, 1·25, 1·13, 1·05.

Table IV.

	$c=0{\cdot}00$		$c=0{\cdot}25$		$c=0{\cdot}50$		$c=0{\cdot}75$		$c=1{\cdot}00$
z	f	g	f	g	f	g	f	g	$f=g$
0·0	0·000	0·000	0·000	0·000	0·000	0·000	0·000	0·000	0·000
0·5	0·134	0·071	0·135	0·095	0·138	0·114	0·140	0·130	0·143
1·0	0·459	0·280	0·466	0·356	0·474	0·412	0·482	0·456	0·492
1·5	0·887	0·609	0·899	0·736	0·913	0·826	0·928	0·892	0·944
2·0	1·362	1·024	1·378	1·188	1·396	1·297	1·413	1·374	1·433
2·5	1·854	1·489	1·872	1·672	1·892	1·789	1·912	1·870	1·932
3·0	2·353	1·978	2·372	2·171	2·392	2·289	2·412	2·370	2·432
3·5	2·852	2·475							
4·0	3·352	2·974							

Thirdly, we may notice that, apart from $c=1$, there is a general tendency for g to approach the mainstream value less rapidly than f, this tendency being most marked at $c=0$. In fact we might artificially speak of two boundary layer thicknesses, one associated with each principal direction, though it must be emphasized that they do not differ vastly. There is a general tendency for both thicknesses to decrease as c increases towards 1, as can be seen from Table II., or from the values of the integrals

$$\int_0^\infty\left(1-\frac{u}{ax}\right)dz,\qquad \int_0^\infty\left(1-\frac{v}{by}\right)dz$$

which are 0·648, 1·026 when $c=0$; 0·628, 0·829 when $c=0{\cdot}25$; 0·608, 0·711 when $c=0{\cdot}50$; 0·588, 0·630 when $c=0{\cdot}75$; and 0·568, 0·568 when $c=1{\cdot}0$.

---

* This is the limiting value as $c\rightarrow 0$, of course.

Finally, it may be remarked that, just as in the corresponding two dimensional solution, the solution given here is in fact a solution of the full equations of viscous motion in Cartesian coordinates.

REFERENCES.

HANNAH, 1947, *Rep. Aero. Res. Coun.*, No. 10, 482 (not yet published).
HOMANN, 1936, *Zeitschr. f. angew. Math. u. Mech.*, **16,** 153–164.
HOWARTH, 1934, *Rep. Memor. Aero. Res. Coun.*, No. 1632 ; 1951, *Phil. Mag.* [7], **42,** 239–243.
PRANDTL, 1945, *Volkenrohde Report and Translation*, No. 64.
SEARS, 1948, *J. Aero. Sci.*, **15,** 49–52.

CXLV. CORRESPONDENCE.

On the Calculation of Characteristic Temperatures from the Elastic Constants.

By M. Blackman,
Physics Department, Imperial College, London *.

[Received September 18, 1951.]

Recent work (Leigh 1951) on the free energy of alloys has drawn attention to the calculation of θ_D values in cases where the solids are elastically anisotropic. This anisotropy is due to the smallness of the $(C_{11}-C_{12})$ value, where the elastic constants of the (cubic) solid are C_{11}, C_{12} and C_{44} respectively. In such cases no simple method exists for calculating θ_D. One has either to calculate the mean velocity directly, which is a lengthy procedure, or to use the Hopf–Lechner (1914) method, which in these cases is equally lengthy and tedious. While this is immaterial in single cases, the time spent in calculation can become disproportionately large, where a series of alloys has to be considered.

Table I.

Substance	Li	Na	K	Cu	Pb	Ag	Au	Al
θ_D^*	354	144	77	342	85	212	158	394
θ_D	(351)	147	82	355	91	203	160	400

The purpose of this note is to communicate a semi-theoretical formula for θ_D designed to cover cases where $(C_{11}-C_{12})$ is relatively small. The method used is to consider the shape of the surfaces of constant frequency (*cf.* Blackman 1935). While this does not lead to a definite formula, it does suggest a reasonable form ; a constant which then remains is fixed by fitting close to the value for Lithium calculated by the standard methods.

The resultant form is

$$\nu_D^3 = s \cdot \frac{3\cdot15}{8\pi} \cdot \frac{1}{\rho^{3/2}\Delta} (C_{11}-C_{12})^{1/2}(C_{11}+C_{12}+2C_{44})^{1/2}(C_{44})^{1/2}, \quad . \quad (1)$$

where Δ=volume of the unit cell, s=number of particles per cell, ρ=density, and ν=Debye frequency. The Debye θ_D value is equal to $h\nu_D/k$ (h=Planck's constant, k=Boltzmann's constant).

Table I. shows the agreement between (1), and the values of ν_D calculated by standard methods. These, it should be remembered, are not exact calculations and may be several per cent in error. The θ values so obtained are labelled θ_D^*.

---

* Communicated by the Author.

The validity of (1) is surprisingly wide, but it should be emphasized that it is nevertheless limited. When the above formula is used, the elastic constants should be such that the C_{44}/C_{11}, C_{12}/C_{11} ratios lie inside the region covered by Table I, (*cf.* Blackman 1938, p. 76).

As an example, we take the Ag–Au alloys, the elastic constants for which have been given by Roehl (1933). The θ_D values were calculated by Roehl not from these values, but from averaged elastic constants. The result of direct calculation using (1) is given below.

TABLE II.

Substance	Ag	25 At. % Au	50 At. % Au	75 At. % Au	Au
θ_D	203	195	185	172	160

The conclusion to be drawn from this table is the same as that drawn by Roehl, namely that θ_D is not a linear function of the percentage of gold added to silver.

REFERENCES.

BLACKMAN, M., 1934, *Proc. Roy. Soc.* A, **149**, 127 ; 1938, *Ibid.*, **164**, 62.
HOPF, L., and LECHNER, G., 1914, *Verh. Deutsch. Phys. Ges.*, **16**, 643.
LEIGH, R. S., 1951, *Phil. Mag.*, **42**, 876.
ROEHL, H., 1933, *Ann. Phys.*, **16**, 887.

Inelastic Scattering of Deuterons.

By R. HUBY and H. C. NEWNS,
Department of Theoretical Physics, The University of Liverpool *.

[Received September 19, 1951.]

THE inelastic scattering of protons has been much studied in experiments, the results of which seem understandable in terms of the formation and decay of a compound nucleus.

Recently, evidence has been obtained showing that deuterons also can be inelastically scattered by nuclei (Greenlees, Kempton and Rhoderick (1949) ; Holt and Young (1949)). In some cases, *e. g.* the excitation of the 1·38 MeV. level in Mg^{24}, the total cross section seems much larger, at about 10^{-25} cm.^{2}, than would be expected for this process on the theory of compound nucleus formation. Further, the angular distribution, which has been measured in the above-mentioned case by Holt and Young, is of a complicated form, with a strong concentration at rather small angles of scattering, such as would seem unlikely on that theory. The present authors therefore attempted an explanation through electrical interaction of the deuteron with the nucleus, but this was found to yield much too small a cross section to account for the present experiments (Huby and Newns (1951)). In a similar treatment, Mullin and Guth (1951) were able to obtain an angular distribution of approximately the required shape, but to account for the measured total cross section, they would require a dipole moment of the order of three times the nuclear radius, which seems too large to be physically plausible.

---

* Communicated by the Authors.

The purpose of this letter is to propose a very simple mechanism to account for the main features of the experimental results. The mechanism is suggested by the similarity of the observed angular distributions to those obtained in various (d–p) and (d–n) reactions, and it has something in common with the stripping theory for the latter. We assume that only one of the constituents of the deuteron, say the neutron, interacts with the nucleus, the proton being outside the range of the nuclear forces. The neutron interacts at the surface of the nucleus, exciting it and then " bouncing off ", the deuteron emerging as a whole having been inelastically scattered*. A calculation can be made, based on the Born approximation, and following closely a treatment of the (d–p) and (d–n) reactions of Bhatia and Huang (reported by Huby (1950)). Despite its crudity, the latter had considerable success in explaining the observed (d–p) and (d–n) angular distributions, and this seems an encouragement for the present calculation for (d–d*) reactions.

The differential cross section can be written

$$\sigma(\theta)=\frac{2\pi}{\hbar}\left|\int \psi_f^* \chi_f^* \chi_{\mathrm{D}f}^* \mathrm{V} \psi_i \chi_i \chi_{\mathrm{D}i}\, d\tau\, d\mathbf{R}_n\, d\mathbf{R}_p\right|^2,$$

where ψ_i and ψ_f are the initial and final deuteron translational wave functions, χ_i and χ_f the initial and final nuclear wave functions, and $\chi_{\mathrm{D}i}$ and $\chi_{\mathrm{D}f}$ the initial and final internal deuteron wave functions. V represents the interaction between the neuteron and the nucleus. This can be evaluated if we assume (i.) the interaction V operates only on a sphere of " radius of interaction " a, (ii.) the incident and scattered deuterons waves are plane waves of wave number $\mathbf{k}_i$ and $\mathbf{k}_f$ respectively, (iii.) the ground state of the deuteron is a pure triplet-S state, with radial wave function of the form $\exp\{-\alpha|\mathbf{R}_n-\mathbf{R}_p|\}/|\mathbf{R}_n-\mathbf{R}_p|$.

The result obtained is

$$\sigma(\theta)=\sum_l |\mathrm{A}_l|^2\left[\frac{4\alpha}{k}\tan^{-1}\frac{k}{4\alpha}\cdot\left(\frac{\pi}{2ka}\right)^{1/2}\mathrm{J}_{l+1/2}(ka)\right]^2,$$

where $k^2=(k_i-k_f)^2+4k_ik_f\sin^2\frac{1}{2}\theta$, and the A_l's are unknown constants. The formula for σ gives scattering predominantly at small angles. The sum is taken over integers l which are related to the angular momentum change of the nucleus. There are selection rules requiring that if J_i and J_f are the angular momentum of the initial and final states of the nucleus, then $\mathbf{J}_f=\mathbf{J}_i+\mathbf{l}+\mathbf{1}$ (but when $J_i=0$, and $l=0$ then $J_f=0$ or 1), and l is odd or even according as there is a change of parity or not. The values of l can be determined from the angular distribution. If more than one value of l can contribute, the lowest one usually predominates. Thus the angular distribution of inelastically scattered deuterons can lead to information about the spins and parities of nuclear states.

---

* A rather similar model was in fact proposed by E. Guth (*Phys. Rev.*, **68**, 280 (1945)) in predicting inelastic scattering of deuterons.

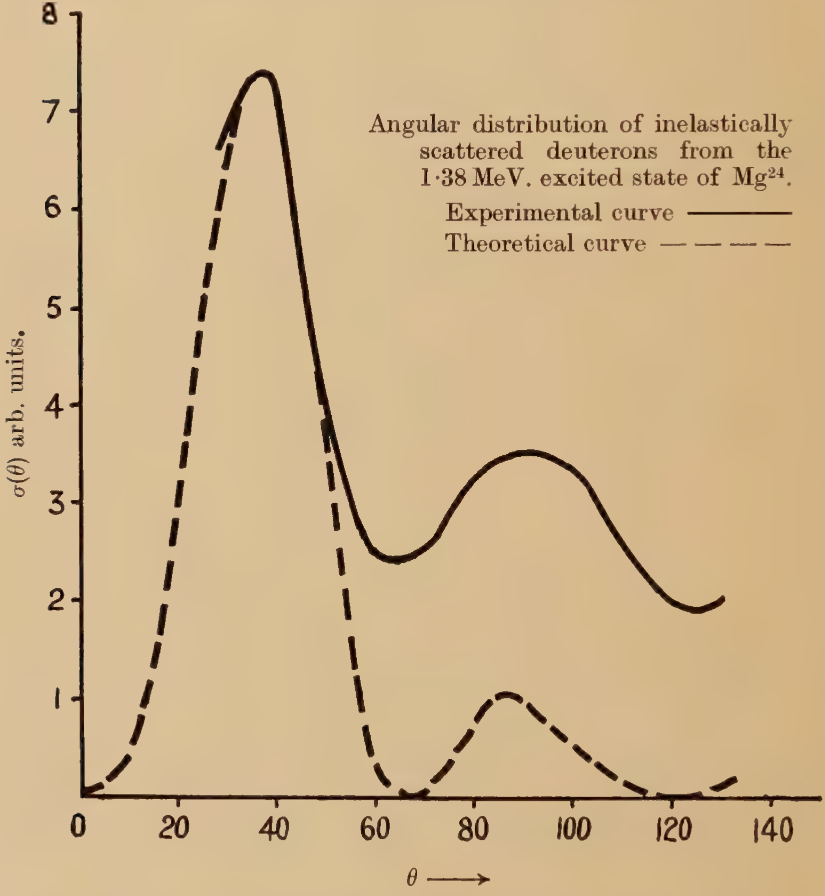

A particular example is the case of deuterons inelastically scattered from the 1·38 MeV. excited state of Mg^{24}. A theoretical curve for $l=2$ is shown in the figure together with the experimental curve (Holt and Young (1949)). Since the ground state of Mg^{24} has spin zero and even parity, the first excited state has spin 1, 2 or 3 and even parity.

The parameter a is not well defined. One might expect it to be given by the Gamow formula (Gamow and Critchfield (1949)) for the nuclear radius, but as in the (d–p) reaction, the values of a needed are always larger than this. In the magnesium case discussed above, we used $a = 7 \times 10^{-13}$ cm. To make curves for different values of l fit, values of a which seem unreasonable would be required. A spin of 2 for the excited state would be in agreement with the experiments on the angular correlation of successive γ-ray emissions from the nucleus (Brady and Deutsch (1948)).

The angular distribution of deuterons inelastically scattered from the 1·66 MeV. excited state of Ne^{20} has been measured by Middleton and Tai (unpublished). This can be fitted by the theoretical curve for $l=1$. Since the ground state of Ne^{20} has spin zero and even parity, the 1·66 MeV. excited state must have spin 0, 1 or 2 and odd parity.

REFERENCES.

BRADY, E. L., and DEUTSCH, M., 1948, *Phys. Rev.*, **74,** 1541.
GAMOW, G., and CRITCHFIELD, G. L., 1949, *Atomic nucleus and nuclear energy sources* (Oxford : Clarendon Press).
GREENLESS, G. W., KEMPTON, A. E., and RHODERICK, E. H., 1949, *Nature, Lond.*, **164,** 663.
HOLT, J. R., and YOUNG, C. T., 1949, *Nature, Lond.*, **164,** 1000.
HUBY, R., 1950, *Nature, Lond.*, **166,** 552 ; also private circulation.
HUBY, R., and NEWNS, H. C., 1951, *Proc. Phys. Soc.* A, **64,** 619.
MULLIN, C. J., and GUTH, E., 1951, *Phys. Rev.*, **82,** 141.

Experiments on the Unsaturated Helium II Film.

By R. BOWERS, D. F. BREWER and K. MENDELSSOHN, F.R.S.,
Clarendon Laboratory, Oxford *.

[Received September 17, 1951.]

THE transfer of the helium II film at pressures lower than the vapour pressure of the liquid has been investigated by a method which consists essentially in measuring the heat conduction of a tube containing He gas under variable percentage saturation.

The principle of the apparatus is shown in fig. 1. The bottom of the (thin-walled german silver) tube is connected to a constant-temperature heat sink, while the top contains a heater and a thermometer. When, under fixed conditions of temperature of the sink and of pressure in the tube, heat is supplied at increasing rates Q, the thermometer remains constant at its original reading until a certain critical heat input Q_c is reached, when it rises sharply. The constancy of temperature is maintained by flow of the film up the inside wall of the tube, the film evaporating at the top, and the helium returning as gas to the bottom of the tube. This circulation provides a powerful means of heat transport, in which the latent heat of the helium is taken up by evaporation at the top, and given off by condensation at the bottom to the heat sink. Incidentally, the heat of evaporation from the film is slightly larger than that of the bulk liquid (L_B), since it also contains the energy of excitation of the superfluid into the normal state ($T\Delta S$). The circulation process must break down when a film flow rate larger than the critical rate r_c is required to maintain it. The critical heat input $\dot{Q}_c$ thus provides an accurate means of determining the critical rate of mass transport of the He II film since

---

* Communicated by the Authors.

$$r_c = \frac{\dot{Q}_c}{(L_B + T\Delta S)}.$$

Fig. 1.

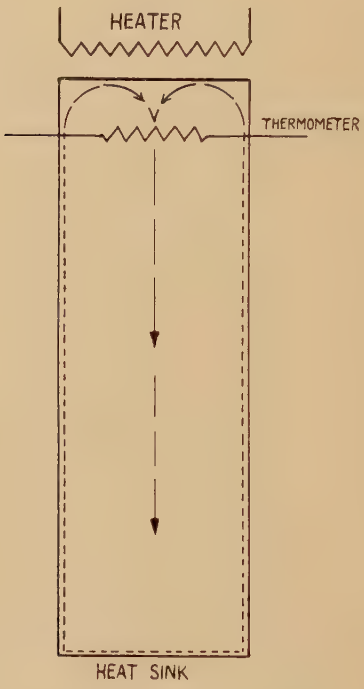

Such factors as might influence the validity of this equation, *e. g.* viscous drag in the returning gas, heat flow by conduction along the metal tube and through the gas, and heat resistance of the partition between the tube and the heat sink, were negligibly small in our case. A check on the validity of the method was provided by plotting the critical flow rates obtained at various temperatures under saturation conditions (r_s) against the absolute temperature. The values derived are in satisfactory agreement with the shape of the curve of transfer rate out of a beaker (Mendelssohn and White 1950).

Transfer rates under various percentage saturations have been obtained for four different temperatures, and the results are given in fig. 2, where the reduced transfer rates r_c/r_s are plotted against the percentage saturation.

The method is sensitive enough to detect mass flow of the order of 0·1 per cent of the saturation flow rates ($r_c/r_s \sim 0{\cdot}001$).

The results show clearly that any appreciable film transfer will only occur near saturation. In fact, even for the lowest temperature (1·37° K.), the flow rate at 90 per cent saturation is only 5 per cent of the full rate ; while nearer the lambda point (1·84° K.), this fraction of the full rate is only reached at 98 per cent saturation. The curves also indicate that for any particular percentage saturation, there exists a temperature above which no film transfer occurs. This " critical " temperature decreases with decreasing percentage saturation.

Fig. 2.

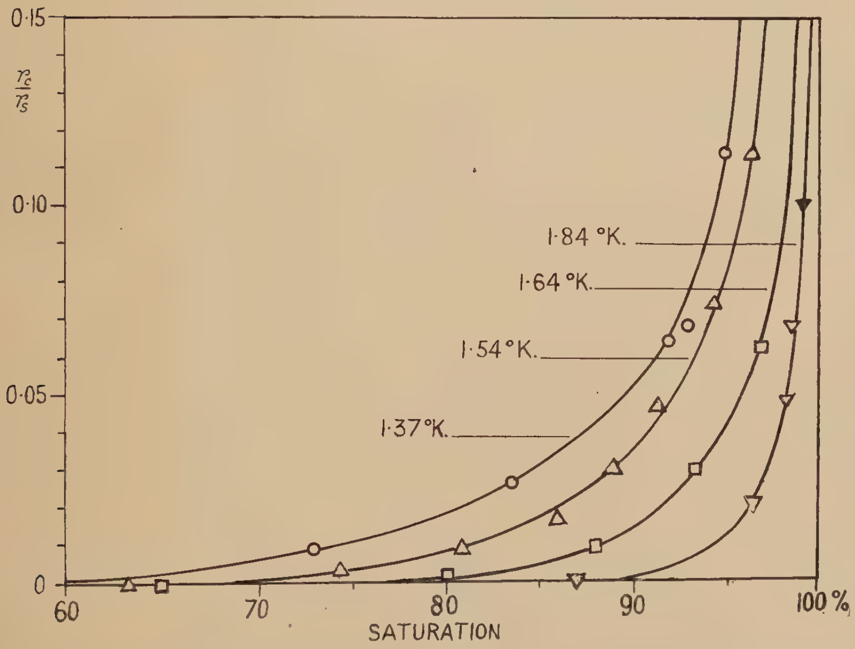

Our values give mass flow rates which can be expressed as a product of the film thickness d, and an average velocity $\bar{v}$. The only measurements of d close to 100 per cent saturation (Long and Meyer 1949) indeed indicate that this quantity is rising rapidly above 90 per cent saturation. At 80 per cent saturation, where according to Frederikse and Gorter (1950) the film thickness is about 10 per cent of that of the saturated film (Daunt and Mendelssohn 1939, Burge and Jackson 1951), d hardly varies with temperature. On the other hand, it is evident from our measurements that the mobility of the film increases rapidly as the temperature is lowered. It is hoped to obtain better determinations of $\bar{v}$ from improved measurements of the adsorption isotherms near 100 per cent saturation, and from more detailed determinations of the transfer rates which are now in progress. So far, our observations do not suggest that $\bar{v} \times d$ is constant.

REFERENCES.

BURGE, E. J., and JACKSON, L. C., 1951, *Proc. Roy. Soc.* A, **205,** 270.
DAUNT, J. G., and MENDELSSOHN, K., 1939, *Proc. Roy. Soc.* A, **170,** 439.
FREDERIKSE, H. P. R., and GORTER, C. J., 1950, *Physica*, **16,** 402.
LONG, E. A., and MEYER, L., 1949, *Phys. Rev.*, **76,** 440.
MENDELSSOHN, K., and WHITE, G. K., 1950, *Proc. Phys. Soc.* A, **63,** 1328.

The Upper Limit for the Neutrino Rest Mass.

By O. KOFOED-HANSEN,
Institute for Theoretical Physics, University of Copenhagen*.

[Received July 9, 1951.]

SINCE the β-spectrum of H^3 has a very low maximum energy it provides us at present with the best possibility for the determination of the rest mass of the neutrino. The following comments on the problem may be of relevance in view of the great experimental progress recently achieved (Curran, Angus and Cockroft 1949, Hanna and Pontecorvo 1949).

For a finite neutrino mass the shape of the β-spectrum is given by

$$P(E)=p\,.\,E\,.\,(E^{\max}+m_\nu-E)\,.\,\{(E^{\max}+m_\nu-E)^2-m_\nu^2\}^{\frac{1}{2}}$$
$$\times[1+bm_\nu m_\beta/(E(E^{\max}+m_\nu-E))]\,.\,F(Z, E) \quad . \quad . \quad . \quad (1)$$

where E is the energy of the β-particle including the rest mass m_β, p is the corresponding momentum, $E^{\max}$ is the maximum energy of the β-particle, m_ν is the rest mass of the neutrino in energy units (we put $c=1$), F(Z, E) is the Coulomb factor and b is a constant which we shall discuss in the following.

It has been shown previously (1947) that even if the neutrino mass is not zero the extrapolated maximum β-energy, if sufficiently large, is the same as for vanishing neutrino mass, *i. e.*, it equals the mass difference Δ between the two nuclei involved in the process. Consequently, in this case the maximum β-energy and the mass of the neutrino can only be determined by the original Fermi method, *i. e.* from the shape of the β-spectra in the immediate vicinity of the upper limit.

Pruett (1948) has pointed out that the term in (1) containing b is important for the discussion of the influence of a finite neutrino mass at low energy β-spectra. Pruett adopted the value -1 for b. However, b may also assume the value $+1$, and if linear combinations of the five coupling cases are used also values between ± 1 may occur. Furthermore, no definite sign of b can be attached to a definite coupling case (Yang and Tiomno 1950).

Many authors assume that the result of an extrapolation of the observed β-spectrum when the term containing b in (1) is taken into account and for low maximum energies leads to an extrapolated upper limit of the spectrum which deviates by $m_\nu/2$ from the value obtained for vanishing neutrino mass. Such a result is found when the β-spectrum is expanded in a series in $m_\nu/(\mathrm{E}^{\max}+m_\nu-\mathrm{E})$. Unfortunately, however, this series is not adequate for the low energy spectra since the condition for such a series development, viz. $m_\nu \ll \mathrm{E}^{\max}+m_\nu-\mathrm{E}$, can not be assumed to hold for the major part of the spectrum. A correct procedure is to apply a numerical evaluation of (1). The result is illustrated in fig. 1 where three hypothetical Kurie (or Fermi) plots are given. In this kind of plot one draws

---

* Communicated by the Author.

$$\{\mathrm{P(E)}/(p\mathrm{E}\,.\,\mathrm{F(Z, E)})\}^{\frac{1}{2}} \quad . \; . \; . \; . \; . \; . \; . \quad (2)$$

Fig. 1.

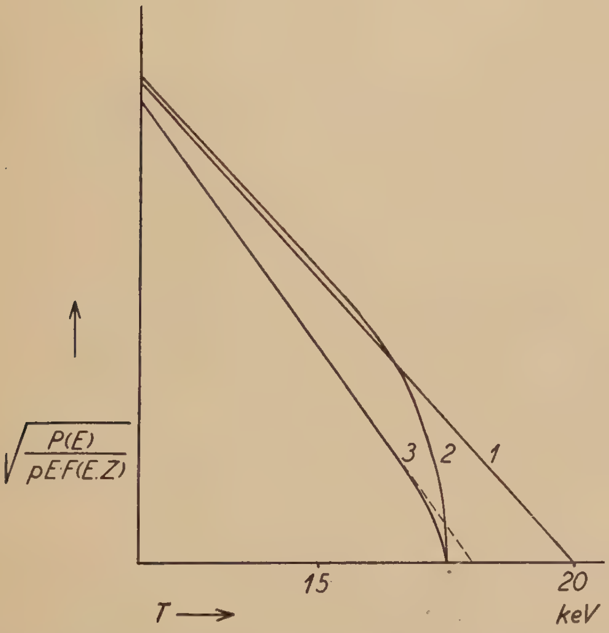

The figure shows hypothetical Kurie plots for $(\Delta-m_\beta)=20$ keV. and for vanishing neutrino mass (curve 1) and for $m_\nu=2{\cdot}5$ keV. and $b=+1$ (curve 2) and $b=-1$ (curve 3). The extrapolated curves will cut the abscissa very close to 20 keV. for curve 2 giving no effect of m_ν and at $\sim$18 keV. for curve 3 giving an effect of $\sim 4/5 m_\nu \simeq m_\nu$. T is the kinetic energy of the β-particle.

as a function of E. If $m_\nu=0$ the Kurie plot is a straight line cutting the abscissa at $\mathrm{E}=\mathrm{E}^{\max}$. For $m_\nu \neq 0$ effects of the neutrino mass appear. In the present low energy case the conclusions as regards the mass of the neutrino are that if $b=1$ one finds a curve which lies rather close to the curve for zero neutrino mass, and in the case $b=-1$ one finds a curve which deviates from the curve for zero neutrino mass by almost the full amount corresponding to m_ν. This means that if ever a finite neutrino mass is observed then this procedure could be used for a determination of b.

In the case of H^3 one does not know the precise value of the mass difference Δ between the H^3 and He^3 nuclei. The main uncertainty comes from the uncertainty in the n-p mass difference. Nuclear cycles involving β-decay processes are our best tools for the determination of the n-p mass difference (Li, 1951) but obviously they involve the assumption of zero neutrino mass so that we cannot apply the Δ value found in this way. Consequently we cannot compare $E_\beta^{\max}$ and Δ directly. However, the shape of the spectrum is known very precisely close to the upper limit of the energy, and thus from the shape of the spectrum one has the possibility of a determination of the neutrino rest mass. The experimental result is (Hanna and Pontecorvo 1949) that the Kurie plot deviates from a straight line by less than 1 keV. Since b is not known this deviation may be a measure of $\sim$1/5 of the neutrino mass only. This represents the lowest curve in fig. 1 corresponding to $b=-1$. Thus we may only conclude that the neutrino mass is smaller than 5 keV. or that the neutrino mass is smaller than 1/100 of the electron mass. This statement is more conservative than the result given by Hanna and Pontecorvo (1949).

REFERENCES.

CURRAN, S. C., ANGUS, J., and COCKROFT, A. L., 1949, *Phil. Mag.*, **40,** 36, 53.
HANNA, G. C., and PONTECORVO, B., 1949, *Phys. Rev.*, **75,** 983.
KOFOED-HANSEN, O., 1947, *Phys. Rev.*, **71,** 451.
LI, C. W., WHALING, W., FOWLER, W. A., and LAURITSEN, C. C., 1951, *Phys. Rev.*, **83,** 512.
PRUETT, J. R., 1948, *Phys. Rev.*, **73,** 1219.
YANG, C. N., and TIOMNO, J., 1950, *Phys. Rev.*, **79,** 495.

ERRATA

A Theoretical Investigation of the Compression of a Ductile Material between Smooth Flat Dies, by A. P. GREEN, 1951, *Phil. Mag.*, **42,** 900.

On page 916 the tranformation equations should read:

$$\left.\begin{array}{llll} u=\bar{y}', & v=-\bar{x}', & \alpha\to\alpha', & \phi=\phi' \quad (b), \\ u=\bar{x}', & v=-\bar{y}', & \alpha\to\beta', & \phi=-\phi' \quad (c), \\ u=\bar{y}', & v=\bar{x}', & \alpha\to .', & \phi=-\phi' \quad (d). \end{array}\right\} \quad . \quad . \quad . \quad (5)$$

Electron and Gamma Ray Spectroscopy with Scintillation Detectors, by R. C. BANNERMAN, G. M. LEWIS and S. C. CURRAN, 1951, *Phil. Mag.*, **42,** 1097.

On page 1102, line 6, the expression " 15 per cent " should read " 1 per cent ".

[*The Editors do not hold themselves responsible for the views expressed by their correspondents.*]

OBITUARY NOTICE

DR. ALLAN FERGUSON

We regret to announce the death of Dr. ALLAN FERGUSON, for many years an Editor of the Philosophical Magazine, who passed away on Friday, November 9th, 1951.

An appreciation and tribute will be published in a later issue of this publication.

INDEX TO VOL. XLII.

ABSORPTION of penetrating shower secondaries (Ritson), 250.
Ahmed (M. S.), ionization of lithium hydride, 997.
Allowed β-transitions, effects of recoil (Kofoed-Hansen), 1411.
Alloys at low temperatures, thermal conductivity (Berman), 642.
α-particles from O_{18} (Seed), 566.
α, α' phases in Al–Zn systems (Leigh), 876.
Amelinckx (S.), interferometric study of cleavage planes of sodium chloride, 324.
Analastic measurements of diffusion in solid solutions (Le Claire), 673.
Analytical continuation of the S-matrix (van Kampen), 851.
Armenteros (R.), Barker (K.), Butler (C. C.) and Cachon (A.), properties of neutral V-particles, 1113.
Ashwell (D. G.), axis of distortion of twisted elastic prism, 820.
Aspinall (A.), Clegg (J. A.) and Hawkins (G. S.), radio echo apparatus for delineation of meteor radiants, 504.
Atkinson (J. R.), *see* Howatson, 1136.
Atmospherics, waveforms and propagation (Bowe), 121.
Attenuation of nucleon cascades in lead (Rosser and Swift), 856.
Bannerman (R. C.), Lewis (G. M.) and Curran (S. C.), electron and γ-ray spectroscopy with scintillation counters, 1097 ; (erratum), 1450.
Bardsley (O.), conditions at sharp leading edge in supersonic flow, 255.
—— and Mair (W. A.), interaction between an oblique shock-wave and a turbulent boundary layer, 29.
Barium titanate, theory (Devonshire), 1065.
Barker (K.), *see* Armenteros, 1113.
^{9}Be$(p, p2n)^7$Be, cross-section (Randle *et al.*), 665.
Berman (R.), thermal conductivity of some alloys at low temperatures, 642.
Beryl crystals, microscopic studies (Griffin).—I., 775.
——, ——. —II., 1337.
Beta decay, interaction in the theory (Pursey), 1193.
β-spectrum of tritium (Insch and Curran), 892.
Bilby (A. H.), *see* Cottrell and Bilby, 573.
Binding energies of 3 and 4 particle nuclei (Irving), 338.
Bishop (J. F. W.) and Hill (R.), plastic properties of poly-crystalline F.C. metal, theoretical derivation, 1298.
——, theory of plastic distortion of a polycrystalline aggregate under combined stresses, 414.
Blackman (M.), calculation of characteristic temperatures from elastic constants, 1441.
Bleaney (B.), hyperfine structure in paramagnetic salts and nuclear alignment, 441.
——, Elliott (R. J.), Scovil (H. E. D.) and Trenam (R. S.), paramagnetic resonance in gadolinium ethylsulphate, 1062.
Bloch-Nordsieck method, covariant formulation (Thirring and Touschek), 244.
Books, new :—Alfven, Cosmical electrodynamics, 118 ; Bouman (J.), Selected topics in X-ray crystallography, 958 ; Butler and Randall, Progress in Biophysics, 118 ; Corner (J.), Theory of interior ballistics of guns, 958 ; Faffingdon (G. H.), Fundamentals of automatic control, 1335 ; Fisher,

Mathematical statistics, 119; Heavyside (O.), Electromagnetic theory, 440; Hill (R.), Mathematical theory of plasticity, 439; Huckel (W.), Structural chemistry of inorganic compounds, 220; Jeffreys (H. and B. S.), Methods of mathematical physics, 119; Jellinck (K.), Weltsystem etc.; Wellenmechanik, 438; London (F.), Super-fluids, 958; MacMillan (R. H.), Theory of control in mechanical engineering, 1335; Pearse and Taylor, Identification of molecular spectra, 959; Progress in physics, Vol. XIV, 1064; Rossini (F. D.), Chemical thermodynamics, 959; Smart (E. H.), Advanced dynamics, 960; Steinhaus (H.), Mathematical snapshots, 439; Vigoureux (P.), Ultrasonics, 439; Wheeler (L. P.), J. Willard Gibbs, 1335; Wilson (W.), Hundred years of physics, 119.

Born-green theory of fluids (Rushbrooke and Scoins), 582.

Bose-Einstein gas, condensation (Fraser).—I., 156.

—— .—II., 165.

Boundary layer on rotating sphere (Howarth), 1308.

Boundary layer in three dimensional flow (Howarth).—I., 239,

—— .—II., 1433.

Bowe (P. W. A.), waveforms of atmospherics and propagation of very low frequency, 121.

Bowers (R.), Brewer (D. F.) and Mendelssohn (K.), experiments on unsaturated helium film, 1445.

Braddick (H. J. J.), Nash (W. H.) and Wolfendale (A. W.), associated penetrating particles of cosmic rays underground, 1277.

Brewer (D. F.), *see* Bowers, 1445.

Brinkworth (M. J.) and Titterton (E. W.), reaction $^{10}B(\gamma, d)2^4He$, 952.

——, Photodisintegration of ^{10}B, 1191.

Bromine, electric quadrupole and magnetic moment of nucleus, 279.

——, hyperfine structure, 284.

Broom (T.), anisotropy of electrical resistance, cold-rolled metals and alloys, 56.

Brown (A. F.) and Honeycombe (R. W. K.), micro-slip in metal crystals, 1146.

Brownian movement, velocity (Macdonald), 219.

Budden (K. G.), propagation of a radio-atmospheric, 1.

——, reflection of low frequency radio waves, 833.

Burcham (W. E.), *see* Freeman, 434.

Burgess (R. E.), rectification and observation of signals in presence of noise, 475.

Butler (C. C.), *see* Armenteros, 1113.

Cachon (A.), *see* Armenteros, 1113.

Calcraft (M. E.) and Titterton (E. W.), reactions $^{11}Be(\gamma\alpha)^7Li$ and $^{11}B(\gamma T)^8Be$, 666.

Calnan (E. A.) and Clews (C. J. B.), deformation textures in metals.—II., 616.

—— .—III., 919.

Camerini (U.), Davies (J. H.), nuclear transmutations of great energy; with Fowler (P. H.) *et al.*—VI., 1241.

——with Franzinetti (C.) *et al.*—VII., 1261.

Capacitance of condenser with anisotropic cylinder in torsion (Mack), 428.

Carborundum growth spirals (Verma), 1005.

—— —— (Frank), 1014.

Cassels (J. M.), *see* Taylor, 20, 328, 751.

——, *see* Randle, 665.

——, Randle (T. C.), Pickavance (T. G.) and Taylor (A. E.), production of neutrons by high energy protons, 215.

Cavanagh (P. E.), *see* Turner, 636.

Characteristic temperatures from elastic constants (Blackman), 1441.

Cherry (C.), non-linear systems possessing reactance, 1161.

Clegg (J. A.), *see* Aspinall, 504.

Clews (C. J. B.), *see* Calnan, 616, 919.

Collision broadening at microwave frequencies (Leslie), 37.

Combined bending and twisting of thin tubes (Hill and Siebel), 722.

Communal entropy of dense systems (Pople), 459.
Compression of ductile material (Green), 900, 1336, 1450.
Cornish (F. H. J.) and MacDonald (D. K. C.), influence of deviations from Debye spectrum on electrical conductivity of metals, 1406.
Cosmic radiation, charge and energy of heavy nuclei (Dainton, Fowler and Kent), 317.
Cosmic rays, origin of stars (Harding), 63.
—— ——, disintegration of nuclei (Hodgson), 82, 955.
—— ——, emission of Li^8 (Hodgson), 207.
—— ——, neutrons in ice (Lattimore), 331.
—— ——, events in glacier (Harding), 651.
—— ——, stars, cascade production (Thomson and Hodgson), 978.
—— ——, associated particles underground (Braddick, Nash and Wolfendale), 1277.
Cottrell (A. H.) and Bilby (B. A.), mechanism for growth of deformation twins in crystals, 573.
Cottrell (T. L.) and Paterson (S.), virial theorem in quantum mechanics, 391.
Critical magnetic fields of Al, Cd, Ga and Zn (Goodman and Mendoza), 594.
Cross-sections for neutrons (Taylor *et al.*), 20, 328, 751, 1336.
Crystal dislocations (Frank), 809.
Crystal plasticity (Nabarro), 213.
Crystalline structure and strength of metals (Wood), 310.
Curran (S. C.), *see* Wilson, 762; Insch, 892; Bannerman, 1097.
Dainton (A. D.), Fowler (P. H.) and Kent (D. W.), new method of determining charge and energy of heavy cosmic nuclei, 317.
Dainton (A. D.), Gattiker (A. R.) and Lock (W. O.), processing of thick emulsions, 396.
Dalitz (R. H.) and Ravenhall (D. G.), Tomonaga method in meson field theory, 1378.
Danysz (M.) and Yekutieli (G.), loading emulsions with wires, 1185.
Davies (J. H.), *see* Camerini, 1241, 1261.
Deflection of cable, single point load (Markland), 990.
Deformation textures in metals (Calnan and Clews).—II., 616.
—— .—III., 919.
—— twins in crystals (Cottrell and Bilby), 573.
Density of states, 3*d* electrons in nickel (Fletcher and Wohlfarth), 106.
Devonshire (A. F.), theory of barium titanate.—II., 1065.
Dickson (J. M.), *see* Randle *et al.*, 665.
Dingle (R. B.), two-fluid model of helium II., 1080.
Dirac's matrices, trace of product (Yang), 1333.
Directive wave propagation (Nodtvedt), 1022.
Dislocation fields synthesis (Nabarro), 1224.
—— in thin plates (Eshelby and Stroh), 1401.
—— reaction in F.C. lattice (Lomer), 1327.
Domb (C.), melting curve at high pressures, 1316.
Dymond (E. G.), *see* Pullar, 663.
Elastic constants of aluminium (Leigh), 139.
Electrical conductivity of metals (Cornish and MacDonald), 1406.
—— resistance, anisotropy, cold-rolled metals and alloys (Broom), 56.
—— —— of gold, silver and copper at low temperatures (Mendoza and Thomas), 291.
Electron and γ-ray spectroscopy (Bannerman, Lewis and Curran), 1097, 1450.
Elliott (R. J.), *see* Bleaney, 1062.
Emulsions, loading with wires (Danysz and Yekutieli), 1185.
Energy loss of slow deuterons in D_2O (French and Seidl), 537.
Equilibrium of linear arrays of dislocations (Eshelby, Frank and Nabarro), 351.
Eshelby (J. D.), Frank (F. C.) and Nabarro (F. R. N.), equilibrium of linear arrays of dislocations, 351.

Eshelby (J. D.) and Stroh (A. N.), dislocation in thin plates, 1401.

Feather (N.), isomeric state of RaE, 568.

Ferromagnetism, collective electron (Wohlfarth), 374.

Field theories with non-localized interaction (Rayski), 1289.

Fletcher (G. C.) and Wohlfarth (E. P.), density of states, 3*d* electrons in nickel, 106.

Forty (A. J.), growth of cadmium iodine from aqueous solution, 670.

Fowler (P. H.), Menon (M. G. K.), Powell (C. F.) and Rochat (O.), masses and decay of heavy τ-mesons.—II., 1040.

Fowler (P. H.), *see* Dainton, Fowler and Kent, 317 ; Camerini, 1241.

Frank (F. C.), crystal dislocations, 809.

——, growth of carborundum, 1014.

——, *see* Eshelby, 351.

Frank (S. G. F.), Frisch (O. R.) and Scarrott (G. G.), mechanical kick-sorter, 603.

——, localizing Geiger counter, 612.

Franzinetti (C.), *see* Camerini, 1241, 1261.

Fraser (A. R.), condensation of a perfect Bose-Einstein gas.—I., 156.

—— .—II., 165.

Freeman (J. M.) and Burcham (W. E.), range-energy relation for slow α particles in air, 434.

French (A. P.) and Seidl (G. F. P.), energy loss of slow deuterons in D_2O, 537.

——, matrix elements for octupole radiative transitions, 263.

Frisch (O. R.), *see* Frank (S. G. F.), 603.

Gattiker (A. R.), *see* Dainton, 396.

Geiger counter, localizing (Frank, S. G. F.), 612.

Gibson (W. M.), Grotdal (T.), Orlin (J. J.) and Trumpy (B.), photodisintegration of the deuteron, 555.

Gold (T.), ultrasonic delay line, design, 787.

Goldsack (S. J.) and Page (N.), example of *n*, *p* ; π^--reaction in emulsion, 570.

Goodman (B. B.) and Mendoza (E.), critical magnetic fields of Al, Cd, Ga, and Zn, 594.

Gottstein (K.), Menon (M. G. K.), Mulvey (J. H.), O'Ceallaigh (C.) and Rochat (O.), multiple scattering of particles in emulsions.—I., 708.

—— and Mulvey (J. H.), multiple scattering in emulsions.—IV., 1089.

Grain boundary diffusion in metals (Le Claire), 468.

Green (A. P.), flow of metals, plasticine models, 365.

——, compression of ductile material between flat dies, 900 ; (errata), 1336, 1450.

Griffin (L. J.), microscopic studies on beryl crystals.—I., 775.

—— .—II., 1337.

Grodtal (T.), *see* Gibson, 555.

Growth of cadmium iodide from solution (Forty), 670.

Gunn (J. C.) and Irving (J.), photoelectric disintegration of 3- and 4-particle nuclei, 1353.

——, Power (E. A.) and Touschek (B. K.), production of mesons in proton–proton collisions, 523.

Hammer tracks in neutron and proton produced stars (Titterton), 113.

Harding (J. B.), origin of cosmic ray stars, 63.

——, cosmic ray events in a glacier, 651.

Hawkins (G. S.), *see* Aspinall, 504.

Hayes (J. G.) and Vickers (T.), fitting of polynomials to unequally-spaced data, 1387.

Helium II film, unsaturated (Bowers, *et al.*), 1445.

Helium II, quantum mechanics (Penrose), 1373.

——, two-fluid model (Dingle), 1080.

Helium, ultrasonic propagation in liquid (Pippard), 1209.

Henisch (H. K.), internal barriers in semi-conductors, 734.

Highly forbidden transitions in Na^{24} (Turner and Cavanagh), 636.

Hill (R.), stress in a plastic-rigid body at yield point, 868.

—— and Siebel (M. P. L.), combined bending and twisting of thin tubes in the plastic range, 722.

Hill (R.), *see* Bishop and Hill, 414, 1298.
Hodgson (P. E.), disintegration of lead nuclei by cosmic rays, 82.
Hodgson (P. E.), emission of Li^8, 207.
——, disintegrations of light nuclei, 955.
——, τ-meson, 1060.
——, *see* Thomson, 978.
Honeycombe (R. W. K.), *see* Brown, 1146.
Hooper (J. E.), King (D. T.) and Morrish (A. H.), pair production by fast electrons, 304.
Howarth (L.), boundary layer on a rotating sphere, 1308.
——, boundary layer in three dimensional flow.—I., 239.
—— .—II., 1433.
Howatson (A. F.) and Atkinson (J. R.), nuclear scattering of electrons and positrons, 1136.
Huang (K.), thermal pressures in solids, Hildebrand's approximation, 202.
Huby (R.) and Newns (H. C.), inelastic scattering of deuterons, 1442.
Hutchinson (G. W.) and Scarrott (G. G.), high precision pulse height analyser of moderately high speed, 792; (Erratum), 957.
Incompressible viscous fluid, unsteady flow (Sowerby), 176.
Inelastic scattering of deuterons (Huby and Newns), 1442.
Insch (G. M.) and Curran (S. C.), β spectrum of tritium, 892.
Interaction, oblique shock-wave and turbulent boundary-layer (Bardsley and Mair), 29.
Irving (J.), binding energies of 3- and 4-particle nuclei, 338.
——, *see* Gunn, 1353.
Keith (H. D.) and Mitchell (J. W.), lattice defects in silver bromide at room temperature, 1331.
Kent (D. W.), *see* Dainton, 317.
King (D. T.), *see* Hooper, 304.
Kofoed-Hansen (O.), allowed β transitions, effects of recoil, 1411.
——, upper limit for neutrino rest mass, 1448.
Kuper (C. G.), model of intermediate state of superconductors, 961.
Landau diamagnetism and Meissner effect (Papapetrou), 95.
Lattimore (S.), rate of production of neutrons in ice by cosmic rays, 331.
Le Claire (A. D.), grain boundary diffusion in metals, 468.
——, analastic measurements of diffusion in solid solutions, 673.
Leigh (R. S.), α, α' phases in Al–Zn systems, 876.
——, elastic constants of aluminium, 139.
Leslie (D. C. M.), collision broadening at microwave frequencies, 37.
Lewis (G. M.), *see* Bannerman, 1097.
Lidiard (A. B.), influence of exchange energy on specific heat of free electrons in metals, 1325.
Lithium hydride, ionization (Ahmed), 997.
Liquid helium, ultrasonic propagation (Pippard), 1209.
Little (C. G.) and Maxwell (A.), radio waves from galactic sources, fluctuations in intensity, 267.
Lock (W. O.), *see* Dainton, 396; Camerini, 1241, 1261.
Lomer (W. M.), dislocation reaction in F.C. lattice, 1327.
Luchak (G.), generalization of Wilson's Hypothesis, 807.
Macdonald (D. K. C.), velocity in brownian movement, 219.
——, transit-time phenomena in electronstreams.—III., 515.
——, metallic conduction—Internal size-effect, 756.
——, *see* Cornish, 1406.
—— and Templeton (I. M.), resistance-minimum in gold, 432.
Mack (C.), capacitance of parallel-plate condenser with anisotropic dielectric cylinder in torsion between, 428.
Mair (W. A.), *see* Bardsley, 29.
Markland (E.), deflection of cable, single point load, 990.
Masses and modes of decay of heavy mesons.—I., κ particles (O'Ceallaigh), 1032.
—— — .—II., τ particles (Fowler, *et al.*), 1040.
Matthews, (P. T.) meson–photon–nucleon interaction, 221.
Maxwell (A.), *see* Little, 267.

Mechanical kick-sorter (Frank, *et al.*), 603.
Melting curve at high pressures (Domb), 1316.
Mendelssohn (K.), *see* Bowers, 1445.
Mendoza (E.) and Thomas (J. G.), electrical resistance of gold, silver and copper at low temperatures, 291.
——, *see* Goodman, 594.
Menon (M. G. K.), O'Ceallaigh (C.) and Rochat (O.), multiple scattering of ionizing particles in emulsions.—II., 932.
—— and Rochat (O.), multiple scattering of ionizing particles.—V., 1232.
——, *see* Gottstein, 708; Fowler, 1040.
Meson field theory, intermediate coupling (Dalitz and Ravenhall), 1378.
Meson–photon–nucleon interaction, (Matthews), 221.
Meson production in atmosphere (Pullar and Dymond), 663.
Mesons, production in proton–proton collisions (Gunn, *et al.*), 523.
Metallic conduction—Internal size-effect (MacDonald), 756.
Meteor radiants, radio echo apparatus (Aspinall *et al.*), 504.
Micro-slip in metal crystals (Brown and Honeycombe), 1146.
Middleton (D.), distribution of energy in randomly modulated waves, 689.
Millar (W.), non-linear systems possessing resistance, 1150.
Mitchell (J. W.), *see* Keith, 1331.
Morrish (A. H.), *see* Hooper, 304.
Moving Griffith crack (Yoffe), 739.
Muirhead (H.), *see* Camerini, 1241.
Multiple scattering of ionizing particles in emulsions.—I. (Gottstein *et al.*), 708.
—— —— .—II. (Menon *et al.*), 919.
—— —— .—III. (O'Ceallaigh and Rochat), 1050.
—— —— .—IV. (Gottstein and Mulvey), 1089.
—— —— .—V. (Menon and Rochat), 1232.
Mulvey (J. H.), *see* Gottstein, 708, 1089.
(n, p; π^-) reaction (Goldsack and Page), 570.
Nabarro (F. R. N.), law of constant resolved shear stress in crystal plasticity, 213.
Nabarro (F. R. N.), synthesis of dislocation fields, 1224.
——, *see* Eshelby *et al.*, 351.
Nash (W. F.), *see* Braddick, 1227.
Neutral V-particles (Armenteros *et al.*), 1113.
Neutrino rest mass, upper limit (Kofoed-Hansen), 1448.
Neutron emission from excited nuclei (Skryme and Williams), 1187.
Neutrons, production by protons (Cassels *et al.*), 215.
Newns (H. C.), *see* Huby, 1442.
Nodtvedt (H.), correlation function in analysis of directive wave propagation, 1022.
Non-linear systems possessing resistance (Millar), 1150.
—— —— —— reactance (Cherry), 1161.
Nuclear transformations by cosmic ray particles of great energy.—VI. (Camerini, Davies, Fowler *et al.*), 1241.
—— —— .—VII. (Camerini, Davies, Franzinetti *et al.*), 1261.
Nuclear scattering of electrons and positrons (Howatson and Atkinson), 1136.
Nuclear explosions, helium and lithium emission (Sorensen), 188.
Octupole transitions (French), 263.
O'Ceallaigh (C.), masses and decay of heavy (κ) mesons, 1032.
—— and Rochat (O.), multiple scattering in emulsions.—III., 1050.
——, *see* Gottstein, 708; Menon, 932.
Orlin (J. J.), *see* Gibson, 555.
Page (N.), *see* Goldsack and Page, 570.
Pair production by fast electrons (Hooper, King and Morrish), 304.
Papapetrou (A.), Landau diamagnetism and Meissner effect, 95.
Paramagnetic salts, hyperfine structure and nuclear alignment (Bleaney), 441.
—— resonance (Bleaney *et al.*), 1062.

Paterson (S.), *see* Cottrell, 391.

Penrose (O.), quantum mechanics of helium II., 1373.

Perkins (D. H.), *see* Camerini *et al.*, 1241, 1261.

Perturbation treatment of closed states in field theories (Touschek), 1178.

Photodisintegration of ^{10}B (Brinkworth and Titterton), 1191.

—— of the deuteron (Gibson *et al.*), 555.

Pickavance (T. C.), *see* Cassels, 215 ; Taylor, 20, 328, 751.

Pippard (A. B.), ultrasonic propagation in liquid helium near the lambda point, 1209.

Plastic distortion, theory (Bishop and Hill), 414.

—— flow of metals (Green), 365.

—— properties of F.C. metal (Bishop and Hill), 1298.

—— -rigid body at yield point (Hill), 868.

Polytypism of silicon carbide, dislocation theory (Vand), 1384.

Pople (J. A.), communal entropy of dense systems, 459.

Positronium, three-photon decay (Radcliffe), 1334.

Powell (C. F.), *see* Fowler, 1040.

Power (E. A.), *see* Gunn, 523.

Processing of thick emulsions (Dainton *et al.*), 391.

Pullar (J. D.) and Dymond (E. G.), meson production in atmosphere, 663.

Pulse height analyser (Hutchinson and Scarrott), 792 ; (Erratum), 957.

Pursey (D. L.), interaction in β decay, 1193.

Quadrupole moments and nuclear shell model (Touschek), 312.

Quantum mechanics of helium II (Penrose), 1373.

Radcliffe (J. M.), three-photon decay of positronium, 1334.

Radiations of ^{203}Hg (Wilson and Curran), 762.

Radio - atmospheric, propagation (Budden), 1.

Radio waves from galactic sources, intensity fluctuations (Little and Maxwell), 267.

RaE, isomeric state (Feather), 568.

Ranade (J. D.), hyperfine structure in bromine spectrum.—II., 284.

——, electric quadrupole and magnetic moment of bromine nucleus, 279.

Randle (T. C.), Dickson (J. M.) and Cassels (J. M.), cross-section of reaction ^{8}Be$(p, p2n)^7$Be at 156 MeV, 665.

Randle (T. C.), *see* Taylor, 20, 328, 751.

——, *see* Cassels, 215.

Range-energy relations, slow alpha particles in air (Freeman and Burcham), 434.

Randomly modulated waves (Middleton), 689.

Ravenhall (D. G.), *see* Dalitz, 1378.

Rayski (J.), field theories with nonlocalized interaction, 1289.

Reaction ^{10}B$(\gamma, d)2^4$He (Brinkworth and Titterton), 952.

—— ^{11}Be$(\gamma\alpha)^7$Li and ^{11}B$(\gamma T)^8$Be (Calcraft and Titterton), 666.

Recrystallization texture of drawn Al wire (Sawkill and Thornley), 1369.

Reflection of low frequency waves (Budden), 833.

Resistance - minimum in gold (MacDonald and Templeton), 432.

Reversion formulae, application to differential equations (Sim), 228.

Ritson (D. M.), absorption of penetrating shower secondaries, 250.

Rochat (O.), *see* Gottstein, 708 ; Menon, 932, 1232 ; Fowler, 1040 ; O'Ceallaigh and Rochat, 1050.

Rosser (W. G. V.) and Swift (M. W.), attenuation of nucleon cascades in lead, 856.

Rushbrooke (G. S.) and Scoins (H. I.), virial coefficients and Born-Green theory of fluids, 582.

Sawkill (J.) and Thornley (N.), recrystallization texture of drawn Al wire, 1369.

Scarrott (G. G.), *see* Frank (S. G. F.), 603 ; Hutchinson, 792.

Scoins (H. I.), *see* Rushbrooke, 582.

Scovil (H. E. D.), *see* Bleaney, 1062.

Seed (J.), alpha-particles from proton bombardment of O_{18}, 566.

Seidl (G. F. P.), *see* French and Seidl, 537.

Semi-conductors, internal barriers (Henisch), 734.
Siebel (M. P. L.), *see* Hill and Siebel, 722.
Signals in presence of noise (Burgess), 475.
Silver bromide, lattice defects (Keith and Mitchell), 1331.
Sim (A. C.), reversion formulae with application to non-linear differential equations, 228.
Skryme (D. M.) and Williams (W. S. C.), neutron emission from nuclei excited by high energy protons, 1187.
Sodium chloride, study of cleavage planes (Amelinckx), 324.
Sorensen (S. O. C.), emission of helium and lithium fragments in nuclear explosions, 188.
Sowerby (L.), unsteady flow of incompressible viscous fluid, 176.
Specific heat, free electrons, exchange energy (Lidiard), 1325.
Stars in emulsions by 150 MeV neutrons (Titterton), 109.
Stroh (A. N.), *see* Eshelby, 1401.
Superconductors intermediate state (Kuper), 961.
Supersonic flow, conditions at sharp leading edge (Bardsley), 255.
Swift (M. W.), *see* Rosser, 856.
τ meson (Hodgson), 1060.
Taylor (A. E.), Pickavance (T. G.), Cassels (J. M.) and Randle (T. C.), cross-sections of hydrogen and carbon for neutrons, 20, 328.
—— —— —— —— of elements for 156 MeV neutrons, 751; (Erratum), 1336.
——, *see* Cassels, 215.
Temperley (H. N. V.), velocity of second sound in helium II., 74.
Templeton (I. M.), *see* Macdonald, 432.
Thermal convection in a magnetic field (Thompson), 1417.
—— pressure in solids (Huang), 202.
Thirring (W.) and Touschek (B.), covariant formulation of Bloch-Nordsieck method, 244.
Thomas (J. G.), *see* Mendoza, 291.
Thompson (W. B.), thermal convection in a magnetic field, 1417.
Thomson (G. P.) and Hodgson (P. E.), cascade production of cosmic ray showers, 978.
Thornley (N.), *see* Sawkill, 1369.
Three and four particle nuclei, disintegration (Gunn and Irving), 1353.
Titterton (E. W.), *see* Calcraft, 666; Brinkworth, 952, 1191.
——, stars in emulsions by 150 MeV neutrons, 109.
——, hammer tracks in neutron and proton produced stars, 113.
Touschek (B.), quadrupole moments and nuclear shell model, 312.
——, perturbation treatment of closed states in field theories, 1178.
——, *see* Thirring and Touschek, 244.
——, *see* Gunn *et al.*, 523.
Transit-time phenomena in electron streams.—III. (MacDonald), 515.
Trenam (R. S.), *see* Bleaney, 1062.
Trumpy (B.), *see* Gibson, 555.
Turner (J. F.) and Cavanagh (P. E.), highly forbidden transitions in Na^{24}, 636.
Twisted elastic prism, distortion (Ashwell), 820.
Ultrasonic delay line, design (Gold), 787.
Unequally-spaced data, polynomials (Hayes and Vickers), 1387.
Vand (V.), polytypism of silicon carbide, dislocation theory, 1384.
van Kampen (N. G.), analytical continuation of the S-matrix, 851.
Velocity of second sound in helium II. (Temperley), 74.
—— —— (Ward and Wilks), 314.
Verma (A. R.), carborundum growth spirals, 1005.
Vickers, *see* Hayes, 1387.
Virial theorem in quantum mechanics (Cottrell and Patterson), 391.
Ward (J. C.) and Wilks (J.), velocity of second sound in helium near absolute zero, 314.
Wave-form analysis, uncertainty (Woodward), 883.
Williams (W. S. C.), *see* Skryme, 1187.
Wilson (H. W.) and Curran (S. C.), radiations of ^{203}Hg, new method, 762.
Wilson's hypothesis (Luchak), 807.

Wohlfarth (E. P.), *see* Fletcher and Wohlfarth, 106.
——, collective electron ferromagnetism; rectangular energy bands, 374.
Wolfendale (A. W.), *see* Braddick, 1277.
Wood (W. A.), intrinsic crystalline structure and strength of metals, 310.
Woodward (P. M.), time and frequency uncertainty in wave-form analysis, 883.
Yang (L. M.), trace of the product of Dirac's matrices, 1333.
Yekutieli (G.), *see* Danysz, 1185; Camerini, 1241, 1261.
Yoffe (E. H.), moving Griffith crack, 739.

END OF THE FORTY-SECOND VOLUME.

PRINTED BY TAYLOR AND FRANCIS, LTD., RED LION COURT, FLEET STREET, E.C.4.

U of Haw.